HYDROFORMYLATION OF C3 AND C8 OLEFINS IN HYDROCARBON GAS-EXPANDED SOLVENTS

By

Dupeng Liu

Submitted to the graduate degree program in Chemical & Petroleum Engineering and the Graduate Faculty of the University of Kansas in partial fulfillment of the requirements for the degree of Doctor of Philosophy.

Chairperson: Bala Subramaniam

Raghunath V. Chaudhari

Jon Tunge

Aaron Scurto

Kevin Leonard

Date Defended: April 30th, 2018

The dissertation committee for Dupeng Liu certifies that this is the approved version of the following dissertation:

HYDROFORMYLATION OF C3 AND C8 OLEFINS IN HYDROCARBON GAS-EXPANDED SOLVENTS

_____

Chairperson: Bala Subramaniam

Date Approved: May 8th, 2018

Abstract

Hydroformylation involves the addition of syngas to the double bond of an alkene yielding aldehydes used to produce basic building blocks for myriad consumer goods. Resource-efficient technologies that conserve feedstock and energy continue to be of interest to industry. It has been shown previously by our group that the use of CO_2-expanded liquids significantly enhances the Rh-catalyzed 1-octene hydroformylation rate and selectivity. This dissertation extends this concept by employing light alkanes such as propane and *n*-butane as compressed solvents in propylene and 1-octene hydroformylation, respectively.

Phase behavior measurements demonstrate that at identical H_2 or CO fugacities in the vapor phase, the H_2 and CO solubilities in either propane- or propylene-expanded solvents (PXLs) are greater than those in the corresponding neat solvents by as high as 76% at 70 °C and 1.5 MPa. The H_2/CO ratio in PXLs is enhanced by simply increasing the propane partial pressure. In contrast, the H_2/CO in the neat solvent at a given temperature is constant at all syngas partial pressures. For Rh/triphenylphosphine catalyzed propylene hydroformylation between 70 to 90°C and pressures up to 2.0 MPa, the *n/i* aldehyde ratio in PXL media is increased by up to 45% compared to conventional media. However, with Rh/BiPhePhos catalyst complexes, the *n/i* ratio and turnover frequency (TOF) in PXL media are comparable with those observed in conventional processes in neat solvent. Thus, refinery-grade propane/propylene mixtures, rather than polymer-grade propylene, can be used in industrial propylene hydroformylation obviating purification by distillation. Technoeconomic analyses show ~ 30% lower capital costs and ~ 20% lower utilities costs for the PXL process compared to the conventional process. The reduced material and energy consumption in the PXL process also lowers adverse environmental impacts (greenhouse gas emission, air pollutants emission, and toxic release) associated with the PXL process. For Co-

catalyzed 1-octene hydroformylation at 180°C, the use of *n*-butane expanded liquids (BXLs) as reaction media was demonstrated. The results show that the TOF for alcohol formation was enhanced by more than 20% in BXL system with a 20% reduction in organic solvent usage. These results pave the way for the rational application of gas-expanded solvents in hydroformylations.

Acknowledgments

First of all, I would like to express my heartfelt thanks to my supervisor Prof. Bala Subramaniam, director of Center for Environmentally Beneficial Catalysis (CEBC), for introducing me to the world of gas-expanded solvents, and his tremendous help and constructive suggestions during my Ph.D. program. I appreciate his constant encouragement, precious guidance and unwavering support. His optimistic, enthusiastic and meticulous style influences me profoundly in the way of pursuing research and being professional. The knowledge he imparted to me will be a great asset throughout my career.

I would like to acknowledge Prof. Raghunath Vitthal Chaudhari, my project collaborator and committee member, for his valuable suggestions and critical review for my research work.

I am also grateful to the rest of my committee members Prof. Jon Tunge, Prof. Aaron Scurto and Prof. Kevin Leonard for their precious time, critical evaluations, valuable inputs during my comprehensive examination to help me learn and improve.

I would like to express my special thanks to Dr. Zhuanzhuan Xie for her patient guidance when I started my research work and insightful advice in the development of analytical methods.

I would like to sincerely acknowledge Dr. Kirk Snavely for his kind help and support in experiment setup design and instrument training and maintenance.

I would like to thank Ed Atchison, and Dr. Fenghui Niu for their constant assistance with the experiment setup and instrumentation.

I would like to thank Dr. Claudia Bode and Nancy Crisp for their assistance and arrangements with courses and meetings, particularly on the preparation of research posters and presentation.

I would also like to thank my KU friends and colleagues from the CEBC family, Dr. Swarup K. Maiti, Dr. Anand Ramanathan, Dr. Hyun-Jin Lee, Dr. Xiaobin Zuo, Dr. Jianfeng Wu, Dr. Simin Yu. Ziwei Song, Xuhui Chen, Pallavi Bobba and Kakasaheb Nandiwale. We have a great time collaborating and contributing together.

Special thanks should go to Dr. Xin Jin, Dr. Wenjuan Yan, Dr. Hongda Zhu, Dr. Yuson So, Dr. Rich Lorenzo and Kunjie Guo. Your assistance, friendship and company always warm my heart and make my life in Lawrence colorful and memorable.

I would like to acknowledge CEBC for providing the financial support under the US Department of Agriculture and the National Institute of Food and Agriculture through Grant No. 2011-10006-30362 and the joint National Science Foundation and Environmental Protection Agency program Networks for Sustainable Material Synthesis and Design (NSF-EPA 1339661).

Last but certainly not the least, I would like to thank my parents back in China for their unconditional love, enduring support and financial aid for my oversea study. Thanks to my wife Honghong Shi, without her love, understanding, scarifies and encouragement, I would have never been able to finish my degree. Thanks to Grace's entry in my life, her birth gets a fresh start of my life.

DEDICATED TO

My wife Honghong Shi and my daughter Grace Shiyi Liu

Table of Contents

List of Figures

List of Tables

Chapter 1: Introduction

The grand challenges facing the chemical industry in the 21st century is the transition to greener, more sustainable and economical beneficial manufacturing processes that efficiently use raw materials, eliminate waste and avoid the use of toxic and/or hazardous substances.[1] The twelve principles of green chemistry and twelve principles of green chemical engineering provide qualitative guidelines for the design of chemical products and processes that reduce or eliminate the use and generation of hazardous substances.[2-3] To implement these principles, chemists and chemical engineers should continue evaluating alternative products and manufacturing processes or improving existing processes to meet customer needs, to maintain process safety and to enhance environmental protection while ensuring economic viability.

The mission of Center for Environmentally Beneficial Catalysis (CEBC) in University of Kansas is to invent cleaner, safer, energy-efficient technologies that protect the planet and human health. Guided by the principles of green chemistry and quantitative sustainability analysis, alternate technology concepts have been demonstrated on a laboratory scale by CEBC researchers in diverse areas such as selective oxidation,[4-6] hydroformylation,[7-8] metathesis[9-10] and hydrogenolysis[11-12]. The new technologies are characterized by one or more of the following attributes: highly active and selective catalysts, use of benign media and process intensification via novel reactor types. Among the CEBC core projects, hydroformylation of olefins has been investigated extensively in an effort to develop greener alternatives to the conventional process. One of the key published findings to date is that the use of CO_2-expanded liquids significantly improves catalyst activity and selectivity to desired products.[13-14]

This dissertation research complements previous work by CEBC researchers on the subject of olefin hydroformylation and extends the concept of CO_2-expanded liquids by employing light

alkanes such as propane and butane as compressed solvents in propylene and 1-octene hydroformylation, respectively. In this chapter, the state-of-the-art in hydroformylation technology and the use of gas-expanded liquids as reaction media are reviewed to rationalize the motivation for the proposed research and hypotheses thereof.

1.1 Hydroformylation reaction and industrial applications

The hydroformylation reaction, also known as "oxo synthesis", comprises the addition of syngas (the mixture of hydrogen and carbon monoxide) to the double bond of an alkene aided by a metal catalyst yielding the aldehydes. (Figure 1-1).[15-16]

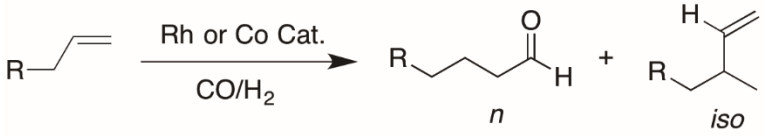

Figure 1-1 Hydroformylation reaction scheme

The product aldehydes are versatile intermediates and building blocks for pharmaceuticals, agrochemicals, and fine chemicals in organic synthesis. They can be converted to corresponding alcohols, acids and amines to make valuable commercial products via hydrogenation, oxidation and reductive amination, respectively (see Figure 1-2).[17] The global market in 2015 was ~4.4 billion and is expected to reach ~5.7 billion in 2022, with annual growth rate of ~3.9% between 2016-2022.[18] Hence, there is opportunity for adopting novel resource-efficient (conserving feedstock and energy) hydroformylation technologies in future plants that are also economically viable.

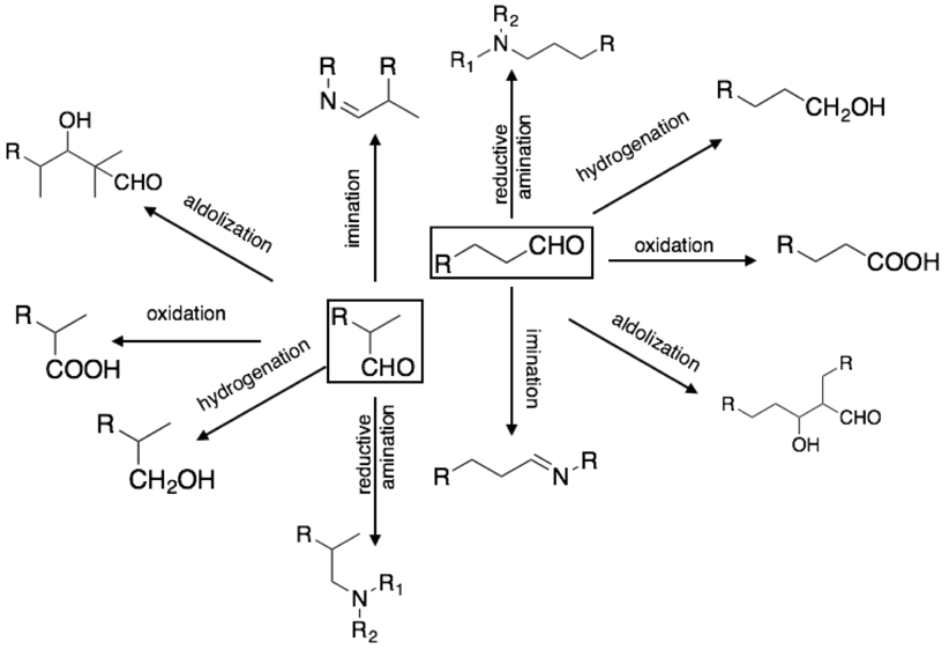

Figure 1-2 Typical uses of aldehydes in organic synthesis

Ever since it was first discovered by Otto Roelen in 1938, the reaction has been under extensive investigation, because of its industrial importance. The first generation of hydroformylation catalysts was based on cobalt carbonyl without phosphine ligand. The reaction was typically operated at temperatures from 110 °C to 180 °C and under H_2/CO pressure from 20 MPa to 30 MPa with low activity and selectivity.[19] After that, the electron-donating ligand, especially phosphine, was introduced into the cobalt catalytic center to increase the reaction selectivity.[20] The process employing phosphine ligand-based cobalt complex could be conducted at much lower syngas pressures than unmodified Co-catalyzed process and is still used today by companies such as BASF, Exxon, Sasol, and Shell for the production of high-boiling aldehydes or alcohols.[21]

In the 1960s, Wilkinson and coworkers discovered that rhodium complexes modified by phosphine ligands can also catalyze hydroformylation with high catalyst activity and aldehyde selectivity.[22-24] Compared to cobalt-based catalyst, the rhodium catalysts are less toxic and in

general much more reactive and selective. Based on the phosphine modified Rh catalyst, the so called "Low pressure Oxo Process" (LPO) was then developed by several companies (Celanese, Union Carbide/Davy Powergas/Johnson Matthey and BASF) independently in the 1970s.[25] The preferred catalyst system for these processes is Rh/Triphenylphosphine (TPP) in a high-boiling solvent such as condensation products of butanal. The solvent and an excess of ligand are used to stabilize the catalyst. Because of its superior performance, the Rh based LPO process gradually replaced the cobalt catalysts in propylene and butene hydroformylation since the mid-seventies. By 1995, more than 80% of hydroformylation processes employed rhodium based catalyst.[26-27] Following the industrial application of monodentate phosphine ligand (TPP), various modified phosphine ligands including monodentate P-O ligands, bidentate ligands and multidentate ligands have been synthesized and tested for hydroformylation reactions.[16] The latest version of the LPO process for propylene hydroformylation employs the bisphosphite-modified rhodium catalyst that provides high activity and regioselectivity for producing linear aldehydes. In this process, hydroformylation takes place in the liquid phase with high purity propylene and syngas feedstock in the presence of homogeneous catalysts. High single pass conversion of propylene (>98%) and *n/i* ratio (>20) are achieved at moderate temperatures (85-95 °C) and pressures (1.5-2.0 MPa).[28]

Rh is a noble metal that costs 750 times more than Co.[29-30] Therefore, the efficient separation and recycle of Rh is key to successful commercialization of Rh-based processes. One promising method to recover the Rh is by employing biphasic systems. The first biphasic hydroformylation process was developed by Rhone Poulenc and Ruhrchemie AG in 1982 and commercialized in 1984.[31-32] In this process, the the reaction occurs in the aqueous phase containing the catalyst while the products separate into the organic phase. However, the substrates for this process are restricted to short chain olefins because of the low solubility of higher olefins

in water. Table 1-1 outlines the characteristic features of industrial hydroformylation processes practiced by leading companies.

As seen in Table 1-1, the Rh catalysts are widely used for short-chain olefin hydroformylation. For long chain olefins containing more than four carbons, organic solvents must be used to dissolve the olefins and achieve reasonable hydroformylation rates. Hence, the catalyst, reactants and products have to be separated by distillation. The Rh catalyst complex will decompose during product distillation due to the relatively high boiling points of the aldehydes.[25] As a result, in current industrial processes involving higher olefins, the cobalt based catalysts are still in use even though it requires rather harsh temperatures and pressures.

Table 1-1 Characteristics of industrial hydroformylation processes

Catalyst (active species)	Operation conditions		*n/i* ratio	Hydrogenation activity	Feedstocks	Developers
	T, °C	P, MPa				
$CoH(CO)_4$	110-180	20-30	80:20	Middle	Long-chain olefin: C_7-C_{14}	BASF, Exxon
$CoH(CO)_3(PR_3)$ R=n-C_4H_9	160-200	5-10	88:12	High		Shell
$RhH(CO)(PR_3)_3$ R=n-C_6H_5	85-115	1.5-2.0	92:8	Low	Short-chain olefin: C_2-C_4	Union Carbide, BASF, Johnson Matthey
$RhH(CO)(POR_3)_3$ R=n-C_6H_5	<130	<2.0	90:10	Low		Mitsubishi
$RhH(CO)(POR_3)_3$ R=n-$C_6H_4SO_3Na$	50-130	1.0-10	95:5	Low		Ruhrchemie Rhone-poulenc
BIPHOS	85-95	1.2-2.0	30:1	Low		Dow Chemical

1.2 Novel developments and research areas in hydroformylation

Hydroformylation research continues to be active. A survey of patent activities and academic publications between 2010 and 2017 offers clear evidence that hydroformylation is still an important focus of both industrial and academic research (Table 1-2).

Table 1-2 Patents and publications connected with hydroformylation from 2010 to 2017

	2010	2011	2012	2013	2014	2015	2016	2017
Grant patents	405	416	372	385	334	195	81	23
Journal articles	261	196	184	233	199	211	237	182
Reviews	17	14	10	16	14	14	16	12

The research areas are mainly concerned with: (1) solving the problem of recycling homogeneous catalysts by immobilizing the homogeneous catalysts on various supports,[33-35] application of nanofiltration separation techniques to retain organometallic complexes[13, 36-38]and usage of multiphase systems to separate reactant and product,[39-41] (2) developing functional ligands and utilizing alternative metals to improve activity and selectivity,[42-45] (3) employing novel solvent media, such as ionic liquids, supercritical CO_2, and gas-expanded solvents to make the process greener.[8, 46-48]

In this section, some of the advances in catalytic hydroformylation reactions of relevance to this dissertation are described.

1.2.1 Alternative metals for homogeneous catalyzed hydroformylation reactions

Although rhodium is the preferred catalyst for hydroformylation, the increased worldwide demand for rhodium for chemical and technical processes has elevated the price of this already expensive precious metal necessitating the search for more readily available alternative transition-metal catalysts.[49] Besides Co and Rh, Ru, Ir, Pd, Pt as well as other metals of the VIII group are generally capable of forming complexes that catalyze hydroformylation reactions.[50-53] The accepted order of hydroformylation activity based on unmodified monometallic catalysts is Rh >> Co > Ir, Ru > Os ~Tc > Pt > Pd > Mn > Fe > Ni >> Re.[54] In the past five years, the research of alternative metal for hydroformylation reaction has advanced significantly, especially on Ru and Ir based catalysts.

The pioneering work for application of ruthenium catalysts in hydroformylation was reported by Wilkinson and coworkers back in1965.[55] However, Ru-based catalysts possess significantly lower activity compared to rhodium. The various ligands developed for Rh catalysts (such as TPP and bisphosphate ligands) have also been demonstrated to show enhanced activity and selectivity with Ru catalysts.[56] Compared to Rh based catalysts, the high hydrogenation activity of Ru catalysts results in higher yields of the alcohols and alkanes. Very recently, Beller et al. developed ruthenium-based hydroformylation catalysts with high *regio*-selectivity and activity. In addition to terminal alkenes, the more challenging internal olefins have been reported to preferentially yield linear alcohols in high yield (up to 88%) and regioselectivity (*n/i* up to 99:1) on Ru based catalysts.[57-58] In 2016, the ruthenium-catalyzed hydroformylation of 1-octene was successfully demonstrated in a continuously operated miniplant.[45] Following optimization of the reaction conditions in a batch reactor, continuous operation with the ruthenium catalyst was demonstrated for nearly 90 h.

Another research hotspot for Ru-catalyzed hydroformylation is using CO_2 as feedstock. The utilization of carbon dioxide as a nontoxic and inexpensive C-1 building block is of widespread interest in the chemical industry since CO_2 could be converted to CO under reverse water-gas-shift (RWGS) reaction ($CO_2 + H_2 = CO + H_2O$). Pioneering work in this area has been reported by Tominaga and Sasaki, who found that for ruthenium-catalyzed hydroformylation of alkenes with CO_2, the olefins could be converted to higher alcohols under a tandem RWGS-hydroformylation-reduction reaction pathway.[59-60] The most recent work showed that by using specific bulky phosphite ligands, the Ru based catalysts allow for a highly efficient hydroformylation of terminal and internal olefins with carbon dioxide at a lower temperature.[61]

Given that iridium and rhodium have similar chemical properties and coordination geometries, it was hypothesized that the closely related chemical properties of carbonyliridium complexes may result in comparable hydroformylation activity.[52] However, Ir based catalysts have a much lower catalytic activity and the competing hydrogenation activity of iridium complexes under hydroformylation conditions led to large amounts of unwanted alkanes as byproducts. In 2011, Beller et al. reported new iridium/phosphine complexes facilitate hydroformylation of olefins at mild conditions. The addition of inorganic salts such as LiCl was reported to suppress the hydrogenation of 1-octene and increase the yield of desired hydroformylation products.[62] Such a catalyst system is also applicable to other alkenes such as 1-pentene or 1-dodecene.[63] Most recently, the scale-up of iridium-catalyzed hydroformylation for continuous operation has been successfully demonstrated. Under optimized condition, high conversions (up to 83%) and *chemo*-selectivity towards the desired aldehydes (88%) were obtained. Long term experiments (up to 100 h) showed extended catalyst stability and activity.[64]

Despite the significant progress, the reported activity of these alternative metal-catalyzed hydroformylation (TOF of Ir = 163 h^{-1}, TOF of Ru = 41 h^{-1}) is still significantly lower than Rh-based catalysts system (TOF = 1255 h^{-1}).[62] In other words, the TOFs of Ir and Ru complexes need to be enhanced by one to two orders of magnitude to be practically viable.

1.2.2 Heterogeneously catalyzed hydroformylation reaction

Although homogeneous hydroformylation processes are dominant in industry for their superior performance with respect to activity and selectivity, catalyst separation from product is a major operating cost. Hence, efforts to immobilize homogeneous Rh catalysts on various types of solid supports to achieve facile separation continue to attract research interest.

Table 1-3 Summary of the key methodologies for the heterogenization of catalysts

Types of attachment	Key features	Pros/cons
Covalent	One or more covalent bonds between catalyst and support	Generally stable link and more than one route to form catalysts. Requirement for covalent attachment can add complexity and may alter nature of catalyst.
Supported liquid phase	Thin film of catalyst on high surface area solid	Relatively simple to carry out with catalyst soluble in supported liquid phase. Leaching a problem in liquid phase.
Entanglement	Physical restriction on the mobility and coalescence of catalyst	Simple synthesis and polysaccharides generally inexpensive. Need for interaction between catalyst precursor and polymer.
Ship in a bottle	Physical entrapment	Effective immobilization but introduces diffusion limitations.

The various types of heterogenized catalysts can be distinguished by the kind of attachment between the support and catalytically active metal or metal compound such as fixation by covalent bonding, ionic bonding, chemi- or physi- sorption, entrapment in porous materials, dissolution in supported liquids and grafting. The key features of these different methods of heterogenization are given in Table 1-3.[65] Over the last few years, several studies of the catalytic hydroformylation of olefins in the presence of immobilized metal complexes have been published.[66] Silica-based mesoporous materials, including SiO_2,[67-68] MCM-41,[69] SBA-15[70-71] have been the most widely studied supports for their diverse mesostructures and suitable spacers. However, both the activity as well as selectivity are adversely affected by confinement effects and diffusion limitations that deter facilely accessibility of the active sites within the supporting matrixes. Besides silica, other support materials including lamellar hydrotalcites,[72] zeolites,[73] active carbons,[74] porous organic polymers[75] and nanoparticles[76] have also been tested for hydroformylation. Compared to homogeneous catalysts, the activity and selectivity of these heterogenized catalysts are significantly reduced and the avoidance of metal leaching is a major challenge. To combat these challenges, several novel concepts have been proposed in recent years.

Xiao et al. synthesized a series of diphosphine ligand constructed porous polymers for hydroformylation. Rather than just immobilizing homogeneous catalysts, these porous polymers also serves as organic ligands and demonstrate even better catalytic performance than the analogous homogeneous catalysts. In addition, the catalyst preserves its activity and *regio*-selectivity even after 5 recycle studies.[77]

Lang et al. prepared single-atom Rh catalysts supported on ZnO nanowires. The single-atom catalysts have the advantages of both homogeneous catalysts, such as "isolated sites", and heterogeneous catalysts, such as stability and reusability. These catalysts demonstrated similar activity (TON = 40000) compared to that of homogeneous Wilkinson's catalyst (TON = 19000). The catalysts were reused four times without any observable decline in activity.[78]

Combing the concept of single atom catalyst and porous organic ligands (POL), Li and co-workers developed a solvent free catalytic process. By employing polymer-supported Rh catalyst Rh/CPOL-bp&P (copolymerization of tris(4-vinphenyl)phosphine and vinyl biphephos) in a fixed-bed reactor, the hydroformylation of propylene to linear aldehyde was achieved with high regioselectivity ($n/i > 24$), activity (TOF > 1200 h^{-1}) and stability (over 1000 h) at mild conditions (70 °C, 0.5 MPa).[33]

1.2.3 Hydroformylation using ionic liquid and supported ionic liquid phase (SILP) catalysts

Ionic liquids (ILs) are salts with melting points below 100 °C, consisting of an organic cation and an inorganic or organic anion. Thus, they exist as liquids even at room temperature.[79] Their unique properties such as negligible vapor pressure, tunable melting points, complete miscibility with conventional solvents and ability to dissolve a wide range of inorganic and organic compounds make them attractive alternatives to organic solvents. In the past 20 years, numerous

benefits associated with the use of ionic liquids as either additive or solvent for catalysis have been identified.[80-81]

The first investigation of the rhodium-catalyzed hydroformylation in IL was published in 1996. In this study, the reaction of 1-pentene with $Rh(acac)(CO)_2$/triphenylphosphine(TPP) complex was carried out using $[C_4min][PF_6]$ as the ionic liquid.[82] However, the use of TPP ligand resulted in significant leaching of Rh catalyst into the product phase. Efficient immobilization of rhodium hydroformylation catalyst was achieved by attaching phosphine ligands to ionic groups with high similarity to the ionic liquid cations.[83-84] The combination of $Rh(acac)(CO)_2$ and guanidinium-modifed triphenylphosphine (Figure 1-3 A) catalyzed the hydroformylation of 1-octene in $[C_4min][PF_6]$ with a TOF of 276 h^{-1} and a *n/i* ratio of 2.7 with no evidence of leaching. When applied to phenylguanidinium-modied xantphos ligand (Figure 1-3 B), a TON of 3500 and *n/i* ratio between 18.0 and 21.3 are obtained for 1-octene hydroformylation in $[C_4min][PF_6]$ with less than 0.07% rhodium leaching after ten cycles. The catalytic activity of xantphos-based catalysts was improved further when replacing the diphenylphosphino groups with phenoxophosphines (POP) (structures of phenylguanidinium and phenoxaphosphino modified xantphos ligands). Ligand C in Figure 1-3 gave the best results (TOF >300, *n/i* >40) in the rhodium-catalyzed hydroformylation of 1-octene in $[C_4min][PF_6]$ with undetectable Rh and P leaching throughout seven recycle experiments.[85]

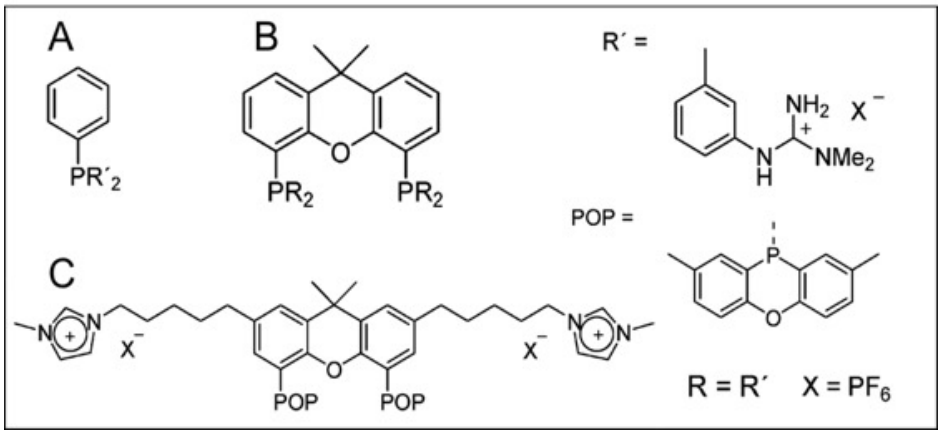

Figure 1-1 Structures of phenylguanidinium and phenoxaphosphino modified xantphos ligands

The influence of the cation and anion combination in different ionic liquids has been studied for Rh-catalyzed hydroformylation of alkenes using sodium tris(m-sulfonatophenyl)-phosphine (TPPTS) ligands as well.[86] In 1-hexene hydroformylation, the catalyst activity was significantly increased when replacing $[C_4min][PF_6]$(TOF = $54h^{-1}$) with $[C_4min][p\text{-}CH_3C_6H_4SO_3]$ (TOF = 2070 h^{-1}). The TOF enhancement was attributed to better solubility of the TPPTS ligand in these ionic liquids. When using longer chain alkenes such as 1-octene, 1-decene, and 1-dodecene as substrates, the activity was observed to increase with increasing alkyl chain length of the imidazolium cation, attributed to improved alkene and ligand solubilities in the redesigned ILs. In all cases however, the selectivity was less affected by the change in ionic liquid.[87]

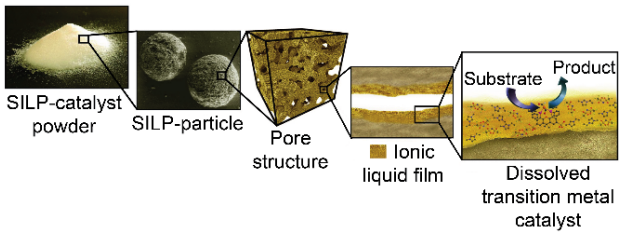

Figure 1-4 Schematic of SILP catalyst components

The concept of supported ionic liquid phase (SILP) catalysis was introduced by Mehnert and co-workers[88-89] and Wasserscheid and co-workers[90] in 2002 and 2003, respectively. The

schematic of SILP catalyst is shown in Figure 1-4. In this concept, a thin film of ionic liquid containing homogeneous catalyst complex is immobilized on a high surface area porous support material to afford a heterogenized version of a homogeneous catalyst dissolved in the ionic liquid. The IL is "impregnated" into supports such as silica as a thin film. Because of the negligible vapor pressure of the IL phase, it was hypothesized that the catalyst containing IL phase will remain in the support at reaction conditions. In this manner, transition metal complexes are immobilized without the need for sophisticated ligand modification. By ensuring that the IL layer is sufficiently thin, mass transport limitations are minimized. Thus, SILP catalysts can be viewed as immobilized homogeneous catalysts retaining their activity and selectivity but obviating post reaction solvent- and energy intensive catalyst recovery steps. And its properties can be easily tuned by tuning properties such as polarity and solubility parameter of the supported IL via various cation and anion combinations to optimize catalyst performance.

Researchers at the Friedrich Alexander Universität (FAU) in Erlangen, Germany have demonstrated the SILP concept could be applied to gas-phase hydroformylation of propylene and 1-butene using a Rh/sulfoxantphos catalyst achieving a TOF of 501 h^{-1} at 140°C and 564 h^{-1} at 120 °C separately.[91-92] Collaborating with an industry partner, a fixed-bed reactor loaded with a SILP catalyst containing a Rh/ligand complex was demonstrated (Figure 1-5).

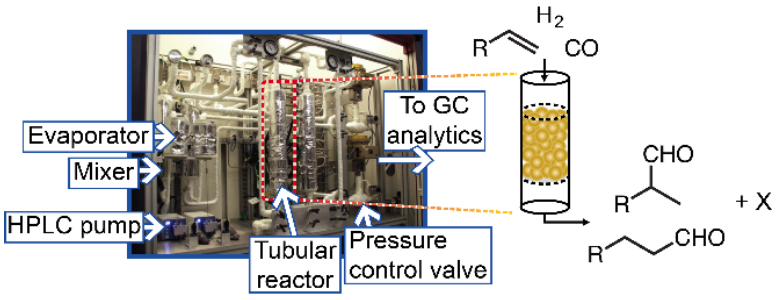

Figure 1-5 SILP-based hydroformylation process

With SILP catalyst with biaryl phosphite as ligand, remarkably stable performance for gas phase hydroformylation of industrial, mixed C4 feeds was demonstrated.[93] While retaining product quality, the space-time-yield was significantly higher for the SILP system compared to the conventional process. This demonstration opens new avenues for exploiting SILPs in other industrially significant reactions. However, leaching of the IL phase is a key barrier to the use of SILPs in liquid-phase reactions.[94]

We hypothesize that the presence of a gas such as dense CO_2 in the liquid phase helps regulate the polarity of the reaction mixture. Thus, it may be possible to minimize, if not totally eliminate, leaching with optimal design of the IL phase and the carbon dioxide-expanded liquid phase.

1.2.4 Hydroformylation in supercritical CO_2

Carbon dioxide is a ubiquitous and environmentally benign compound. Above the critical point (Tc =31.1°C, Pc = 7.38 MPa), it transformed into a fluid ($scCO_2$) that has attracted interest in the last few decades as reaction medium for several transition-metal-catalyzed organic transformations.[95] Reported benefits of employing $scCO_2$ in reactions include the following features: (1) non-flammable nature and general chemical inertness; (2) nontoxic to humans; (3) lower viscosity compared to conventional liquids; (4) improved mass transfer; (5) simple separation of catalysts and reaction products by pressure reduction. Even though CO_2 production contributes to global warming, its sequestration and use/reuse as a solvent lessens the rate at which it is emitted into the atmosphere.

The first hydroformylation reaction in $scCO_2$ was carried out by Rathke et al. in 1991 in high-pressure NMR tubes with an unmodified Co complex and propylene.[96] The reaction proceeded more slowly than in organic solvent. This work demonstrated that, although the catalyst

is soluble in the supercritical media, CO_2 does not participate in the equilibrium exchange processes involving the cobalt carbonyl complex, H_2 and CO.[97] One challenge of using $scCO_2$ as reaction medium is that most common rhodium catalyst complexes have poor solubilities in carbon dioxide rich reaction mixtures.[98] Strategies to deal with this poor solubility include the use of co-solvents and modification of ligands with perfluoroalkyl substituents.[99] The advantage of using perfluoroalkylated phosphorus ligands include catalyst solubility enhancement in $scCO_2$ and operation at lower pressures (<30 MPa) than what would be needed without the modification. In addition to concerns about synthesis cost and persistence, ligand modification by fluorinated compounds could also adversely influence catalyst activity.[100] Erkey et al. reported on the influence of temperature, olefin concentration, CO_2 and syngas pressure on 1-octene hydroformylation in $scCO_2$ by $HRh(CO)[P(p\text{-}CF_3C_6H_4)_3]_3$ and $HRh(CO)[P(3,5\text{-}(CF_3)_2C_6H_3)_3]_3$ catalyst complexes.[100-103] The reaction outcomes were found to be similar in either $scCO_2$ or conventional solvents. The main difference is the disappearance of the inhibitory effect of high olefin concentration that generally occurs in conventional solvents, which was attributed to the difficulty of formation of dimeric rhodium species in the supercritical media.

Supercritical CO_2-ionic liquid biphasic system has also been studied for hydroformylation reactions. Cole-Hamilton and co-workers developed a continuous-flow hydroformylation of long-chained olefins employing the concept of biphasic ionic liquid/$scCO_2$ systems.[104-105] The olefins, syngas and $scCO_2$ are fed into a stirred tank reactor containing an ionic liquid with dissolved catalyst. While $scCO_2$ is typically highly soluble in ionic liquid phases, the ionic liquid is essentially insoluble in $scCO_2$. Hence, the products dissolved in $scCO_2$ may be easily separated from the ionic liquid catalyst phase. Scurto et al. conducted detailed phase equilibrium studies to determine the volumetric expansion of the IL phase along with the multiphase equilibria and

mixture critical points involving the reactant, product and IL ([HMIm][Tf_2N]) with CO_2. The viscosity of the IL with CO_2 pressure and self-diffusion coefficients were also measured in concert with kinetic studies in an attempt to better understand the interplay between mass transfer and kinetic effects.[106-107] Cole-Hamilton demonstrated that by using supercritical carbon dioxide ($scCO_2$) as a carrier, under optimum conditions the using supported ionic liquid phase catalysts catalyst was stable for 40 h and gave steady production of aldehyde at a TOF of 500 h^{-1} and 42% conversion of 1-octene.[108-109]

A compilation of different catalytic systems in the Rh-catalyzed hydroformylation of 1-octene was previously made by Cole-Hamilton in 2003[110] and is updated here in Table 1-4.

Table 1-4 Rh-catalyzed hydroformylation of 1-octene in different catalyst systems

System	P, MPa	T, ºC	TOF, h-1	n/i	Problem
Homogeneous (Biphephos)[111]	3.0	120	7800	49	-
Homogeneous (TPP)[110]	1.5	95	770	8.8	S
Nano filterable homogeneous[8]	0.6	50	165	2.8	E, S
Supported on SiO_2[112]	5.0	80	287	40	L, R
Supported on POL-dppe[71]	2.0	90	nr	2.4	E, S
Fluorous biphasic[113]	1.0	100	837	4.5	S, L, E
Thermomorphic solvent[114]	1.5	90	383	9.7	E, L
$scCO_2$[115]	20.0	65	430	5.5	P, E
IL[116]	2.8	100	863	2.5	E, S
Supported IL[89]	10.0	100	3600	2.4	S, L, E
$scCO_2$/IL[117]	20.0	100	272	11.5	P, E
$scCO_2$/Supported IL[108]	10.0	100	686	3.0	P, S, E

Abbreviations: nr, not recorded; R, low rate; P, high pressure; S, low selectivity to linear aldehyde; L, high catalyst leaching; E, expensive ligand and/or solvent.

1.3 Gas-expanded liquids and its application for hydroformylation reaction

1.3.1 Introduction of gas-expanded liquids

Solvents play a vital role in multiphase catalysis. They are selected to perform functions during liquid phase catalytic transformations like solubilizing reactants, facilitating product/catalyst separation, increasing reaction rates, enhancing solubilities of gaseous reactants (such as O_2, CO, H_2) in the liquid phase, and providing heat capacity to effectively manage the

heat of reaction.[118] During the last two decades, gas-expanded liquids (GXLs) have received much attention as versatile solvent media and been investigated extensively for chemical reactions. Their properties and applications have been reviewed extensively in recent journals and books.[119-121]

GXL is defined as a continuum of tunable solvents generated by mixing liquid solvents and compressed near-critical gases. At ambient temperatures, gases such as carbon dioxide (CO_2) and light alkanes (such as propane and propylene) are close to their critical temperatures (i.e. between 0.7 and 1.3T_c). When these gases are mildly compressed (to a few MPa) at even ambient temperatures, they attain liquid-like densities and dissolve in most conventional solvents while creating the so-called GXL phase.

GXLs provide many unique benefits over traditional organic solvents and supercritical fluids. For example, they provide enhanced transport properties with increased diffusivity and decreased viscosity compared to traditional solvents. Typical operating pressure (a few MPa) required for CO_2-expanded solvents is much lower than scCO_2 (tens of MPa). The solubilities of permanent gases (H_2, CO, O_2 etc.) may be enhanced in GXLs compared to traditional organic solvents.[122-124] Moreover, the H_2/CO ratio in the GXL phase is tunable with pressure of the gas used to create the GXL.[13, 125] In addition, by using an inert gas such as carbon dioxide as the expansion gas, vapor flammability envelope is significantly reduced if not totally eliminated, which is particularly attractive for oxidation reactions.[126] When a substantial amount of the organic solvent is replaced with a non-toxic solvent such as CO_2, the GXL also provides environmental advantages. A graphical illustration of GXL and a few reported applications is shown in Figure 1-6.

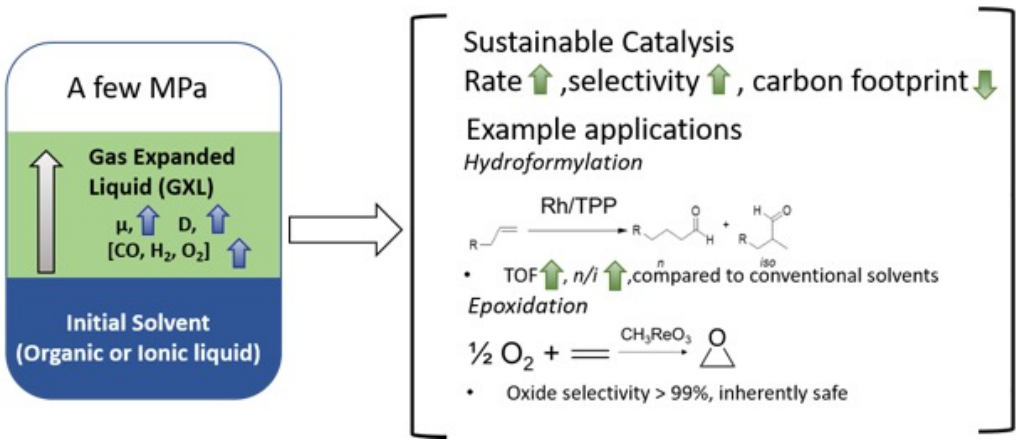

Figure 1-6 Illustration the unique property of GXLs and its application[119, 127]

1.3.2 Hydroformylation in CO_2-expanded liquids

Solvents have a remarkable effect on the hydroformylation of olefins. It was shown that for Co-catalyzed propylene hydroformylation, the *n/i* ratio was increased from 1.2 to 24 when replacing toluene with methyl ethyl ketone as the solvent.[128] For Rh-catalyzed hydroformylation, it was shown that the syngas uptake rate in polar solvents such as butyraldehyde was initially rapid but decreased with time. In contrast, the rate in nonpolar solvent such as benzene was initially accelerated with an increase in aldehyde concentration (which increases the polarity) and then decreased with time.[129] It was also found that higher H_2 pressure and lower CO pressures are generally required to enhance both the overall rate and the *regio*-selectivity to the linear aldehyde. However, CO is generally more soluble than H_2 in most conventional solvents which results in the H_2/CO ratio being lower than unity even though equimolar amounts of H_2 and CO present in the syngas feed.[130] Thus, it is generally not possible to achieve the desired H_2/CO ratios in conventional solvents without adding additional hydrogen to the gas phase.

The Subramaniam research group has conducted extensive studies of hydroformylation in CO_2-expanded liquids (CXLs). Jin et al. demonstrated that both turnover frequency (TOF) and aldehyde *regio*-selectivity can be improved in CXLs. For Rh-catalyzed 1-octene hydroformylation,

the TOF increased from 195 to 290 h^{-1}, and the *n/i* ratio increased from 4 to 11 when 5.8 MPa of syngas (out of 6.4 MPa) was replaced by 0.6 MPa syngas and 5.8 MPa CO_2 in CXLs run. Lower temperatures and higher H_2 concentration were reported to favor the aldehydes selectivity and reaction rate, respectively.[14, 131] Fang et al. demonstrated that the use a soluble polymer-bound Rh catalyst complex in conjunction with a size-selective nanofiltration membrane can substantially retain the bulky Rh catalyst in solution while allowing the lighter components to pass through.[36] A polymer bound bidentate ligand (JanaPhos) modifed homogeneous Rh catalyst complex was shown to display stable activity (TOF = 125 h^{-1}) and *regio*-selectivity (*n/i* = 3.5) at 50 °C during continuous 1-octene hydroformylation under 3.0 MPa of syngas in a stirred reactor equipped with a nanofiltration membrane. Economic and environmental analysis, which compares a CXL-based Rh-catalyzed hydroformylation in membrane-based reactor with a conventional industrial Co-catalyzed process, shows that the utilization of CXLs combined with membrane filtration has the potential to be a practically viable technology for Rh-catalyzed continuous hydroformylation of higher olefins.[132] Xie et al. conducted systematic phase equilibrium studies and demonstrated that the enhanced TOF and *regio*-selectivity toward linear aldehydes could be attributed to the tunability of syngas solubility in CO_2-expanded liquids. The H_2/CO ratios in the CXL phase are either comparable to or greater than those observed in conventional solvents at much lower syngas pressures, thus avoiding syngas inhibition.[124-125] In addition, continuous hydroformylation in CXL media with soluble Rh-catalyst complex as a model system was successfully demonstrated. The continuous run reflected the previously reported advantages with batch CXL systems producing steady activity, >95% chemoselectivity*, n/i* ratio of nearly 8, and effective Rh retention that exceeded the economic viability benchmark.[8, 13] The schematic of the setup for continuous run in CXL and its performance is shown in Figure 1-7.

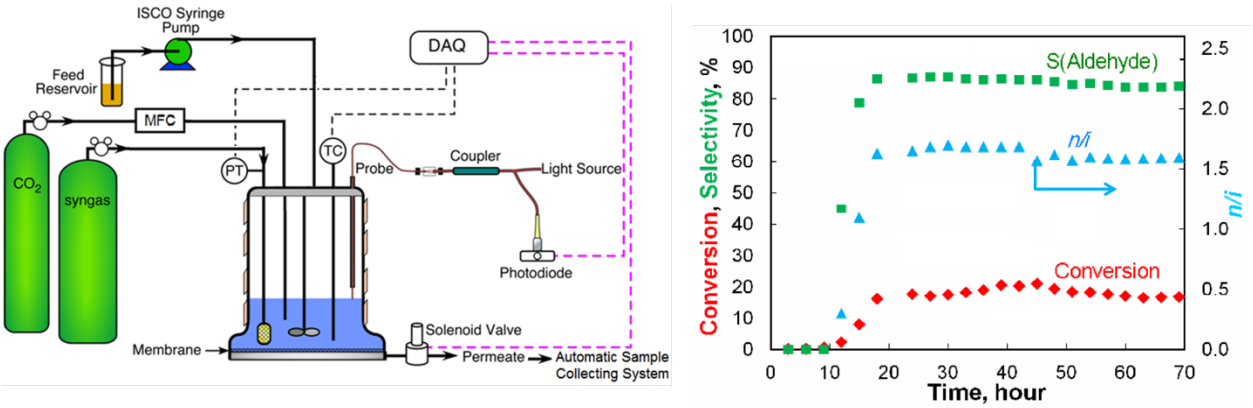

Figure 1-7 Reactor setup for continuous run in CXLs with membrane filtration and its performance

The benefits of using CXL as reaction medium has also been reported by other groups. For example, Hallett el al. used CXL to recover catalyst and products when running hydroformylation in organic-aqueous tunable solvents (OATS). They demonstrated by using CO_2 as an antisolvent, more than 99.9% of Rh is recovered by separating OATS into a product-rich organic phase and a catalyst-rich aqueous phase.[133]

1.4 Objective and overview of this work

This dissertation is aimed at extending the concept of gas-expanded liquids (GXLs), from CO_2 as expanding gas to light alkanes, to investigate the feasibility and potential benefits for hydroformylation reaction. Compared to CO_2 (Tc = 31.0 °C; Pc = 7.38 MPa), propane (Tc = 96.6 °C; Pc = 4.25 MPa) and n-butane (Tc = 152.0 °C; Pc = 3.70 MPa) possess much higher critical temperatures but lower critical pressures. Given that the critical temperatures of the light alkanes are close to the typical operation temperature of conventional Rh-catalyzed propylene hydroformylation (T: 70-110 °C) and Co-catalyzed l-octene hydroformylation (T: 160-200 °C), propane expanded liquids (PXLs) and n-butane expanded liquids (BXLs), we hypothesize that they have the potential to enhance these hydroformylation processes in similar ways as CXLs.

Toward this end, the goal of this dissertation is investigating the feasibility of using PXLs and BXLs in industrial hydroformylation thorough systematic investigations of phase equilibrium,

reaction kinetics, economic viability and environmental sustainability, employing complementary experimental and theoretical approaches. Specific objectives are to:

- Perform phase behavior studies of propylene hydroformylation reaction systems in neat and PXL media, focusing on the tunability of H_2 and CO concentrations in the propylene- and propane-expanded phases.
- Investigate PXL effects on Rh-catalyzed propylene hydroformylation activity and selectivity through semi-batch reaction studies (T = 70-90 °C, pressure up to 2.0 MPa).
- Perform comparative economic and environmental impact assessments of the PXL process and conventional process based on plant-scale process simulations.
- Investigate BXL effects on Co-catalyzed hydroformylation reaction activity and selectivity through semi-batch reaction studies. (T = 160-180 °C, pressure up to 1.8 MPa), guided by experimental measurements of the volumetric expansion of typical hydroformylation mixtures by n-butane.
- Perform preliminary investigations of SILPs for 1-octene hydroformylation in CXL media with Rh-based containing various ligands (triphenylphosphine, sulfxantphos, xantphos) provided by FAU researchers, aimed at determining the extent of leaching of the SILP phase compared to operating in conventional solvents

The various chapters following this introductory chapter are organized as follows. In Chapter 2, the solubilities of H_2 and CO (syngas components used in hydroformylation) in the presence of either propane or propylene are investigated and VLE data of such systems are modeled using the Peng-Robinson equation of state (PR-EoS). In Chapter 3, a detailed study is presented to discern the effects of PXL media on the H_2/CO ratio in the liquid phase along with the activity and selectivity of the hydroformylation reaction with various ligands. In addition, it is

shown that refinery-grade propane/propylene mixtures can be used directly for propylene hydroformylation without the need for energy-intensive purification. Chapter 4 covers the economic and environmental aspects of the conceptual PXL process based on plant-scale simulation to assess the economic viability and the environmental benignity of the alternative process for hydroformylation. Chapter 5 describes the effects of BXLs on Co-catalyzed 1-octene hydroformylation reaction through semi-batch reaction studies. Reaction parameters such as n-butane partial pressure, syngas partial pressure as well as H_2/CO ratio are examined to test the activity and selectivity of hydroformylation in BXL medium. In collaboration with FAU researchers, Chapter 6 reports preliminary results of the application of SILP catalysts for liquid-phase hydroformylation in PXLs, including the extent of metal leaching in neat solvents and CXLs. Finally, in Chapter 7, a summary of the conclusions of the current work and recommendations for future work are provided.

Chapter 2: Enhanced solubility of hydrogen and carbon monoxide in propane- and propylene-expanded liquids

2.1 Introduction

Carbon dioxide-expanded liquids (CXLs) have been extensively investigated for performing homogenous catalytic reactions (oxidation,[134-136] hydrogenation,[137-140] and hydroformylation,[13, 131, 141-142] as well as in heterogeneous catalysis[139, 143-144]. For Rh-catalyzed 1-octene hydroformylation, turnover frequencies (TOFs) are enhanced by approximately 65% and the regioselectivity (*n/i*) is enhanced by approximately 250% in CO_2-expanded toluene relative to neat toluene.[13] The presence of CO_2 in the CXL phase increases the solubilities of H_2 and CO yielding increased H_2/CO ratio in the CXL phase at progressively higher CO_2 pressures. The increased H_2/CO ratios result in increases in the reaction rates and regioselectivity.[13, 122-125]

In comparison to CO_2 (T_c = 31.0 °C; P_c = 73.8 bar), propane (T_c = 96.6 °C; P_c = 42.5 bar) and propylene (T_c = 91.1 °C; P_c = 45.5 bar) possess much higher critical temperatures but lower critical pressures than CO_2. Consequently, propane and propylene can expand organic solvents at higher temperatures and lower pressures than CO_2. Similar to CXLs, reaction media expanded by either propylene or a mixture of propylene and propane have the potential to enhance propylene hydroformylation. More than 75% of the existing industrial hydroformylation units in the world make butyraldehyde from polymer-grade propylene (99.5 % purity).[27, 145] At typical operating conditions (70 to 110 °C and 10 to 18 bar), the reaction mixture is in all likelihood expanded by propylene (the substrate). However, it is not clear if and how the propylene-expanded reaction medium enhances the reaction in a manner similar to how CXLs enhance 1-octene hydroformylation. Furthermore, it is also not clear if instead of polymer-grade propylene, crude propylene/propane mixtures from propane dehydrogenation unit may be used as feed without the

need for the energy-intensive propylene/propane purification step. In other words, can propylene/propane mixtures be used to expand the reaction mixture in which propylene is selectively reacted to form aldehydes? To fully understand and evaluate the potential of using propylene- and propane-expanded solvents for hydroformylation, an unambiguous understanding of the volumetric expansion of the reaction mixture and the solubilities of CO and H_2 in such gas-expanded solvents is essential.

In this chapter, we report the solubilities of H_2 and CO (syngas components used in hydroformylation) in the presence of either propane or propylene in two typical hydroformylation solvents, toluene and 2,2,4-trimethyl-1,3-pentanediol mono(2-methylpropanoate), commonly denoted as NX-795.[63, 115] NX-795 is used for hydroformylation because of its high boiling point and its inertness in the hydroformylation reaction mixture.[146-147] The solubility measurements were performed at temperatures and pressures of relevance in industrial propylene hydroformylation.

Previously reported solubilities of syngas components in various solvents including NX-795 serve to benchmark measurements reported herein. Still et al. reported the solubilities of alkene, carbon monoxide and hydrogen in NX-795 at various temperatures.[146] Xie et al. reported the solubilities of CO and H_2 in neat and CO_2-expanded hydroformylation reaction mixtures containing 1-octene and nonanal.[124] To the best of our knowledge, the phase equilibria of systems involving propane- or propylene expanded organic solvents have not been previously reported in the literature. In addition to reporting ternary VLE data of such systems, we also model the ternary phase behavior data (propane or propylene/solvent/H_2 or CO) using the Peng-Robinson equation of state (PR-EoS).

2.2 Experimental

The experimental apparatus for obtaining vapor-liquid equilibrium data is shown in Figure 2-1. The details of the setup and procedure have been described previously.[124] Briefly, the apparatus consists of a SFT phase monitor II, CCD camera with a fiber optic light source, TV/VCR monitor, multi-port sampling valves for liquid and vapor phases in the gas chromatograph, temperature controller, fluid mixing system, temperature and pressure indicators, gas cylinder and syringe pump. The volume of the view cell in the SFT phase monitor II may be varied manually from 3 to 30 mL. Fluid mixing is achieved through rare earth magnets coupled to an internally mounted impeller as well as by the circulation of the liquid phase with a micro-pump. The sample lines were heated to avoid condensation. Following attainment of equilibrium, the vapor and liquid phases were sampled independently and analyzed by using a gas chromatograph (GC, Varian CP-3800) equipped with a thermal conductivity detector (TCD) and a flame ionization detector (FID).

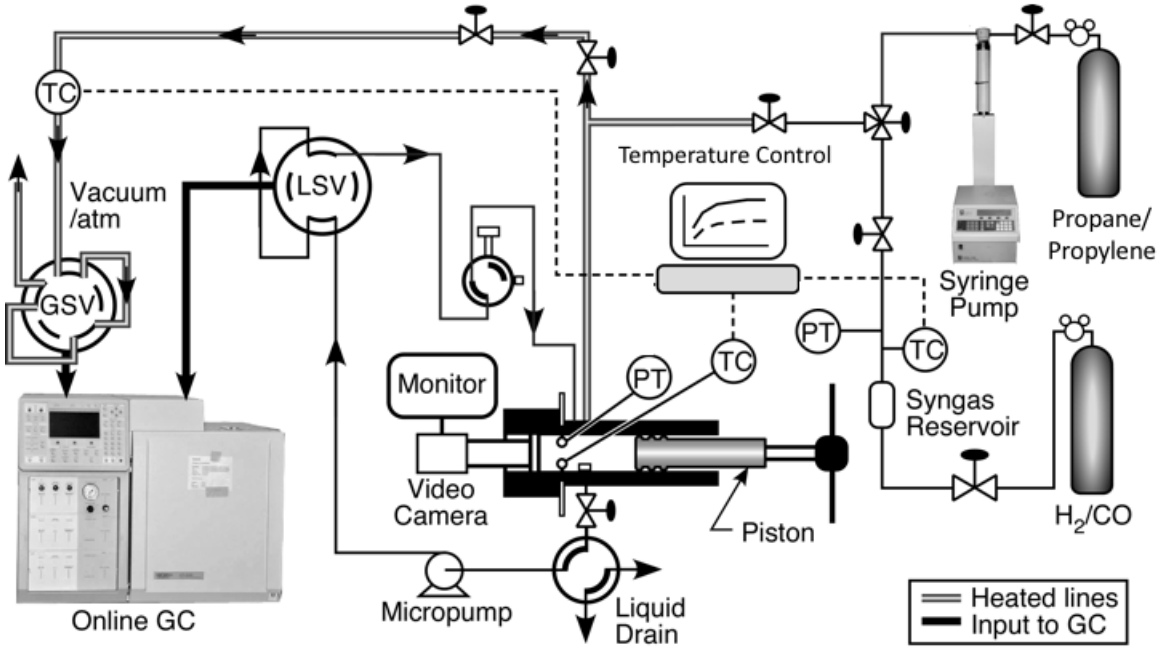

Figure 2-1 . Schematic of experimental apparatus to measure vapor liquid equilibrium

Toluene (HPLC grade) was obtained from Sigma-Aldrich, Inc.; 2,2,4-Trimethyl-1,3-pentanediol monoisobutyrate (99%) was acquired from Sigma-Aldrich, Inc. All organic compounds were used as received. Hydrogen (ultra-high purity grade, 99.99 %), carbon monoxide (ultra-high purity grade, 99.9%), propylene (ultra-high purity grade, 99.9 %), and propane (ultra-high purity grade, 99.9 %) were purchased from Matheson Tri-Gas Co.

In a typical run, the entire apparatus was rinsed several times with the expansion gas to remove any residual air. The experimental measurements were made in a view cell at a fixed volume. A predetermined amount of the liquid solvent (10 mL) was syringed into the view cell and then heated to the desired temperature. For the binary system, the second component (propane, propylene, CO or H_2) was then introduced to the desired pressure. For the ternary system, either propane or propylene was introduced into the cell as liquid from an ISCO syringe pump followed by the addition of either H_2 or CO from a syngas reservoir to reach the final desired pressure. The system is stirred and allowed to equilibrate for at least one hour (confirmed by no measurable pressure or temperature change with time). The moles of either propane or propylene introduced into the system were measured from the pump volume change and the pump temperature. The moles of either H_2 or CO added were calculated from knowing the pressure decrease in the external reservoir and the reservoir temperature. A sample calculation for determining the overall composition of a ternary system along with the overall compositions for the various ternary systems investigated in this work are provided in the Appendix E and Table E1.

Following equilibration, three samples are withdrawn from both the vapor and liquid phases at each equilibrated pressure and analyzed. The vapor phase is sampled by the static gas sampling method by withdrawing a small amount of gas from the top of the view cell. The pressure drop in the cell upon sampling is less than 0.1 MPa. After each sample is withdrawal, the cell

pressure is maintained constant by suitably moving the piston. The sampled gas phase fills two sample loops (200 μL and 250 μL in size) in a 10-port gas sampling valve. The helium carrier gas sweeps the sample in the 200 μL loop and injects it into a Supelco precolumn (4′ × 1/16″, 1.5 % OV-101 on Chromasorb GHP) and a Hayesep D column (6′ × 1/8″ SS, 80/100 mesh) in series, connected to a TCD for analyzing permanent gases. An identical sample in the 250 μL loop is injected into a Varian CP-Wax 52CB capillary column (50 m × 0.25 mm × 0.2 μm), also using He as the carrier gas. The gas samples were injected from the loops into the GC by the atmospheric balancing technique described elsewhere.[124, 148] The liquid phase is sampled using an 8-port sampling valve containing two sampling loops measuring 0.2 μL and 0.5 μL in internal volume. During each sample withdrawal, the two sample loops in each sampling valve are filled simultaneously to enable parallel analysis. The liquid phase samples in the loops were injected directly under pressure using He as the carrier gas. As in the case of vapor phase analysis, the packed column and TCD are used for analysis of the nonpolar gas components while the capillary column/FID combination is used for analyzing the organic components.

External standardization method was applied for on-line gas chromatographic (GC) analysis of liquid and vapor phase samples as described elsewhere.[148] Details of the calibration procedure are detailed in the Appendix A.

2.3 Vapor-liquid-equilibrium (VLE) modeling

The PR-EoS is used for predicting the VLE of the binary and ternary systems in this study. The approach is similar to that reported previously for binary and ternary gas-expanded liquid systems involving CO_2 as the expansion gas.[122-124] The PR-EoS for a pure component is as follows:

$$P = \frac{RT}{(V-b)} - \frac{a(T)}{V(V+b)+b(V-b)} \tag{2-1}$$

where the variables a and b are defined for pure components as follows:

$$a(T) = a_c \alpha$$

$$a_c = 0.45723553 \frac{R^2 {T_c}^2}{P_c}$$

$$\alpha = [1 + (0.37464 + 1.54226\omega - 0.26993\omega^2)(1 - \sqrt{T_r})]^2$$

$$b = 0.07779607 R \frac{T_c}{P_c}$$

$$T_r = \frac{T}{T_c}$$

where T_c, P_c and ω represents the critical temperature, critical pressure and acentricity factor, respectively. The liquid and vapor phases of the ternary systems were simulated as pseudo-binary systems given that the permanent gas (either CO or H_2) concentrations in the liquid phase and the concentrations of the organic solvent in the vapor phase are relatively low. Hence, van der Waals' mixing rules and binary interaction parameters are used for the mixtures as follows.

$$a = \sum_i \sum_j x_i x_j a_{ij}$$

$$b = \sum_i x_i b_i$$

where

$$a_{ij} = \sqrt{a_i a_j}(1 - k_{ij})$$

and k_{ij} is the binary interaction parameter.

The critical parameters and acentric factor obtained from the NIST database are summarized in

Table 2-1.[149] The binary interaction parameters shown in Table 2-2 were generated by Aspen Plus® simulator by fitting experimental VLE data for the binary systems.[150-154]

Table 2-1 Critical temperatures *Tc*, critical pressure *Pc* and acentricity factor ω of the substances

Substance	T_c (°C)	P_c (MPa)	ω
H_2	-239.97	1.293	-0.218
CO	-138.97	3.499	0.049
Propane	96.72	4.253	0.152
Propylene	91.8	4.591	0.143
Toluene	318.74	4.126	0.264
NX-795	392.65	0.201	1.018

The average absolute relative deviation (*AARD*) compares the experimental and predicted values in each phase at equilibrium, and is defined as follows for the individual phases.

$$AARD_x = \frac{1}{ND}\sum_1^{ND} \frac{|x_{cal}^i - x_{exp}^i|}{x_{exp}^i} \tag{2-2}$$

$$AARD_y = \frac{1}{ND}\sum_1^{ND} \frac{|y_{cal}^i - y_{exp}^i|}{y_{exp}^i} \tag{2-3}$$

ND represents the number of data points, x_{exp}^i, y_{exp}^i and x_{cal}^i, y_{cal}^i represent the experimental and calculated mole fractions of each component in the liquid and vapor phases, respectively.

To understand the effect of either propane or propylene addition on syngas solubility, the syngas solubility in pure toluene (i.e., without propane), is compared with that in propane-expanded toluene at identical hydrogen fugacity and temperature. This ratio, termed as the Enhancement Factor (EF), is defined as follows:

$$\text{EF} = \frac{x_{PXL}}{x_{neat\ solvent}} \tag{2-4}$$

where x_{PXL} and $x_{neat\ solvent}$ represent the mole fractions of the permanent gas component in the PXL (either propane- or propylene-expanded phase) and neat solvent phases, respectively. The mole fraction of the solute gas in the neat solvent phase is estimated using the Henry's law constants determined for the binary systems. A sample calculation is included in the Appendix B.

Table 2-2 Binary interaction parameters k_{ij} used in the PR-EoS in this work

Substance	T (°C)	k_{ij}
Propane + CO	70.0	-0.015[b,152]
	80.0	-0.014[b,152]
	90.0	-0.013[b,152]
Propane + H_2	70.0	-0.512[b,151]
	80.0	-0.549[b,151]
	90.0	-0.586[b,153]
Propane + Toluene	70.0	0.04[a]
	80.0	0.036[a]
	90.0	0.040[a]
Propane + NX-795	90.0	-0.025[a]
Propylene + H_2	70.0 - 90.0	-0.104[b,154]
Propylene + CO	70.0 - 90.0	0.026[155]
Propylene + Toluene	70.0	0.033[a]
	80.0	0.035[a]
	90.0	0.039[a]
Propylene + NX-795	90.0	-0.034[a]
CO + NX-795	90.0	-0.091[a]
CO + Toluene	70.0	0.022[a]
	80.0	0.032[a]
	90.0	0.035[a]
H_2 + Toluene	70.0	0.120[a]
	80.0	0.107[a]
	90.0	0.017[a]
H_2 + NX-795	90.0	-1.374[a]

[a] from model fit of binary VLE data from this work

[b] extrapolated from k_{ij} values fit to literature data

The gas phase fugacity of either H_2 or CO in the ternary system was estimated using the PR-EoS.[149]

$$\hat{f}_i = \hat{\phi}_i y_i \mathrm{P} \tag{2-5}$$

where $\hat{f}_i$, y_i, $\hat{\phi}_i$ and P represent the fugacity of component *i*, mole fraction in gas phase, fugacity coefficient and total pressure, respectively. The fugacity coefficient $\hat{\phi}_i$ was estimated using the following equation and the PR-EoS.

$$RT \ln\hat{\phi}_i = \int_0^P \left(\overline{V}_i - \frac{RT}{P}\right) dP \tag{2-6}$$

The formula embedded in the software for estimating the fugacity coefficient is provided in the Appendix C.

2.4 Results and discussion

The binary and ternary systems studied along with the experimental conditions are summarized in Table 2-3.

Table 2-3 Binary and ternary systems studied

System	*T* (°C)	P_{total} (MPa)	H_2 or CO partial pressure (MPa)	Propane or propylene partial pressure (MPa)
Toluene/H_2	70, 80, 90	0.1 - 3.0	0.1 - 3.0	-
Toluene/CO	70, 80, 90	0.1 - 3.0	0.1 - 3.0	-
NX-795/H_2	70, 80, 90	0.1 - 3.0	0.1 - 3.0	-
NX-795/CO	70, 80, 90	0.1 - 3.0	0.1 - 3.0	-
Propane or Propylene/Toluene	70, 80, 90	0.1 - 2.0	-	0.1 to 2.0
Propane or Propylene/NX-795	90	0.1 - 2.0	-	0.1 to 2.0
Propane/H_2/Toluene	70, 80, 90	1.5	0.2 - 1.3	Remainder
Propylene/H_2/Toluene	70, 80, 90	1.5	0.2 - 1.3	Remainder
Propane/CO/Toluene	70, 80, 90	1.5	0.2 - 1.3	Remainder
Propylene/CO/Toluene	70, 80, 90	1.5	0.2 - 1.3	Remainder
Propane/H_2/NX-795	90	1.5	0.2 - 1.3	Remainder
Propane/CO/NX-795	90	1.5	0.2 - 1.3	Remainder
Propylene/H_2/NX-795	90	1.5	0.2 - 1.3	Remainder
Propylene/CO/NX-795	90	1.5	0.2 - 1.3	Remainder

Experimental measurements of binary VLE data involving either CO or H_2 in a conventional solvent were aimed at reproducing published data to establish the reliability of the experimental unit and procedures.

The solubility of either H_2 or CO in conventional solvents was measured at 70 to 90 °C and at pressures between 1.0 and 3.0 MPa. As expected, the solubility of either H_2 or CO in conventional solvents increases linearly with gas pressure. The Henry's law constants (K_H) for H_2 and CO solubilities in conventional solvents were estimated as follows:

$$K_H = \frac{P}{c_2} \tag{2-7}$$

where P represents the partial pressure of the solute gas and c_2 is the concentration of the solute gas in the solvent. The uncertainty in experimental measurements is ± 5% around the mean values. As inferred from Table 2-4, the Henry's law constants obtained in this work match well with previously reported values.[146, 155-157] In both solvents, the solubility of CO is higher than that of hydrogen. In addition, the solubilities of both gases are greater in toluene than in NX-795.

Table 2-4 Solubility of H_2 and CO in different solvents (K_H, MPa·m^3/kmol)

		H_2			CO		
		70 °C	80 °C	90 °C	70 °C	80 °C	90 °C
Toluene	This work	29.7	27.9	26.2	11.7	11.8	11.7
	Literature	30.69[156]	26.80[155]	25.64[157]	-	11.53[155]	11.51[157]
NX-795	This work	34.3	32.7	30.4	17.2	16.8	16.8
	Literature[146]	33.26	31.57	30.10	17.37	17.08	16.85

The K_H values from this work have an uncertainty of ± 5% around mean values.

2.4.1 Propane/Toluene and Propylene/Toluene Systems.

Figure 2-2 shows the measured VLE data for the propylene/toluene and propane/toluene systems in the 70 to 90 °C range at various pressures up to 2.0 MPa.

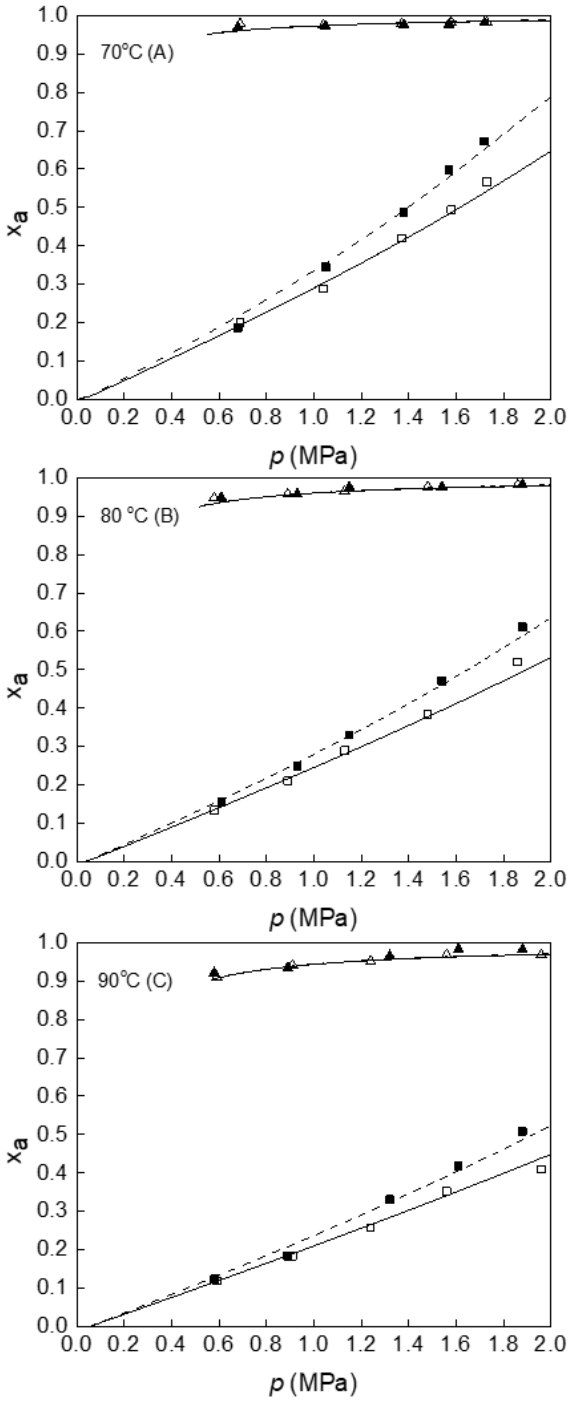

Figure 2-2 Vapor-liquid equilibrium of binary mixtures propane + toluene & propylene + toluene at T = 70 °C (A), 80 °C (B) and 90 °C (C), and pressures up to 2.0 MPa. Mole fractions x_a: ■, propane, liquid phase; □, propylene, liquid phase; ▲, propane, vapor phase; Δ, propylene, vapor phase; ——, propylene simulation; ---, propane simulation

At identical pressure and temperature, the solubility of propane in toluene is higher than that of propylene. For example, at 1.6 MPa and 70 °C , the solubility of propane in toluene is approximately 12% greater than that of propylene. As expected, higher temperatures at a given pressure reduce the solubility. Further, VLE simulations using the PR-EoS match the experimental data well. As discussed later, the binary interaction parameters for these systems were also used in predicting their ternary VLE in the presence of either H_2 or CO.

2.4.2 Propane/NX-795 and Propylene/NX-795 Systems.

The VLE data for the propylene/NX-795 and propane/NX-795 systems were measured at 90 °C and various total pressures up to 2.0 MPa summarized in Figure 2-3. Given its high boiling point, the NX-795 solvent exists mainly in the liquid phase. Propane and propylene solubilities in NX-795 were similar within experimental error.

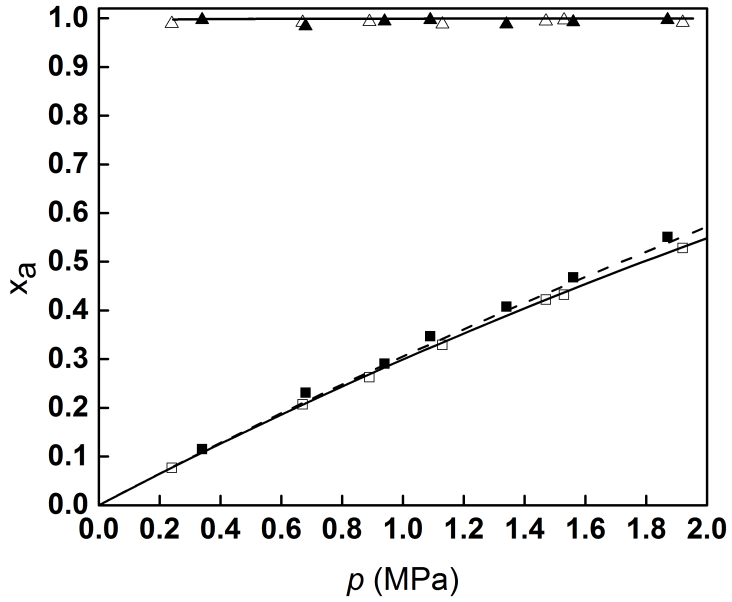

Figure 2-3 Vapor-liquid equilibrium of binary propane + NX-795 & propylene + NX-795 mixtures at T = 90 °C, and pressure up to 2.0 MPa. Mole fractions x_a: ■, propane, liquid phase; □, propylene, liquid phase; ▲, propane, vapor phase; Δ, propylene, vapor phase; ——, propylene simulation; ---, propane simulation

2.4.3 Propane/H_2/Toluene and Propane/H_2/NX-795 Systems.

The experimental VLE results for the propane/H_2/toluene system in the 70 - 90 °C range and total pressures of either 0.8 or 1.5 MPa are shown in Table 2-5 and Figure 2-4.

The equilibrium compositions of the vapor and liquid phases were measured as described in the experimental section. Only the measured H_2 and propane mole fractions in the two phases are shown in Table 2-5, with the balance being toluene.

Table 2-5 Vapor-liquid equilibrium of H_2(1) + propane(2) + toluene(3) systems*

T (°C)	P_{total} (MPa)	Liquid phase composition		Vapor phase composition		f_{H_2} (MPa)[a]	x_{H_2}, neat solvent	EF
		x_1	x_2	y_1	y_2			
90	0.80	0.0023	0.042	0.663	0.265	0.52	0.0023	1.00
90	0.80	0.0021	0.048	0.573	0.356	0.46	0.0020	1.05
90	0.80	0.0013	0.085	0.307	0.620	0.26	0.0011	1.18
90	0.80	0.0009	0.111	0.211	0.716	0.16	0.0007	1.29
90	1.50	0.0043	0.092	0.631	0.331	0.92	0.0040	1.08
90	1.50	0.0031	0.139	0.371	0.590	0.61	0.0027	1.15
90	1.50	0.0025	0.190	0.330	0.630	0.48	0.0021	1.19
90	1.50	0.0015	0.248	0.155	0.806	0.25	0.0011	1.36
80	1.50	0.0047	0.111	0.706	0.265	1.06	0.0043	1.09
80	1.50	0.0033	0.234	0.440	0.533	0.64	0.0026	1.27
80	1.50	0.0025	0.310	0.280	0.692	0.45	0.0018	1.39
80	1.50	0.0015	0.340	0.152	0.820	0.26	0.0010	1.50
70	1.50	0.0046	0.143	0.727	0.254	1.09	0.0041	1.12
70	1.50	0.0038	0.209	0.558	0.422	0.89	0.0033	1.15
70	1.50	0.0032	0.302	0.422	0.559	0.64	0.0024	1.33
70	1.50	0.0016	0.472	0.151	0.831	0.25	0.0009	1.78

*Overall compositions for each entry given in Appendix E. (Table E1); [a]estimated using Eq. (2-5).

At the experimental conditions, the fugacity coefficients were found to be close to unity. The fugacity of H_2 is shown in Table 2-5. As seen from Table 2-5, the EF values are greater than unity at all the conditions studied. At constant temperature and total pressure, the EF values increase with increasing propane mole fraction in the liquid phase. The EF value reaches as high as 1.78 at 70 °C and 1.5 MPa. This is attributed to the high propane solubility in the liquid phase, which increases the free volume in the liquid phases and thereby enhances H_2 solubility. Similar enhancements for H_2 and CO solubilities have previously been reported in CO_2-expanded liquids.[22, 24, 122]

Figure 2-4 compares the propane/H_2/toluene system at 90 °C at two different total pressures. The tie lines connect the vapor and liquid phases at equilibrium.

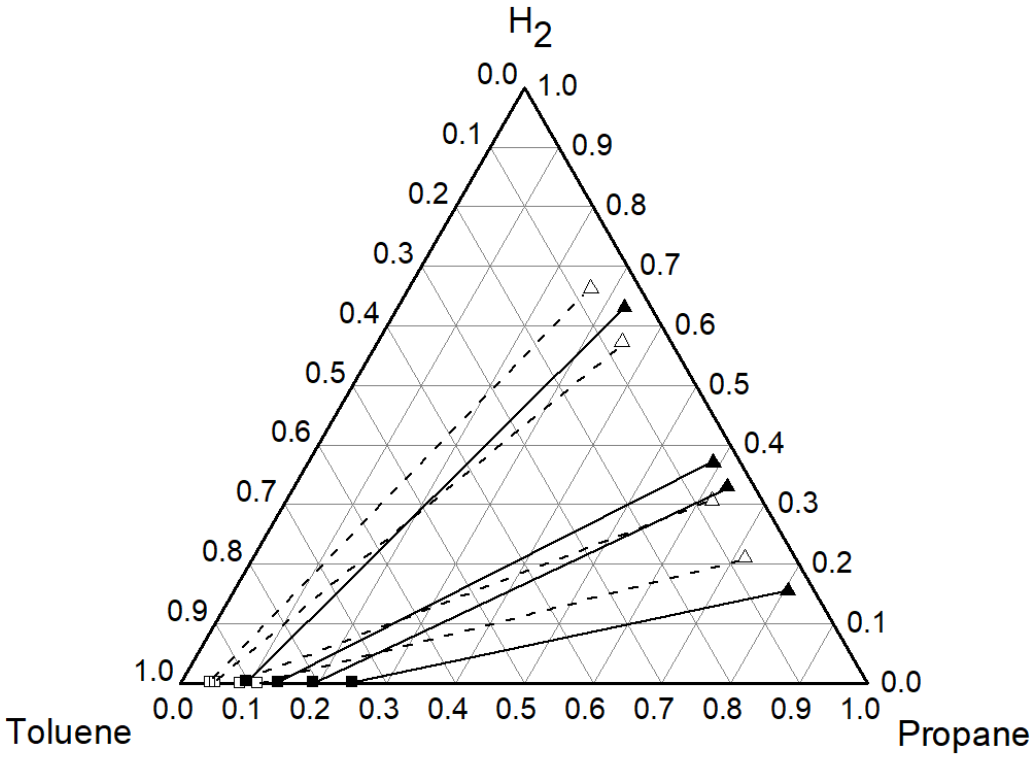

Figure 2-1 Vapor-liquid equilibrium of ternary mixtures of hydrogen(1) + propane(2) + toluene(3) at T =90 °C and p = 0.8 MPa (□, liquid phase; Δ, vapor phase) and 1.5 MPa (■,liquid phase; ▲, vapor phase).

That the equilibrium liquid phase compositions lie close to the bottom axis is a reflection of the limited H_2 solubility in the liquid phase compared to the other two compnents. On the other hand, the equilibrium vapor phase compositions close to the right axis reflecting the relatively small presence of toluene in the vapor phase compared to either propane or H_2. Compared to tie lines at 1.5 MPa, the tie lines at 0.8 MPa have a smaller slope. At the lower pressure, the liquid phase contains less propane and hydrogen while at 1.5 MPa, both the propane and hydrogen mole fractions in the liquid phase are greater. This is also reflected in the higher EF for H_2 at the higher pressures (Table 2-5).

Table 2-6 summarizes the VLE data for the propane/H_2/NX-795 system at 90 °C. Compared to toluene, NX-795 has a much higher normal boiling point (255 °C) and therefore much lower vapor pressure (<0.001 MPa at 20 °C). As in the case of toluene as solvent, EF values exceeding unity are obtained and increase with propane addition at constant temperature and total pressure.

Table 2-6 Vapor-liquid equilibrium of H_2(1) + propane(2) + NX-795(3) at 90 °C*

P_{total} (MPa)	Liquid phase composition		Vapor phase composition		f_{H_2} (MPa)[a]	$x_{H_2,\ \text{neat solvent}}$	EF
	x_1	x_2	y_1	y_2			
1.50	0.0106	0.053	0.887	0.113	1.33	0.0099	1.07
1.50	0.0073	0.188	0.578	0.422	0.87	0.0065	1.12
1.50	0.0055	0.254	0.421	0.579	0.63	0.0047	1.17
1.50	0.0037	0.320	0.266	0.734	0.40	0.0030	1.23

*Overall compositions for each entry given in Appendix E. (Table E1); [a]estimated using Eq. (2-5).

2.4.4 Propane/CO/Toluene and Propane/CO/NX-795 Systems.

The VLE data for propane/CO /toluene and propane/CO/NX-795 ternary systems are shown in Table 2-7 and Table 2-8, respectively. The fugacities and EF values for CO are calculated

following similar methods decribed earlier for the H_2-based ternary systems. Similar to the trends observed for H_2, the EF values for CO also exceed unity with propane addition. In other words, at identical CO fugacity, the CO solubility in the propane-expanded liquid phase is greater than that in the neat solvent. The effect of temperature on the VLE behavior for the propane/CO/toluene system at 1.5 MPa is easily seen from Figure 2-5. Clearly, the slopes of the tie lines at 90 °C are less than those at 70 °C. This is a reflection of the fact that at higher temperatures, propane and H_2 are less soluble in the liquid phase causing the ends of the tie lines to move towards the toluene apex. Comparison of Table 2-5 and Table 7 shows that EF values are higher for H_2 than CO at constant temperature and pressure which generally favor TOF and *regio*-selectivity for Rh-catalyzed hydroformylation reaction using simple triphenylphosphine ligand.[16,44]

Table 2-7 Vapor-liquid equilibrium of CO(1) + propane(2) + toluene(3) systems*

T (°C)	P_{total} (MPa)	Liquid phase composition		Vapor phase composition		f_{CO} (MPa)[a]	$x_{CO,\ neat\ solvent}$	EF
		x_1	x_2	y_1	y_2			
90	1.50	0.0097	0.076	0.655	0.302	0.97	0.0094	1.03
90	1.50	0.0081	0.120	0.502	0.454	0.76	0.0074	1.09
90	1.50	0.0057	0.182	0.335	0.622	0.47	0.0046	1.24
90	1.50	0.0023	0.242	0.122	0.835	0.18	0.0018	1.28
80	1.50	0.0099	0.127	0.615	0.356	0.97	0.0092	1.08
80	1.50	0.0065	0.221	0.392	0.578	0.59	0.0057	1.14
80	1.50	0.0052	0.261	0.293	0.677	0.42	0.0040	1.30
80	1.50	0.0026	0.363	0.136	0.836	0.20	0.0019	1.37
70	1.50	0.0101	0.180	0.628	0.351	0.95	0.0090	1.12
70	1.50	0.0073	0.321	0.402	0.577	0.61	0.0059	1.24
70	1.50	0.0042	0.412	0.203	0.778	0.32	0.0031	1.35
70	1.50	0.0037	0.464	0.165	0.817	0.25	0.0024	1.54

*Overall compositions for each entry given in Appendix E. (Table E1); [a]estimated using Eq. (2-5).

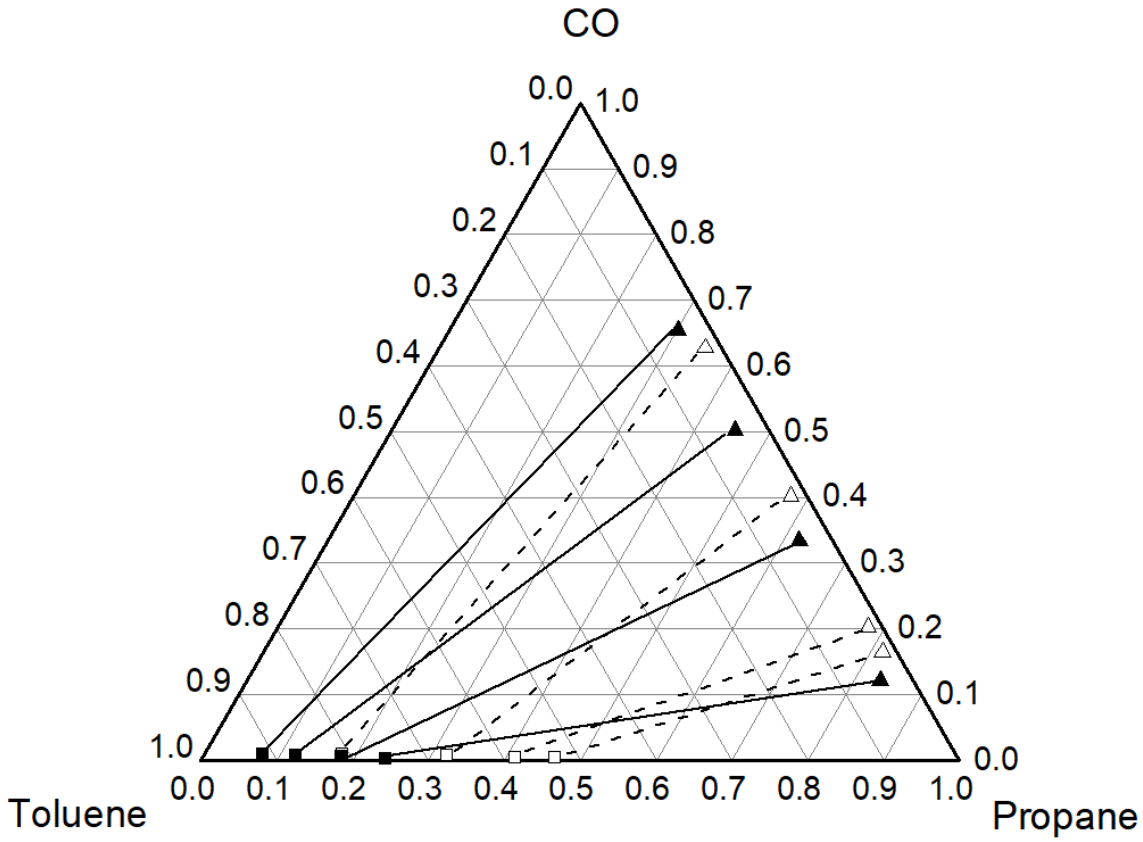

Figure 2-2 Vapor-liquid equilibrium of ternary mixtures CO(1) + propane(2) + toluene(3) at T = 90 °C (■,liquid phase; ▲, vapor phase) and 70 °C (□, liquid phase; Δ, vapor phase) and p = 1.5 MPa.

Table 2-8 Vapor-liquid equilibrium of CO(1) + propane(2) + NX-795(3) at 90 °C*

P_{total} (MPa)	Liquid phase composition		Vapor phase composition		f_{CO} (MPa)[a]	$x_{CO,\ neat\ solvent}$	EF
	x_1	x_2	y_1	y_2			
1.50	0.0173	0.073	0.836	0.164	1.25	0.0167	1.04
1.50	0.0117	0.202	0.536	0.464	0.80	0.0108	1.08
1.50	0.0088	0.266	0.388	0.612	0.58	0.0078	1.13
1.50	0.0058	0.329	0.244	0.756	0.37	0.0049	1.18

*Overall compositions for each entry given in Appendix E. (Table E1); [a]estimated using Eq. (2-5).

2.4.5 Propylene/H_2/Toluene and Propylene/H_2/NX-795 Systems.

Table 2-9 shows the VLE data for propylene/H_2/Toluene at 70 - 90 °C and a total pressure at 1.5 MPa. Again, the EF values are greater than unity in all cases, indicating that propylene dissolution in the liquid phase has a similar enhancement effect on liquid phase H_2 solubility as observed in the propane-based ternary systems involving H_2 and NX-795. Given that propylene solubility in NX-795 decreases at the higher temperatures, the enhancement factor is lower at 90 °C than at 70 °C.

Table 2-9 Vapor-liquid equilibrium of H_2(1) + propylene(2) + toluene(3) systems*

T (°C)	P_{total} (MPa)	Liquid phase composition		Vapor phase composition		f_{H_2} (MPa)[a]	x_{H_2}, neat solvent	EF
		x_1	x_2	y_1	y_2			
90	1.50	0.0049	0.069	0.721	0.239	1.08	0.0047	1.04
90	1.50	0.0044	0.089	0.618	0.343	0.95	0.0041	1.07
90	1.50	0.0026	0.165	0.347	0.614	0.54	0.0024	1.08
90	1.50	0.0014	0.218	0.205	0.756	0.28	0.0012	1.17
80	1.50	0.0043	0.118	0.620	0.352	0.96	0.0039	1.10
80	1.50	0.0027	0.241	0.360	0.613	0.56	0.0023	1.17
80	1.50	0.0018	0.266	0.226	0.746	0.35	0.0014	1.29
80	1.50	0.0008	0.321	0.089	0.883	0.14	0.0006	1.33
70	1.50	0.0044	0.145	0.712	0.271	1.06	0.0040	1.10
70	1.50	0.0035	0.251	0.519	0.463	0.77	0.0029	1.21
70	1.50	0.0029	0.282	0.365	0.618	0.60	0.0023	1.26
70	1.50	0.0015	0.463	0.147	0.835	0.25	0.0010	1.50

*Overall compositions for each entry given in Appendix E. (Table E1); [a]estimated using Eq. (2-5).

The EF values for the propane/H_2/toluene system (Table 2-5) are greater compared to those for the propylene/H_2/toluene system (Table 2-9) at the same temperature and pressure, implying that that propane has a better enhancement effect for liquid phase H_2 solubility compared to

propylene. The maximum EF value observed in the propylene-based ternary system is 1.50 (70 °C and 1.5 MPa total pressure) at a hydrogen fugacity of 0.25 MPa (row#12, Table 2-9) which is approximately 16% lower than in propane system (1.78) at the same hydrogen fugacity (0.25 MPa). This can be attributed to the higher solubility of propane in toluene that in turn increases the free volume in the PXL phase favoring H_2 solubility. The VLE data of propylene/H_2/NX-795 ternary system at 90 °C and 1.5 MPa are listed in Table 2-10. Again, the dissolution of propylene in the liquid phase was found to enhance H_2 solubilities in the PXL phase.

Table 2-10 Vapor-liquid equilibrium of H_2(1) + propylene(2) + NX-795(3) at 90 °C*

P_{total} (MPa)	Liquid phase composition		Vapor phase composition		f_{H_2} (MPa)[a]	x_{H_2}, neat solvent	EF
	x_1	x_2	y_1	y_2			
1.50	0.0103	0.066	0.856	0.144	1.28	0.0096	1.07
1.50	0.0069	0.199	0.546	0.454	0.82	0.0061	1.13
1.50	0.0051	0.264	0.390	0.610	0.58	0.0044	1.16
1.50	0.0032	0.328	0.235	0.764	0.35	0.0026	1.23

*Overall compositions for each entry given in Appendix E. (Table E1); [a]estimated using Eq. (2-5).

2.4.6 Propylene/CO/Toluene and Propylene/CO/NX-795 Systems.

The VLE data for these ternary systems are summarized in Table 2-11 and Table 2-12. It is noticed that the liquid phase CO solubility is enhanced even at low propylene mole fraction in the PXL phase. A comparison of the relative EF values in Table 2-7 and Table 2-11 shows that propane has a better enhancement effect than propylene for CO solubility in the PXL phase involving toluene. However, the difference is less pronounced for PXLs involving NX-795 (see Table 2-8 and Table 2-12).

Table 2-11 Vapor-liquid equilibrium of CO(1) + propylene(2) + toluene(3) systems*

T (°C)	P_{total} (MPa)	Liquid phase composition		Vapor phase composition		f_{CO} (MPa)[a]	$x_{CO,\ neat\ solvent}$	EF
		x_1	x_2	y_1	y_2			
90	1.50	0.0101	0.076	0.655	0.302	1.01	0.0098	1.03
90	1.50	0.0084	0.121	0.515	0.444	0.80	0.0079	1.06
90	1.50	0.0049	0.194	0.307	0.652	0.44	0.0043	1.14
90	1.50	0.0028	0.242	0.153	0.805	0.22	0.0022	1.27
80	1.50	0.0103	0.117	0.615	0.356	1.02	0.0097	1.06
80	1.50	0.0085	0.141	0.492	0.478	0.79	0.0076	1.12
80	1.50	0.0042	0.261	0.243	0.727	0.37	0.0035	1.20
80	1.50	0.0028	0.323	0.136	0.836	0.22	0.0022	1.27
70	1.50	0.0101	0.140	0.628	0.351	0.98	0.0093	1.09
70	1.50	0.0083	0.241	0.442	0.537	0.71	0.0068	1.22
70	1.50	0.0055	0.332	0.263	0.718	0.43	0.0042	1.31
70	1.50	0.0036	0.364	0.165	0.817	0.26	0.0025	1.44

*Overall compositions for each entry given in Appendix E. (Table E1); [a]estimated using Eq. (2-5).

Table 2-12 Vapor-liquid equilibrium for CO(1) + propylene(2) + NX-795(3) at 90 °C*

P_{total} (MPa)	Liquid phase composition		Vapor phase composition		f_{CO} (MPa)[a]	$x_{CO,\ neat\ solvent}$	EF
	x_1	x_2	y_1	y_2			
1.50	0.0167	0.086	0.805	0.195	1.21	0.0161	1.04
1.50	0.0110	0.213	0.506	0.494	0.76	0.0102	1.08
1.50	0.0081	0.274	0.360	0.640	0.54	0.0073	1.11
1.50	0.0051	0.334	0.217	0.783	0.33	0.0044	1.16

*Overall compositions for each entry given in Appendix E. (Table E1); [a]estimated using Eq. (2-5).

2.4.7 VLE Simulations

The VLE data were simulated with Aspen Plus® software using PR-EoS as explained in the modeling section. The measured overall ternary compositions serve as the internal mass balance constraint. The average absolute relative deviations (*AARD*) for the various liquid phase and gas phase components are summarized in the Table 2-13 and Appendix D.

Table 2-13 AARD values based on liquid phase (x)and gas phase (y) mole fractions for various ternary systems

System	*T* (°C)	*AARD, %*					
		x_1	x_2	x_3	y_1	y_2	y_3
H_2(1) + Propane(2) + Toluene(3)	90	5.17	6.56	1.64	6.59	5.05	5.50
H_2(1) + Propane(2) + Toluene(3)	80	5.75	4.48	1.60	3.82	4.00	3.88
H_2(1) + Propane(2) + Toluene(3)	70	2.15	4.15	1.68	3.62	3.22	3.31
H_2(1) + Propylene(2) + Toluene(3)	90	1.78	2.58	0.40	6.48	3.73	3.41
H_2(1) + Propylene(2) + Toluene(3)	80	5.43	3.58	2.95	3.91	4.05	3.86
H_2(1) + Propylene(2) + Toluene(3)	70	6.09	4.38	3.52	2.61	7.05	5.23
CO(1) + Propane(2) + Toluene(3)	90	3.73	3.62	0.73	6.26	4.36	2.59
CO(1) + Propane(2) + Toluene(3)	80	2.51	4.21	1.35	7.37	3.76	2.91
CO(1) + Propane(2) + Toluene(3)	70	2.86	4.03	2.25	3.49	1.81	7.03
CO(1) + Propylene(2) + Toluene(3)	90	3.35	3.50	0.79	5.44	2.46	1.29
CO(1) + Propylene(2) + Toluene(3)	80	2.28	8.04	1.67	5.05	5.68	1.96
CO(1) + Propylene(2) + Toluene(3)	70	5.85	5.31	2.01	3.30	2.44	3.56
H_2(1) + Propane(2) + NX-795(3)	90	3.19	7.66	7.61	7.07	6.80	14.54
CO(1) + Propane(2) + NX-795(3)	90	5.26	4.92	3.66	8.81	14.45	18.50
H_2(1) + Propylene(2) + NX-795(3)	90	6.66	5.59	4.81	12.37	11.07	18.00
CO(1) + Propylene(2) + NX-795(3)	90	5.51	4.44	3.94	8.79	9.50	22.35

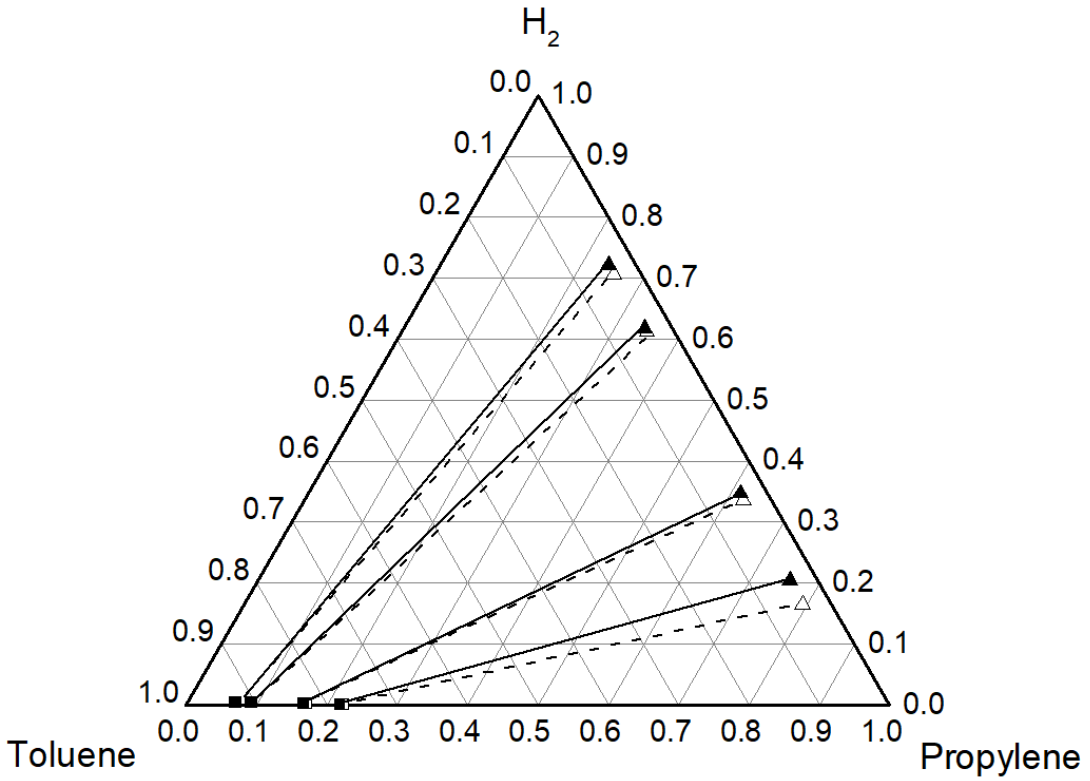

Figure 2-3 The vapor-liquid equilibrium of ternary mixtures H_2(1) + propylene (2) + toluene(3) at T = 90 °C and p = 1.5 MPa. ■, liquid phase experimental data; ▲, vapor phase experimental data; □, liquid phase simulation data; Δ, vapor phase simulation data.

The experimental and simulated VLE data for propylene/H_2/toluene and propylene/H_2/NX-795 ternary systems at 90 °C and 1.5 MPa are compared in Figure 2-6 and Figure 2-7. In general, the simulation results matched the experimental data reasonably well, with better fits for the toluene-based ternary systems compared to the more polar NX-795-based systems. The good fit between the experimental data and PR-EoS predictions justify the approximation of the vapor and liquid phases in the ternary systems as pseudo-binary systems for modeling purposes.

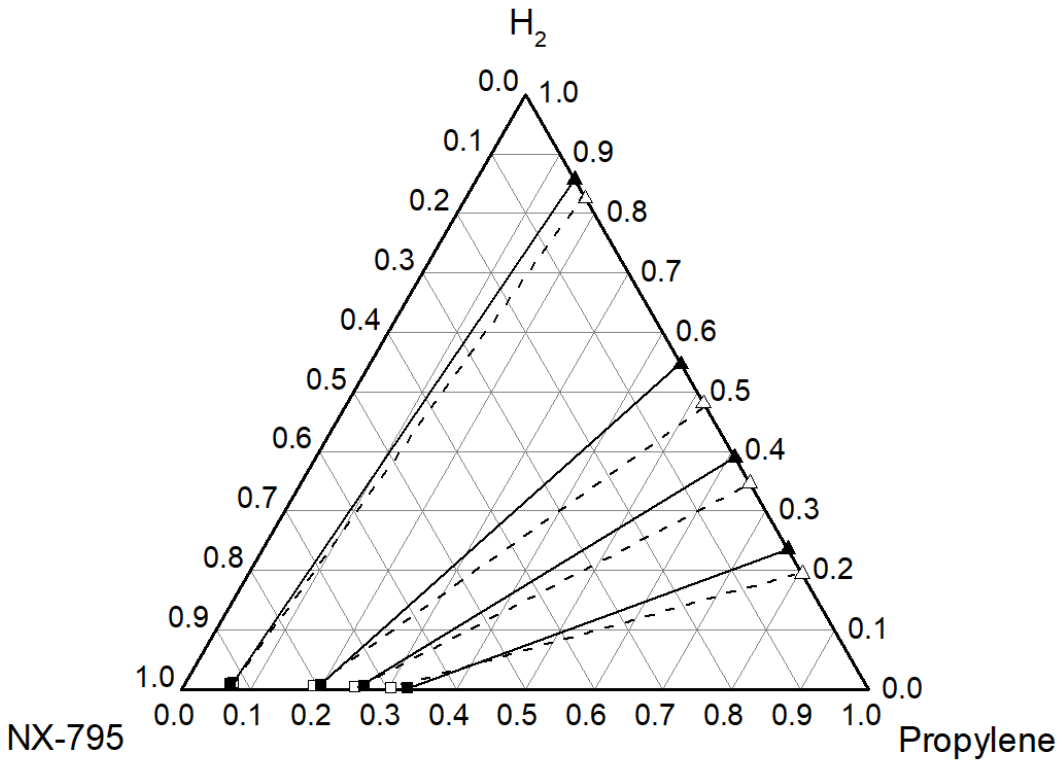

Figure 2-4 The vapor-liquid equilibrium of ternary mixtures H_2(1) + propylene(2) + NX-795(3) at T = 90 °C and p = 1.5 MPa. ■, liquid phase experimental data; ▲, vapor phase experimental data; □, liquid phase simulation data; Δ, vapor phase simulation data;

It must be noted that the composition of the reaction mixture will change with propylene conversion even though the reaction mixture is dominated by the solvent (~65 mol %) in industrial hydroformylation. Even if one assumes the linear aldehyde to be the only product, a multicomponent system (up to 6 components) will result. We have shown that for 1-olefin hydroformylation in carbon dioxide-expanded liquids (CXLs), the ternary VLE models[124] can be extended to reliably model quaternary systems and quinary systems with variable compositions.[125] Models utilizing cubic equation of state and excess Gibbs free energy-based mixing rules (CEoS/GE) were successful for predicting the multicomponent VLE phase behavior of 14 CO_2-expanded liquid systems. These included eight ternary systems, three quaternary systems and one quinary system of 1-octene hydroformylation in CO_2-expanded acetone (with the components H_2,

CO, CO_2, 1-octene, nonanal, and acetone), a CO_2-expanded toluene ternary system and a CO_2-expanded acetonitrile ternary system. Similar modeling approaches can be used to predict the VLE of multicomponent propylene hydroformylation systems. The ternary VLE data presented herein will be useful to validate such models.

2.5 Conclusion

The solubilities of H_2 and CO in either propane or propylene-expanded solvents (toluene and NX-795) are reported for the first time. Enhancement factors (EFs), defined as the ratio of gas (either CO or H_2) solubility in the ternary PXL phase to that in the neat solvent at identical vapor phase fugacities of the gas (either CO or H_2), exceed unity and are generally enhanced at increasing propane or propylene dissolution in the PXL phase. The maximum EF value is 1.78 for H_2 and 1.54 for CO, both in PXL phases involving toluene. The Peng-Robinson equation of state (PR-EoS) with van der Waals' mixing rules and binary interaction parameters modeled the VLE data adequately, with much better fits for the toluene systems compared to the more polar NX-795 systems. The complementary experimental and modeling studies have led to a better understanding of H_2 and CO solubilities in PXL media and paves the way for the rational application of such tunable media in propylene hydroformylation. For example, the tunable H_2/CO ratio in PXL phases may be exploited to enhance rate and product selectivity during propylene hydroformylation. Further, it may be possible to utilize refinery grade propane/propylene mixtures (i.e., without the energy intensive separation of propane and propylene) to perform propylene hydroformylation in PXL phase wherein propane is used as a co-solvent to enhance the hydroformylation reaction.

2.6 Notation

c2	Concentration of the solute gas in the solvent, kmol/m^3
fi	Fugacity of pure component i, MPa
$\hat{f}_i$	Fugacity of component i in a mixture, MPa
KH	Henry's law constants, MPa·m^3/kmol
kij	Binary interaction parameters
Pc	Critical pressure, MPa
P	Total pressure, MPa
R	Gas law constant, J/mol K
T	Temperature, °C
Tc	Critical temperatures, °C
V	Specific volume, m^3/mol
$\overline{V}_i$	Specific volume of component i in a mixture
$\underline{V}$	Total volume, m^3
T	Temperature, °C
Tc	Critical temperatures, °C
V	Specific volume, m^3/mol
$\overline{V}_i$	Specific volume of component i in a mixture
$\underline{V}$	Total volume, m^3
xi	Liquid mole fraction of component i
y_i	Vapor mole fraction of component i
xa	Mole fraction
Z	Compressibility factor

Greek Letters

$\widehat{\phi_i}$	Fugacity coefficient of component i in a mixture
ω	Acentric factor

Chapter 3 Homogeneous catalytic hydroformylation of propylene in propane-expanded solvent media

3.1 Introduction

The hydroformylation reaction, also known as "oxo synthesis", comprises the addition of syngas (the mixture of hydrogen and carbon monoxide) to the double bond of an alkene yielding the aldehydes (Figure 3-1). It is one of the most important homogeneous catalysis reactions industrially used to produce basic building blocks for myriad consumer goods, including pharmaceuticals, detergents, plastics, and many more.[16, 158] More than 75% of the existing industrial hydroformylation units in the world are used for propylene hydroformylation, propylene is reacted with syngas to produce butyraldehyde. Besides the desired linear n-aldehydes, branched isoaldehydes can also be formed in a parallel reaction.

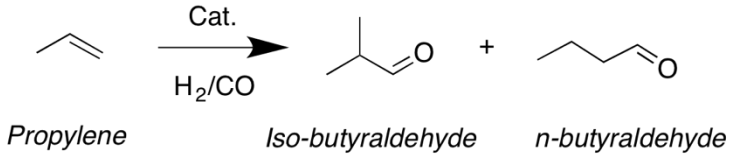

Figure 3-1 Hydroformylation of propylene

Industrial hydroformylation processes use either cobalt- or rhodium-based catalyst complexes. Propylene hydroformylation processes use rhodium-based catalysts that they allow operation at relatively mild conditions, are more active and also selective toward the preferred linear aldehyde.[159] The regioselectivity (*n/i*) is influenced by the type of ligands used to form the Rh complex, the H_2/CO ratio in the reaction phase and the nature of the solvents used.[24, 128, 160-162] In most reported studies of propylene hydroformylation, high purity propylene (up to 99.5% propylene or polymer-grade) is used as feedstock. Polymer-grade propylene costs 50% more than refinery-grade propylene (60-70% purity). The use of polymer-grade propylene makes sense if it

is readily available on site from feedstock that is specifically made for manufacturing polypropylene with a much higher capacity. However, if propylene is made on site from a propane dehydrogenation unit, it may be more economical to use the cheaper propane + propylene mixture as feedstock. Further, propane + propylene mixtures may also provide process advantages because of the increased ability of the mixture to expand the liquid reaction phase. It should be noted that compressed propylene (the substrate) by itself will expand the hydroformylation reaction mixture. However, the addition of unreactive propane expands the reaction mixture further to provide more tunability of the reaction mixture. Throughout this chapter, we refer to the reaction mixture containing propylene and propane as the PXL phase.

We have previously shown that the H_2/CO ratio can be easily tuned in CO_2-expanded liquids (CXLs) with pressure such that the TOF and *n/i* are maximized.[7, 131] In comparison to CO_2 (T_c = 31.1 °C; P_c = 7.38 MPa), propane (T_c = 96.0 °C; P_c = 4.25 MPa) and propylene (T_c = 91.1 °C; P_c = 4.55 MPa) possess much higher critical temperatures but lower critical pressures. Consequently, propane and propylene can expand organic solvents at higher temperatures and lower pressures. Similar to CXLs, reaction media expanded by either propylene or a mixture of propylene and propane have the potential to enhance propylene hydroformylation. In this context, we have recently shown that the solubilities of H_2 and CO in either propane-expanded or propylene-expanded organic solvents are greater than those in the neat solvents, by as high as 78% at 70 °C and 1.5 MPa.[13, 163]

In this manuscript, we experimentally quantify the volumetric expansion of typical hydroformylation mixtures by propane and propylene and investigate homogeneous propylene hydroformylation in PXLs with conventional rhodium-based catalysts modified by various ligands. The experimental results reveal that refinery-grade propane/propylene mixtures may

indeed be directly used for performing propylene hydroformylation. In addition to the tunable syngas solubility and increased regioselectivity afforded by the PXL media, an enriched propane stream is also produced. Thus, this reactive separation alleviates the need for energy-intensive separation of propane and propylene by conventional distillation.

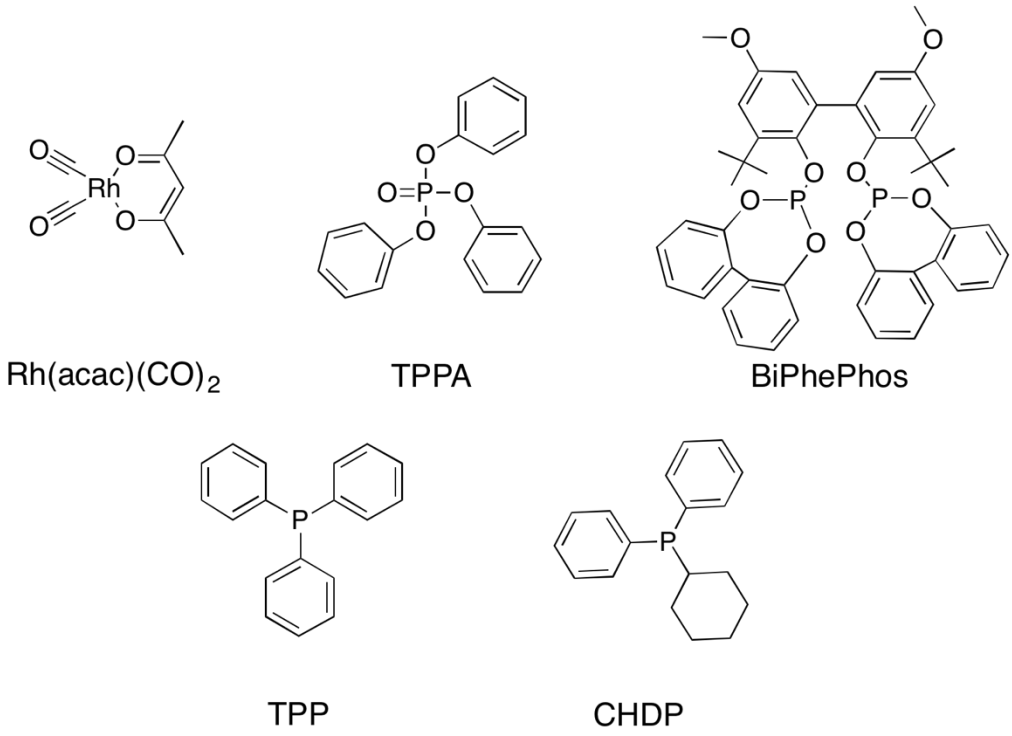

Figure 3-2 Structures of catalysts and ligands investigated in the present work

3.2 Experimental

3.2.1 Materials

The purchased materials are listed in Table 3-1. The various ligands are shown in Figure 3-2. All organic compounds were used as received and stored under argon.

3.2.2 Apparatus and methods

3.2.2.1 Volumetric Expansion and Phase Equilibrium Studies:

The equipment and procedures used for volumetric expansion and phase equilibrium studies are described elsewhere.[13, 131] For measuring the volumetric expansion of organic solvents, a Jerguson® view cell was used. In a typical run, a known quantity of a simulated reaction mixture consisting of the solvent used for propylene hydroformylation was placed in the view cell either with or without dissolved catalyst complex. This liquid phase is then brought to the desired temperature by external heating. Either dense propane or propylene is then gradually introduced through a dip tube immersed in the liquid phase to achieve predetermined partial pressures.

Table 3-1 Materials used in this Work

Material	Purity	Company
Toluene	anhydrous, 99.8%	Sigma-Aldrich, In
1-Butanol	anhydrous, 99.8%	Sigma-Aldrich, In
2,2,4-Trimethyl-1,3-pentanediol monoisobutyrate (NX-795)	99%	Sigma-Aldrich, In
(Acetylacetonato)dicarbonylrhodium(I) ($Rh(acac)(CO)_2$)	98%	Sigma-Aldrich, In
Triphenylphosphine (TPP)	99%	Sigma-Aldrich, In
6,6′-[(3,3′-Di-tert-butyl-5,5′-dimethoxy-1,1′-biphenyl-2,2′-diyl)bis(oxy)]bis(dibenzo[d,f][1,3,2]dioxaphosphepin) (BiPhePhos)	97%	Sigma-Aldrich, In
Cyclohexyldiphenylphosphine (CHDP)	98%	Sigma-Aldrich, In
Triphenyl phosphate （TPPA）	99%	Sigma-Aldrich, In
Hydrogen	100.00%	Matheson Tri-Gas Co.
Syngas	49.5% H_2 with balance being CO	Matheson Tri-Gas Co.
Propane	99.9%	Matheson Tri-Gas Co.
Propylene	99.9%	Matheson Tri-Gas Co.

The expansion of the organic liquid by propane or propylene was recorded in terms of the relative increase in the liquid volume from the initial state (C_3-free, equilibrated pressure, P_0) to

the final state (C_3-expanded, equilibrated pressure, P) at the same temperature. The volumetric expansion ratio was calculated using Equation 3-1.

$$\frac{V}{V_0} = \frac{V(T,P)}{V(T,P_0)} \qquad (3\text{-}1)$$

The solubilities of CO and H_2 in propylene and/or propane-expanded phases are measured by using a Supercritical Fluid Technologies® variable-volume equilibrium cell equipped with on-line sampling of the vapor and liquid phases. Details of this equipment and its operation are provided elsewhere.[124, 164]

Hydroformylation reaction experiments： The hydroformylation reactions were performed in a 50 cm^3 high-pressure Parr reactor. A schematic of the reactor setup is shown in Figure 3-3. Mixing is provided by a magnetic stirrer with a maximum agitation rate of 1700 rpm. Pressure and temperature are monitored by a Labview® data acquisition system and controlled with a Parr 4840 controller. Syngas is introduced from an external gas reservoir equipped with a pressure regulator and a pressure transducer. The pressure regulator, located at the exit of the reservoir, is used to admit syngas and maintain a constant total pressure in the reactor. The pressure transducer monitors the total pressure in the reservoir which drops due to syngas and propylene consumption from the gas phase. The reactor lid is equipped with ports to admit propane and/or propylene, a product sampling line, a pressure transducer, a thermocouple, and a safety rupture disk (HIP rated to 33.6 MPa).

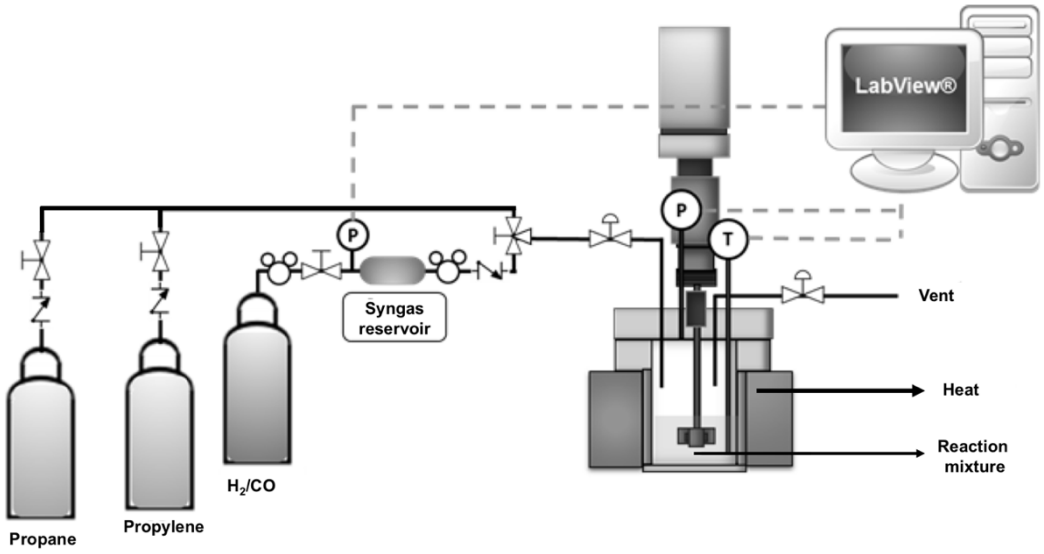

Figure 3-3 Schematic of reactor setup for investigating homogeneous hydroformylation in neat and propane-expanded solvents

In a typical run, a known amount of liquid solution containing the dissolved catalyst precursor, ligand, internal standard (decane) and the organic solvent is first introduced into the reactor and heated to the desired temperature with stirring. Following this step, predetermined amounts of either propylene or propane followed by propylene are pumped to predetermined partial pressures. The partial pressures are chosen based on the volumetric expansion studies to maintain the same initial volume of the homogeneous reaction mixture in all cases. Stirring is temporarily halted and the premixed syngas (molar $CO/H_2 = 1$) from the gas reservoir is then introduced into the reactor to the desired partial pressure. The stirrer speed is then increased to 1000 rpm to start the reaction. The reactor pressure is maintained constant by continuously replenishing syngas from an external reservoir.

The substrate conversion, regioselectivity and turnover frequency (TOF) are defined as follows:

$$\text{Propylene conversion (\%)} = \frac{\text{Moles of monoaldehyde products}}{\text{Moles of propylene fed}} \times 100 \qquad (3\text{-}2)$$

The moles of propylene fed to the reactor are estimated from the volume of liquefied propylene injected by the syringe pump into the reactor. The moles of propylene consumed by reaction are estimated from the monoaldehyde products formed. In most cases, only linear and branched butyraldehydes (> 99%) are detected by GC analysis and hence the conversion calculation can be based on moles of aldehyde products formed. The hydrogen and carbon mole balances were estimated by comparing the moles of syngas consumed with the moles of hydrogen and carbon added to the products. The total moles of hydrogen and carbon depleted from the external reservoir is generally more than what can be accounted for by product formation. However, even at the highest conversion in this manuscript (20%), this discrepancy is no greater than 8%. This is because syngas is also drawn into the reactor from the reservoir when some propylene is transferred from the vapor phase to the liquid phase upon reaction. Sample calculations for propylene conversion and syngas consumption along with the molar carbon + hydrogen balance deficits are provided in Appendix F and Table F1.

The regioselectivity (*n/i*) is estimated as the molar ratio of the linear to branched aldehydes in the product.

$$\text{Regioselectivity } (n/i) = \frac{\text{Moles linear aldehyde}}{\text{Moles branched aldehyde}} \qquad (3\text{-}3)$$

Since each mole of propylene react with two moles of syngas (H_2/CO=1:1), the TOF is estimated as follows, assuming negligible propylene transfer from the vapor phase to the liquid phase at low (~5%) propylene conversion, based on monoaldehydes formation.

$$\text{TOF } (\text{min}^{-1}) = \frac{\text{Moles of syngas consumed corresponding to 5\% substrate conversion}}{(2)(\text{moles of Rh})(\text{min})} \qquad (3\text{-}4)$$

Uncertainties in measured TOF, conversion and selectivity data are within ±5 % of mean values.

3.3 Results and discussion

3.3.1 Volumetric expansion of organic solvents by propane and propylene:

The operating conditions (organic solvent volume, propane/propylene pressures, temperature) for performing homogeneous hydroformylation are determined from volumetric expansion studies of representative reaction mixtures. Figure 3-4 shows the volumetric expansion of toluene by propylene and propane at pressures up to 2.0 MPa at 70 °C. The volume of the liquid mixture increases exponentially upon either propane or propylene pressurization (by up to two-fold at 1.5 MPa for propane and 1.7 MPa for propylene), with propane providing a greater expansion at a given pressure. The results clearly confirm that at typical industrial hydroformylation conditions (1.0-1.8 MPa, 70-110 °C), the reaction mixture undergoes significant volumetric expansion by propylene (the substrate). The experimental expansion data are predicted reasonably well by simulations performed using Aspen Plus® software employing the Peng-Robinson equation of state.[165-166] Our recent work has demonstrated that this methodology satisfactorily predicts the experimental VLE data of these systems.[148, 164]

The volumetric expansion behavior of toluene by propane at 80 °C and 90 °C is presented in Figure 3-5. The volumetric expansion by propane was greater and more sensitive to pressure at the lower temperature (80 °C) as compared to the higher temperatures (90 °C). This trend is to be expected given that the propane density (and, therefore, its solubility) in the PXL phase decreases with an increase in temperature. As inferred from Figure 3-5, no significant variation in the expansion behavior is observed at 90 °C with and without dissolved catalyst complexes because of the relatively dilute catalyst concentrations (2.21 mmol/L).

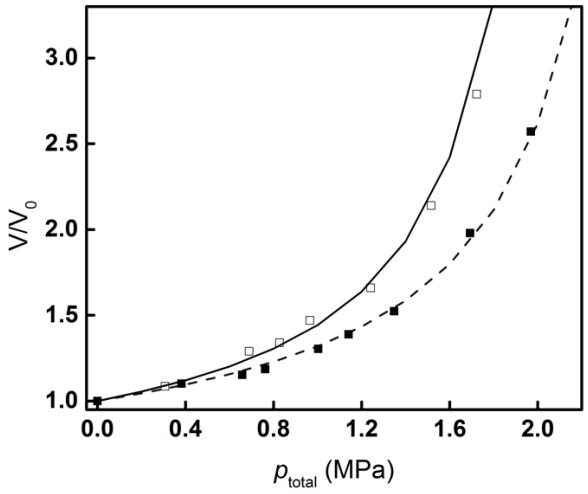

Figure 3-4 Volumetric expansion of toluene by propane and propylene at 70 ℃ (□, toluene/propane experiment; ——, toluene/propane simulation; ■, toluene/propylene experiment; ---, toluene/propylene simulation).

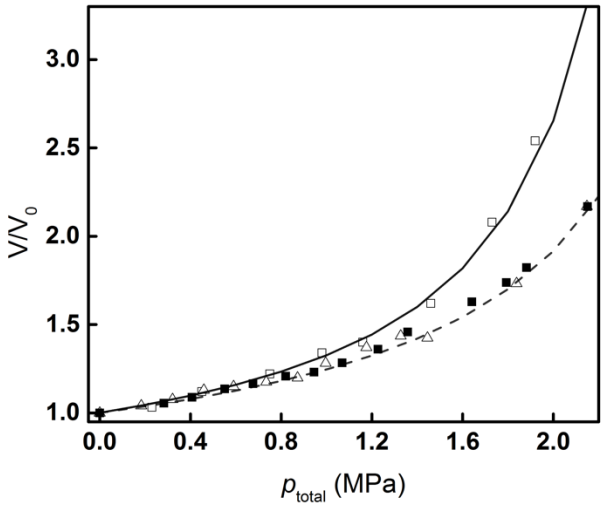

Figure 3-5 Volumetric expansion of toluene by propane at 80 ℃ (□, toluene/propane experiment; ——, toluene/propane simulation) and 90 ℃ (Δ, toluene/propane experiment; ■, toluene/propane/catalyst experiment; ---, toluene/propane simulation). [Rh] = 2.21 mmol/L, molar [TPP/Rh] = 80.

Knowledge of the extent of volume expansion of typical hydroformylation reaction mixtures by compressed propane and propylene at the reactor operating conditions (*P* and *T*) is essential for rational reactor design and operation. Figure 3-6 shows the volumetric expansion effects of propylene (0.60 MPa) and propane (up to 1.6 MPa) on various solvents (toluene, NX-795 and butanol) containing dissolved Rh catalyst complex. NX-795 solvent consists of butyraldehyde oligomers (mostly trimers) and is used in some industrial propylene hydroformylation processes as the solvent. As inferred from the expansion curves (Figure 6), all the tested solvents demonstrate good miscibility with propane/propylene at relatively mild pressures (up to 1.5 MPa, consisting of 0.6 MPa propylene and propane). At identical temperature and pressure. the volumetric expansion for toluene is greater than those of NX-795 and butanol. No catalyst precipitation was observed in the investigated P and T ranges indicating that under typical hydroformylation conditions, the Rh/TPP catalyst complex remains dissolved in these PXL phases. This was found to be the case with all the catalyst complexes listed in Figure 3-2. (See Appendix G and Figure G1).

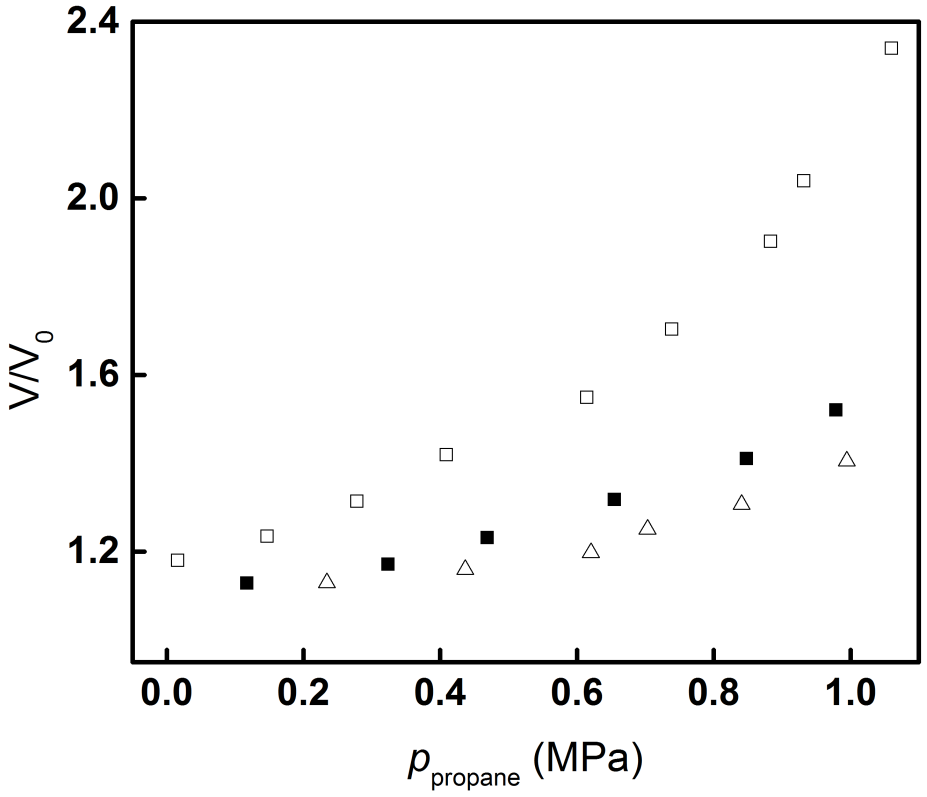

Figure 3-6 Volumetric expansion of mixtures containing dissolved Rh catalyst complex by propane at 90 ℃, propylene = 0.60 MPa; [Rh] = 2.21 mmol/L; molar TPP/Rh = 80 (□, toluene/propane/propylene/catalyst; Δ, NX-795/propane/propylene/catalyst; ■, butanol/propane/propylene/catalyst).

3.3.2 Effects of propane and propylene on H_2/CO ratio in the expanded phase

The equilibrium solubilities of CO and H_2 were measured in typical reaction mixtures expanded by either propylene or propane. To avoid the reaction, catalyst complexes were excluded from the reaction mixture. The H_2 and CO concentrations in the liquid phase at 70 ℃ with and without propane or propylene are shown in Table 3-2. The standard deviations are ± 5% for all data points. The initial composition for the measurement is also presented in the Appendix H, Table H1 & H2.

Table 3-2 CO and H_2 mole fractions (x) in neat and propane- or propylene- expanded toluene at 70 °C

Entry #	*P*, MPa	Syngas Only			Propane-expanded toluene 0.60MPa syngas + Propane			Propylene-expanded toluene 0.60 MPa syngas + Propylene		
		x, H_2	x, CO	H_2/CO	x, H_2	x, CO	H_2/CO	x, H_2	x, CO	H_2/CO
1	0.60	0.0011	0.0025	0.44	-	-	-		-	-
2	1.00	0.0019	0.0043	0.44	0.0013	0.0028	0.46	0.0013	0.0027	0.48
3	1.20	0.0023	0.0051	0.45	0.0015	0.0030	0.50	0.0014	0.0029	0.48
4	1.40	0.0027	0.0060	0.45	0.0016	0.0032	0.50	0.0015	0.0030	0.50
5	1.80	0.0035	0.0077	0.45	0.0021	0.0037	0.57	0.0018	0.0034	0.53
6	2.00	0.0039	0.0085	0.46	0.0024	0.0041	0.59	0.0020	0.0037	0.54

Standard deviations ± 5% for all data points

As can be seen from Table 3-2, both H_2 and CO concentrations increased when pressurized with syngas alone, while the H_2/CO ratio in the liquid phase remains constant. This is because the gas solubilities follow Henry's law and the CO solubility is greater than that of H_2 in toluene. However, when replacing syngas in excess of 0.60 MPa with either propane or propylene, the H_2/CO ratio in the liquid phase is enhanced with increasing partial pressures of either propane or propylene. For example, while the H_2/CO ratio in the neat toluene is 0.46 with 2.0 MPa syngas (Table 2, Entry 6), it increases to 0.59 with 0.60 MPa syngas + 1.40 MPa propane and to 0.55 with 0.60 MPa syngas + 1.40 MPa propylene. Clearly, H_2 is more soluble in propane or propylene-expanded toluene than in the mixture pressurized with syngas alone, causing the H_2/CO to increase as more propane is added. The increased H_2/CO ratio is attributed to the high solubility of pressurized propane and propylene in the liquid phase (Figure 3-4) which increases the free volume of the expanded phase. In addition, the polarity of the expanded phase is continuously diminished by the addition of either propane or propylene. Less polar phases tend to favor syngas solubilities.[167] Further, the enhanced H_2/CO in propane-expanded liquid relative to propylene-expanded liquid correlates with the higher volumetric expansion caused by propane. As seen from Table 3, H_2/CO enhancement is also seen in propane- and propylene expanded NX-795, which is

a polar solvent similar to the aldehyde products. This tunability of H_2/CO ratio in the expanded phase favors TOF and regioselectivity during propylene hydroformylation as discussed in the following section.

Table 3-3 CO and H_2 mole fractions (x) in neat and propane- or propylene-expanded NX-795 at 90 °C

					Propane-expanded NX-795			Propylene-expanded NX-795		
		Syngas Only			0.60MPa syngas + Propane			0.60 MPa syngas + Propylene		
Entry #	*P*, MPa	x, H_2	x, CO	H_2/CO	x, H_2	x, CO	H_2/CO	x, H_2	x, CO	H_2/CO
1	0.60	0.0022	0.0046	0.48	-	-	-	-	-	-
2	1.00	0.0036	0.0076	0.47	0.0023	0.0047	0.49	0.0022	0.0046	0.48
3	1.20	0.0043	0.0091	0.47	0.0023	0.0047	0.49	0.0023	0.0047	0.49
4	1.40	0.0050	0.0106	0.47	0.0024	0.0048	0.50	0.0024	0.0047	0.51
5	1.80	0.0064	0.0135	0.47	0.0026	0.0050	0.52	0.0025	0.0048	0.52
6	2.00	0.0071	0.0150	0.47	0.0027	0.0051	0.54	0.0026	0.0049	0.53

Standard deviations for the various data points are ±5%.

3.3.3 Reaction studies

3.3.3.1 Benchmark reaction

Early industrial process for propylene hydroformylation employed a rhodium-triphenylphosphine (TPP) catalyst in the low pressure oxo (LPO) process. The TPP ligand is used in a large excess (molar P/Rh up to 250) to stabilize the catalyst complex and to maximize the *n/i* ratio.[16, 27] The latest version of the LPO process uses bidentate phosphine ligands (such as Dow LP oxo SELECTOR 30 technology) employing relatively low molar P/Rh ratio (3-15) to obtain high chemo- and regioselectivities. Linear aldehyde selectivity exceeding 95% is attained at a relatively moderate temperature and pressure (e.g., 100 °C, 2.0 MPa).[168]

We first benchmarked propylene hydroformylation with Rh/BiPhePhos catalysts in toluene and PXL media at typical industrial process conditions. The reactions were performed at 90 °C with a syngas partial pressure of 0.60 MPa. As summarized in Table 3-5, more than 95% *n*-butyraldehyde selectivity is obtained in pure toluene which matches well with the conventional process.[168] For the reaction in PXLs, the total pressure is kept constant (1.0 MPa) by partially

replacing propylene with propane, while maintaining an identical volume of both the "neat" and PXL phases. While propane addition dilutes the propylene concentration in the PXL phase and therefore decreases the reaction rate, it has less effect on the *n/i* ratio (Entries 1-3, Table 3-5). To eliminate the dilution effect caused by propane addition in the batch reactor, the propylene and propane partial pressures were varied, based on calculation methods developed previously[164] to ensure that the initial propylene concentration in the PXL phase is identical to the other runs (Entries 4 & 5, Table 3-5).

Table 3-4 Propylene hydroformylation with Rh/BiPhePhos catalysts in toluene and propane-expanded toluene (PXL)

Entry#	Solvent	$p_{propylene}$, MPa	$p_{propane}$, MPa	V/V$_0$	TOF, min^{-1}	*n/i*	*n*-aldehyde selectivity, %	Propylene conversion
1	Toluene	1.00	0.00	1.1	61.2	23.3	95.9	18.5
2	PXL	0.80	0.20	1.1	55.1	23.5	95.9	16.7
3	PXL	0.60	0.40	1.1	45.4	23.8	96.0	13.8
4	PXL	1.15	0.35	1.4	59.0	30.1	96.8	18.5
5	PXL	1.40	0.60	1.8	59.1	22.5	95.7	18.0

[Rh] = 0.62 mmol/L ; molar P/Rh = 4; p_{syngas} = 0.60 MPa; molar [H_2/CO] in feed = 1; reaction time = 10 min; T = 90 °C;

Under such conditions, the regioselectivity and the TOFs are comparable to the values observed without propane addition. Thus, the advantages of using PXLs are as follows: (a) the use of relatively inexpensive refinery grade propylene (that contains more than 30% propane) as feedstock; (b) selective removal of propylene by reaction thereby enriching the propane stream; and (c) > 40% replacement of the organic solvent with compressed propane that is easily separated and recycled.

3.3.3.2 Ligands effect:

Table 3-5 Rh-catalyzed hydroformylation of propylene with different ligands in toluene and propane-expanded toluene (PXL)

Entry #	Ligands	Solvent	$p_{propylene}$, MPa	$p_{propane}$, MPa	V/V_0	TOF, min^{-1}	*n/i*	*n*-aldehyde selectivity, %
1	TPP	Toluene	0.60	-	1.1	26.3	2.51	71.5
2	CHDP	Toluene	0.60	-	1.1	15.4	2.11	67.8
3	TPPA	Toluene	0.60	-	1.1	21.5	1.21	54.8
4	TPP	PXL	0.70	0.40	1.4	25.4	3.12	75.7
5	CHDP	PXL	0.70	0.40	1.4	14.9	2.51	71.5
6	TPPA	PXL	0.70	0.40	1.4	18.9	1.65	62.3

[Rh] = 2.21mmol/L; molar [P/Rh] = 32; reaction time: 10 min; T = 70 °C; p_{syngas} = 0.60 MPa; molar [H_2/CO] =1.

The performances of several conventional mono-phosphine ligands (TPP, CHDP and TPPA) for propylene hydroformylation were also assessed in toluene and PXL media. The results are summarized in Table 3-5. At identical Rh concentration and P/Rh mole ratio, the Rh/TPP catalyst shows higher TOF and *n/i* in neat toluene compared to other monophosphine ligands (entries 1-3, Table 3-5). This is consistent with previous observations.[147] Over all three catalyst complexes, the *n/i* ratio in PXL media (entries 4-6, Table 3-5) is higher than in neat toluene. For the TPPA ligand, the increase is more than 35%. The enhanced catalyst performance was achieved by propylene/propane mixtures with 30 vol% of toluene being replaced with propane in the liquid phase. However, none of the ligands matched the performance of the BiPhePhos ligand Table 3-4) suggesting that electronic effects are far more important compared to solvent effects in determining the yield of the linear aldehyde.

3.3.3.3 Effect of H_2/CO ratio

The Wilkinson mechanism is commonly accepted for phosphine-modified rhodium-catalyzed hydroformylation of terminal olefins.[24, 169]

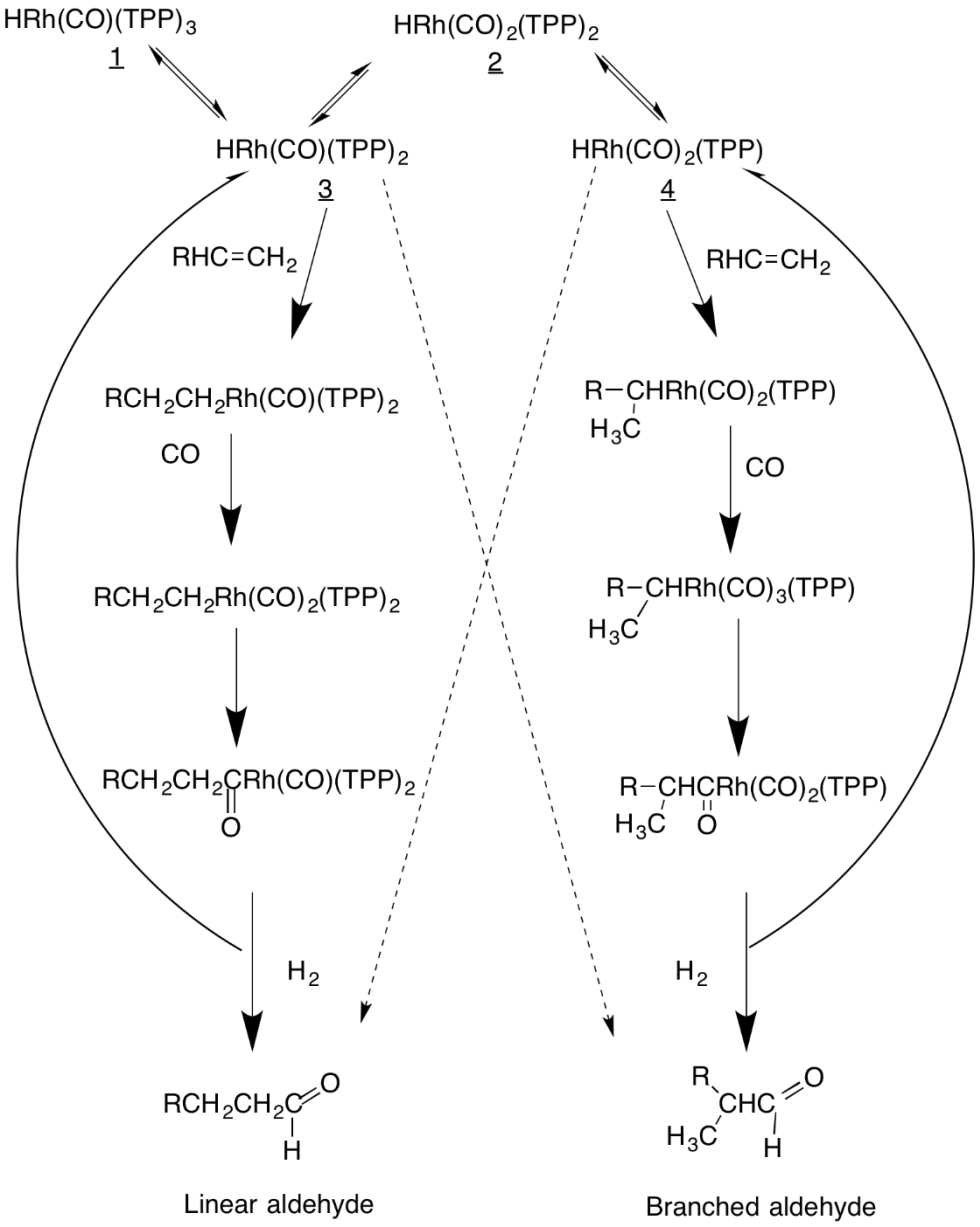

Figure 3-7 Simplified mechanism for Rh-catalyzed hydroformylation to form linear and branched products.

It is believed that the regioselectivity is largely dictated by the competitive reaction of the alkene with the intermediates (3) and (4) shown in Figure 3-7 resulting in either high or low *n/i* ratio, respectively. The progressive substitution of TPP by CO attachment to the Rh center is believed to worsen the regioselectivity. Thus, for a given catalytic system, it is plausible that at

certain CO concentrations in the liquid phase the three PPh_3 ligands could all be displaced by CO, resulting in lower regioselectivities.[147, 170]

The effects of H_2 and CO concentrations on substrate conversions and product selectivities for olefin hydroformylation have been studied in various solvent media, including organic liquids,[147] ionic liquids,[85] $scCO_2$[103] and gas-expanded solvents[13-14]. In general, higher H_2 concentrations and lower CO concentrations in the reaction phase favor higher rates and linear aldehyde selectivity.

Table 3-6 Propylene hydroformylation with Rh/ TPP catalysts in toluene and propane-expanded toluene (PXL) at different H_2/CO ratios

Entry#	H_2/CO	Solvent	$p_{propylene}$, MPa	$p_{propane}$, MPa	V/V$_0$	TOF, min^{-1}	*n/i*	*n*-aldehyde selectivity, %
1	1.0	Toluene	0.60	-	1.1	26.3	2.51	71.5
2	1.5	Toluene	0.60	-	1.1	27.2	3.53	77.9
3	2.0	Toluene	0.60	-	1.1	27.8	4.23	80.9
4	1.0	PXL	0.70	0.40	1.4	25.4	3.12	75.7
5	1.5	PXL	0.70	0.40	1.4	26.9	3.82	79.3
6	2.0	PXL	0.70	0.40	1.4	27.9	4.52	81.9

[Rh] = 2.21mmol/L; Molar [P/Rh] = 32; reaction time: 10 min; T = 70 ℃; psyngas = 0.60 MPa.

Table 3-8 presents the effect of H_2/CO mole ratio in the feed on Rh-catalyzed propylene hydroformylation in neat and propane-expanded toluene. Higher H_2/CO ratios significantly increase the *n/i* ratio in both the neat solvent (entries 1-3, Table 3-8) and PXLs (entries 4-6, Table 3-8). At identical H_2/CO ratio in the feed, the *n/i* ratio in PXLs is more compared to toluene, which is attributed to the higher H_2/CO ratio in the PXL phase. While the TOFs increase slightly with H_2/CO ratio in the case of the neat solvent, there is a ~10 % increase in the case of PXLs (entries 4-6, Table 3-8). This is consistent with the higher H_2/CO ratios in PXLs. It must be noted that higher H_2/CO ratios tend to promote hydrogenation reaction. Approximately 15 mole % of propane

is formed at a H_2/CO ratio of 2, which is not observed at lower H_2/CO ratios in either neat toluene or PXLs.

3.3.3.4 Effect of solvent replacement with propane

Propylene hydroformylation was performed at 70 ℃ with Rh/TPP complexes in PXLs with identical initial propylene concentrations in the PXL phase. This is achieved by varying the volumetric expansion ratios and relative partial pressures of propane and propylene based on modeling results. The propane concentration in the propylene feed is varied from 0% to 37 mol %. The corresponding increase in the V/V_0 ratio ranges from 1.1 to 1.9.

Table 3-7 Propylene hydroformylation with Rh/ TPP catalysts with different propane and propylene replacement

Entry #	Solvent	p_{total}, MPa	$p_{propylene}$, MPa	$p_{propane}$, MPa	V/V_0	TOF, min^{-1}	*n/i*	*n*-aldehyde selectivity, %
1	Toluene	0.60	0.60	-	1.1	26.3	2.51	71.51
2	PXL	1.10	0.70	0.40	1.4	25.4	3.12	75.73
3	PXL	1.30	0.85	0.45	1.7	24.8	3.43	77.43
4	PXL	1.50	0.95	0.55	1.9	23.3	3.62	78.35
5	Toluene	1.10	1.10	-	1.3	34.5	2.63	72.45
6	Toluene	1.30	1.30	-	1.5	45.3	2.92	74.45
7	Toluene	1.50	1.50	-	1.7	52.8	3.20	76.47

[Rh] = 2.21mmol/L in either toluene or PXL; Molar [P/Rh] = 32; reaction time = 10 min; T = 70 ℃; p_{syngas} = 0.60 MPa; molar [H_2/CO] in feed = 1.

As seen in Table 3-7, comparable TOF and higher *n/i* ratio were achieved in the PXL media. The *n/i* ratio increased by 44% as the volumetric expansion ratio (V/V_o) increases from 1.1 to 1.9 (entries 1-4, Table 3-7). The volumetric expansion may be viewed as solvent replacement by the expansion gas. Thus, at the highest expansion ratio (V/V_o = 1.9), toluene replacement by propane in the expanded reaction mixture is approximately 48%. When toluene is expanded by pure propylene alone, the TOF increased from 26.32 min^{-1} at V/V_o = 1 (entry 1, Table 7) to 52.81 min^{-1} at V/V_o = 1.7 (entry 7, Table 3-7). However, the *n/i* ratio increase from 2.51 to 3.2 is approximately 28%. In contrast, the corresponding *n/i* increase in the PXL phase (entries 1 and 4,

Table 3-7) is 44%. This is attributed to the generally higher H_2/CO ratio in the PXL phase (see Table 3-2 & Table 3-3). Similar trends were also observed for cobalt-catalyzed hydroformylation in butane-expanded liquids.[171]

3.3.3.5 Effect of organic solvents

Solvents have a significant effect on the hydroformylation of olefins. The general roles of conventional solvents and gas-expanded liquids in multiphase catalytic processes have been recently reviewed.[118] Conventional hydroformylation reactions usually employ a high boiling mixture of aldehyde condensation products (dimers, trimers and tetramers) as the solvent.[172-173] A solvent used in industrial propylene hydroformylation processes is NX-795 which is composed of butyraldehyde oligomers. Hence, in addition to toluene, we also investigated the reaction in NX-795 and butanol. Table 3-8 summarizes the results of propylene hydroformylation performed in neat solvents as well as PXLs. For the reaction in neat organic solvents, the highest TOF is observed in toluene while butanol shows the highest n/i ratio (Entries 1-3, Table 3-8). In PXL media, while the TOFs were not significantly altered, the n/i ratio increased for all solvents, with propane-expanded butanol showing the largest increase of ~45% (entries 4-6, Table 3-8).

Table 3-8 Propylene hydroformylation with Rh/ TPP catalysts in organic solvents and propane-expanded solvents (PXL)

Entry #	Solvent	$p_{propylene}$, MPa	$p_{propane}$, MPa	V/V_0	TOF, min^{-1}	*n/i*	*n*-aldehyde selectivity, %
1	Toluene	0.60	-	1.1	26.3	2.51	71.51
2	NX-795	0.60	-	1.1	23.2	3.78	79.08
3	Butanol	0.60	-	1.1	20.5	4.18	80.69
4	PXL-Toluene	0.70	0.40	1.4	25.4	3.12	75.73
5	PXL-NX-795	1.00	0.60	1.4	24.7	5.08	83.55
6	PXL-Butanol	0.90	0.50	1.4	21.9	6.07	85.86

[Rh] = 2.21mmol/L; Molar [P/Rh] = 32; reaction time: 10 min; T = 70 °C; p_{syngas} = 0.60 MPa; molar [H_2/CO] = 1

3.4 Conclusion

The homogeneous hydroformylation of propylene in propane- and propylene- expanded solvent media with Rh-based catalyst complexes was investigated. Volumetric expansion studies show that both propane and propylene can significantly expand typical hydroformylation solvents, by approximately 2-fold at a propane pressure of 1.5 MPa and 70 °C. The H_2/CO ratio in the reaction media may be tuned with either propane or propylene addition at fixed syngas feed composition and partial pressure, with the ratio being higher in propane-expanded liquids or PXLs. For Rh-catalyzed propylene hydroformylation using bidentate BiPhePhos ligand, the *n/i* ratio and TOF are comparable with those observed during conventional processes in neat solvent. In contrast, clear increases in *n/i* ratio are observed during Rh-catalyzed propylene hydroformylation in PXL media with monophosphine ligands (triphenylphosphine, cyclohexyldiphenylphosphine, triphenylphosphate). However, the TOFs and regioselectivity are much lower than those obtained with the Rh/BiPhePhos complex. Our results show clearly that refinery grade propylene (rather than polymer-grade propylene) can be used in industrial hydroformylation processes involving Rh/BiphePhos complexes without any adverse effects on TOF or product selectivity. The selective conversion of propylene during hydroformylation produces an enriched propane stream thus providing effective, less energy-intensive separation of propane and propylene.

Chapter 4: Comparative economic and environmental impact analysis of PXL-based hydroformylation, benchmarked with conventional processes

4.1 Introduction

Butyraldehyde is the precursor for a variety of industrial chemicals including 2-ethylhexanol (2EH), one of the most widely used plasticiser alcohols, and butanols, which are used to manufacture pharmaceuticals, polymers, and pyroxylin plastics. The hydroformylation reaction, also known as oxo synthesis, is the dominant industrial technology for aldehyde production. It entails the addition of synthesis gas ("syngas"), a mixture of CO and H_2, to olefins in the presence of catalysts.[16, 169, 172] The global market in 2015 was ~4.4 billion and is expected to reach ~5.7 billion in 2022, with annual growth rate of ~3.9% between 2016-2022.[18]

The industrial hydroformylation catalysts are based on cobalt and rhodium complexes exclusively. Compared to Rh-based processes (T = 85–130 ℃, P = 1.5–5.0 MPa), harsher conditions (T = 140–200 ◦C, P = 50–300 bars) are required to activate the cobalt and intensify the reaction. The Rh-catalyzed hydroformylation is mainly used for propylene hydroformylation reaction. There are two types of commercial processes for propylene hydroformylation: the homogeneous low-pressure oxo process and the aqueous biphasic oxo process.[174-176]

The aqueous biphasic oxo process (also known as Ruhrchemie/Rhone–Poulenc process) was commercially used for hydroformylation in 1984 with water-soluble TPPTS as the ligand to overcome the expensive separation step involving catalyst and the reaction products. In the biphasic process, the active catalyst remains dissolved in the aqueous phase where the reaction occurs, while the reactants and products, which are organic and relatively nonpolar, separate into a second phase which is easily separated from the catalyst solution. However, the activity of water-

soluble catalyst is significantly lower as compared with the standard homogeneous Rh/TPP catalyst.[31-32]

The commercial plant employing homogeneous low-pressure oxo process using TPP modified Rh catalysts to produce butyraldehydes was successfully started up in 1976 at Ponce, Puerto Rico, with a capacity of 136,000 tonnes per year.[27] In the forty years or so since it was first introduced, the homogeneous low-pressure oxo process has maintained its position as the world's foremost oxo process, having undergone much improvement and refinement. For example, instead of using excess TPP as ligands, today several low-pressure oxo plants produce butyraldehyde using a more advanced bisphosphite-modified rhodium catalyst with higher activity and regioselectivity.[177-178] However, for this process, polymer-grade propylene (up to 99.5% purity) is generally used as feedstock.[179-180] Even though polymer-grade propylene costs approximately 50% more than refinery-grade propylene (60-70% purity), its use makes sense if it is readily available on site from feedstock that is specifically made for manufacturing polypropylene with a much higher capacity. However, if propylene is made on site from a propane dehydrogenation unit, it may be more economical to use the cheaper propane + propylene mixture as feedstock.

In Chapter 3, we demonstrated that refinery-grade propane/propylene mixtures can be used directly for propylene hydroformylation without the need for purification to obtain polymer-grade propylene. The mixed propylene/propane feed also provides reaction benefits by volumetrically expanding the reaction mixture to yield gas-expanded liquids (GXLs) with tunable physicochemical properties. Unlike conventional reaction media, the H_2/CO ratio in GXL media can be enhanced by simply increasing the partial pressure of propane.[164] For rhodium/triphenylphosphine catalyzed propylene hydroformylation performed between 70 - 100 °C and pressures up to 2.0 MPa, the *n/i* aldehyde ratio is increased by up to 45% in propane-

expanded liquids (PXLs). In addition, the PXL-based hydroformylation process also has potential energy savings and economic/environmental benefits since the refinery-grade propylene feedstock (55% propylene + 45% propane) costs up to 50% less than polymer-grade propylene.[181]

This chapter provides detailed economic and environmental impact analyses of the integrated propane dehydrogenation and propylene hydroformylation process (termed the CEBC-PXL process) and compares the results with the conventional process that employs distillation to separate the propane/propylene mixtures to obtain polymer-grade propylene. The quantitative analyses identify key operating factors that affect the economics and environmental impacts, and provide valuable guidance for process design and optimization. Analogous comparative analyses have been previously conducted for ethylene and propylene epoxidation,[182] long-chain olefin hydroformylation,[8] terephthalic acid production via spray process,[183] and solid-acid catalyst alkylation processes[184] developed at the CEBC.

4.2 Methodology

The methodological framework for economic and environmental impact assessment are depicted in Figure 4-1. Three tasks are involved in this methodology: (1) plant-scale simulations of the integrated propane dehydrogenation (PDH) and propylene hydroformylation (PHF) in conventional process with propane/propylene separation by distillation and CEBC-PXL process by Aspen Plus® software, (2) comparative economic analysis by estimating capital investment and total production cost for each process, (3) comparative environmental impacts analysis by Economic Input-Output Life Cycle Assessment (EIO-LCA).

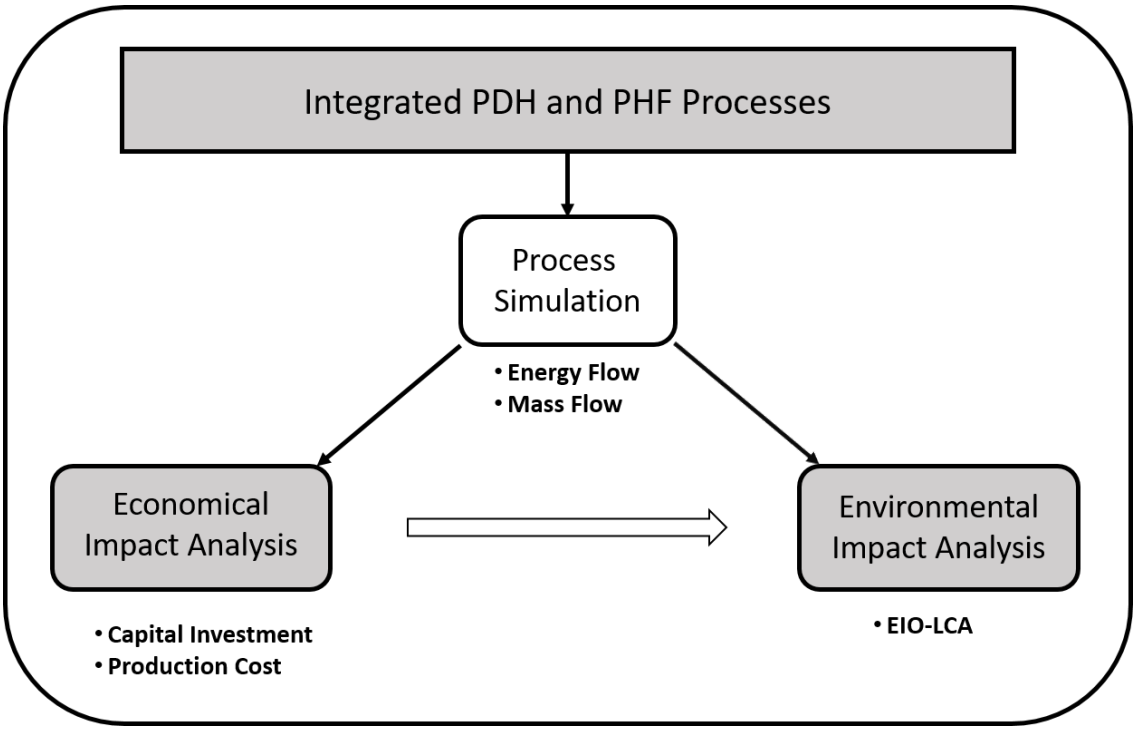

Figure 4-1 Methodological framework for economic and environmental impact assessments of the integrated propane dehydrogenation (PDH) and propylene hydroformylation (PHF)

4.2.1 Process descriptions

Schematics of the integrated PDH and PHF processes under consideration are shown in Figure 4-2.The butyraldehyde is produced through an integrated propane dehydrogenation and propylene hydroformylation process with pure propane as the feedstock. The propane dehydrogenation process is based on CB&I's CATOFIN® PDH process which converts propane to propylene on Cr-based catalysts.[185] The feed stream to the PDH unit is vaporized by heat exchange with various process streams and then raised to reaction temperature in the charge heater. The PDH reactor effluent is routed through a feed-effluent exchanger and trim cooler to the compressor. The compressor discharge is cooled and routed to the low-temperature recovery section to reject light ends which are hydrogen rich.[186] In the conventional process, the C_3 liquid mixture from the condenser is fed to the distillation column to obtain high purity propylene. The

separated (unreacted) propane is recycled back to the PDH reactor. In the CEBC-PXL process, the liquid C_3 stream is routed directly to hydroformylation units without further purification.

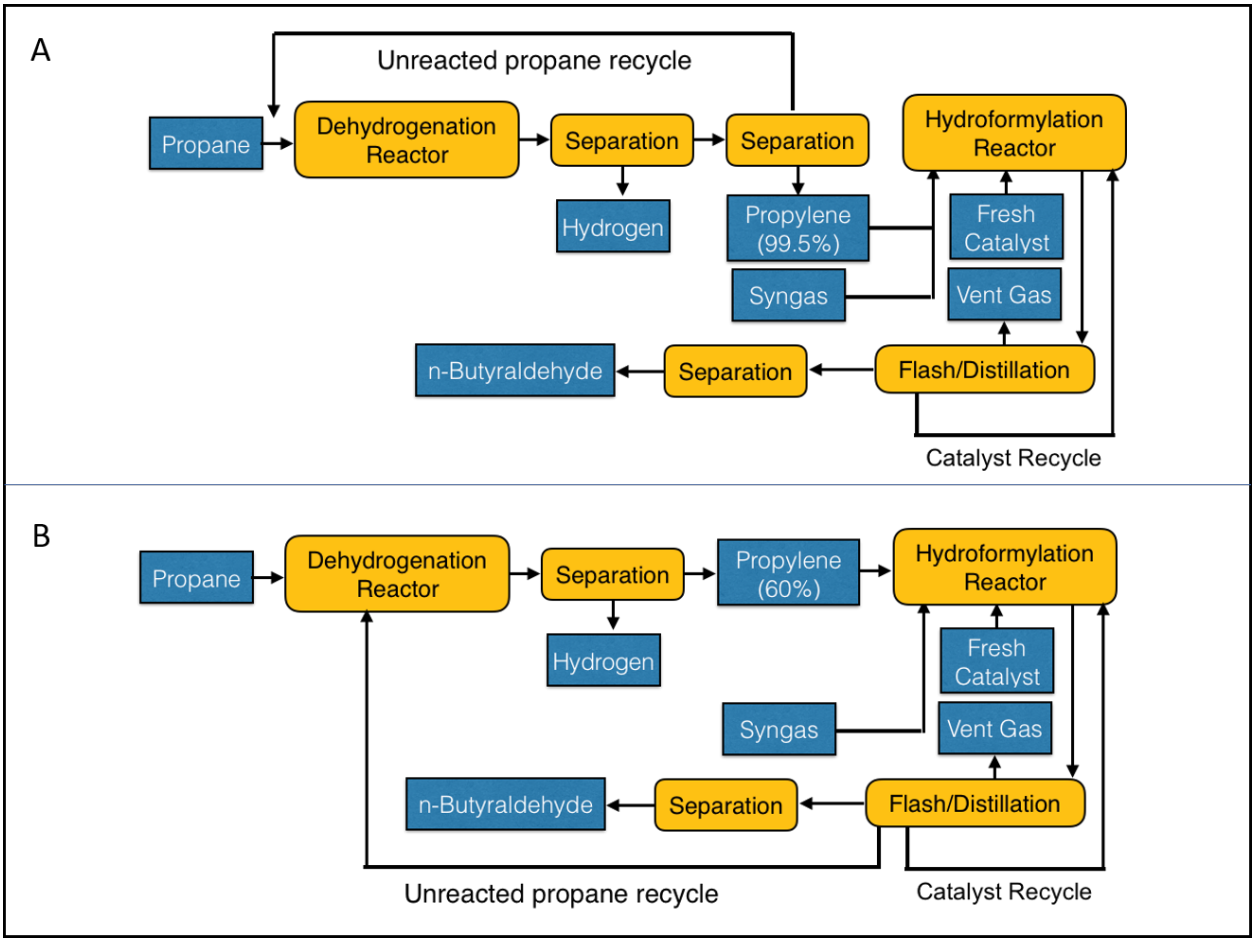

Figure 4-2 The schematic of integrated propane dehydrogenation and propylene hydroformylation processes. (A) conventional process with propane/propylene separation by distillation, (B) PXL process

The conventional process is modified based on Johnson Matthey's SELECTOR 30® technology utilizing proprietary NORMAXTM™ catalyst, an organophosphite ligand available from Dow.[177] In this process, polymer-grade (99.5%) propylene and syngas are introduced into the reactor in the presence of a homogeneous bisphosphite modified rhodium catalyst at moderate temperatures (85-95 °C) and pressures (1.5-2.0 MPa). More than 95% of the propylene feed is converted into butyraldehyde in a single pass with $n/i > 30$. The reactor effluent with unreacted

syngas and propylene are removed during the product vaporization process and burned as fuel. The crude product butyraldehyde is obtained after separation.[28, 187-188] In the PXL process, the mixed propylene/propane effluent stream from the PDH reactor is used as feedstock without further purification under otherwise identical operating conditions as the conventional process. Following reaction and separation, the unreacted propane is recycled back to the PDH reactor.

4.2.2 Process Simulations

Aspen plus® V8.8 software was employed to perform simulations of the integrated PDH and PHF processes. The annual butyraldehyde capacity for the plant scale simulations was set at 300,000 tons/year at a 0.9 on-stream factor (i.e., 328 on-stream days). The data for simulating the CATOFIN® PDH and conventional PHF process were obtained from literature and patents.[185-186] The data for simulating the PXL process were obtained from laboratory-scale experiments. To simplify the process for better convergence, the mass and energy balances for PDH catalyst regeneration are calculated separately. The operating parameters are summarized in Table 4-1. The UNIQUAC package present in Aspen® software was used to predict the relevant thermodynamic properties, while the Peng−Robinson equation of state was employed for phase equilibrium modelling. Although a mixture of different light alkanes is used as raw material in industrial propane dehydrogenation process, identical feeds (pure propane and syngas with equimolar H_2 and CO ratio) were used for all the processes described. The process flow diagrams developed for both the processes (Figure 4-3 and Figure 4-4), with various operating parameters/variables and product specifications as inputs, provide the relevant mass and energy flow rates associated with the process streams.

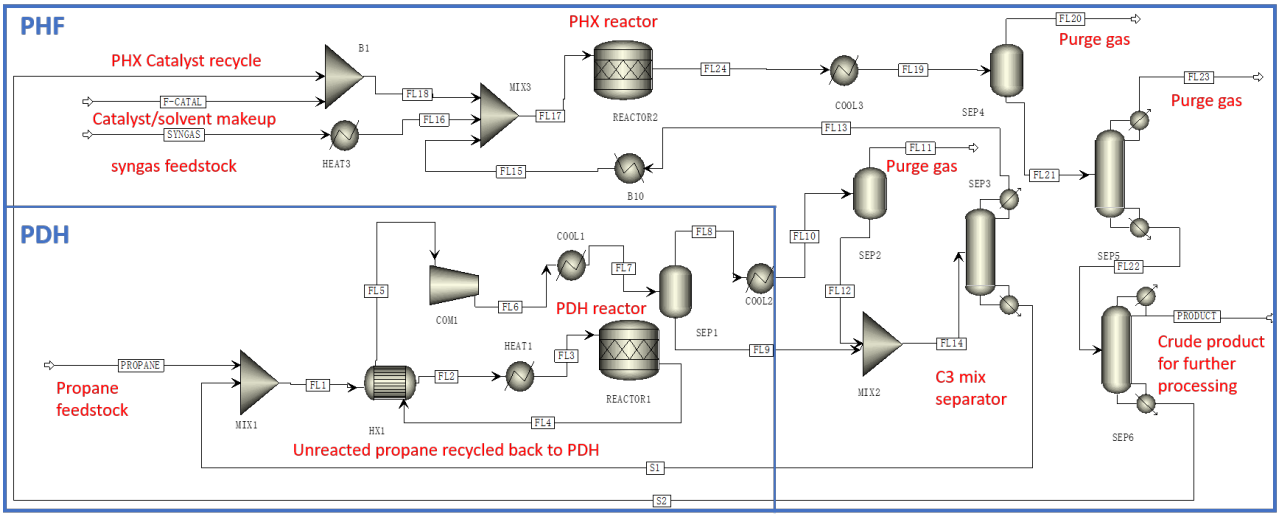

Figure 4-3 Process flow diagram of simulated conventional process

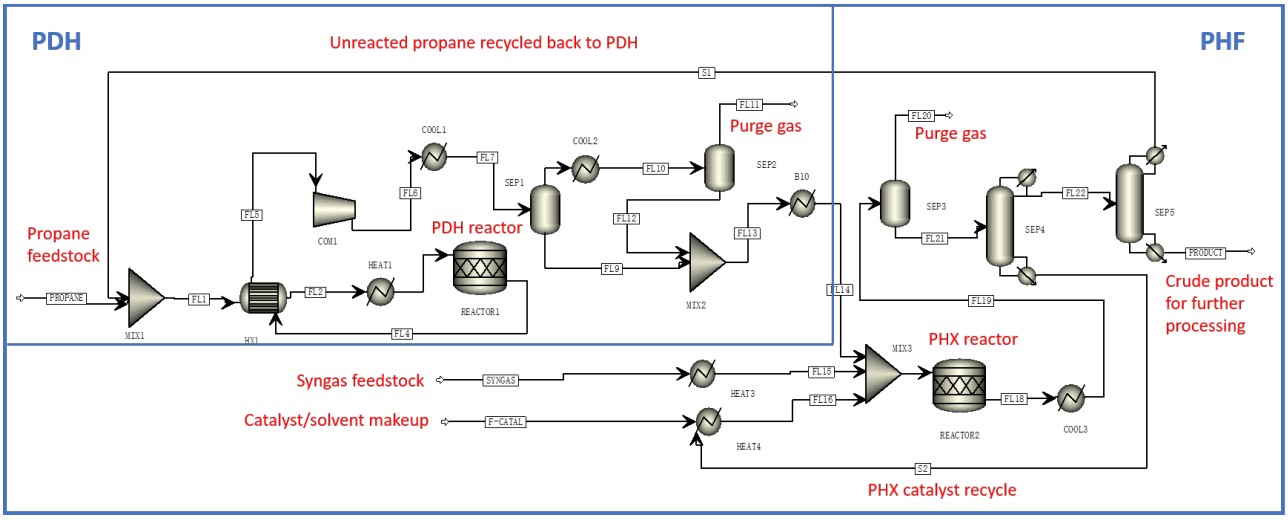

Figure 4-4 Process flow diagram of simulated PXL process

These mass and energy flow rates along with the stream composition information are used in process equipment design and sizing and to perform the economic and environmental impact analyses.

Table 4-1 Key operating parameters for process simulations

Butyraldehyde capacity, kiloton /year	300	
Feed	100% propane	
PDH Reactor (identical for both conventional and CEBC-PXL processes)		
Cr_2O_3/Al_2O_3, ton	4/25	
Operation Temperature / °C	600	
Operation Pressure / MPa	0.05	
Conversion % (propane)	60	
Chemo-Selectivity, %	98	
Catalyst regeneration temperature / °C	690	
Catalyst regeneration pressure / MPa	0.2	
PHF Reactor		
	Conventional process	CEBC-PXL Process
Feed	Propylene (99.5%) Propane (0.5%)	Propylene (60%) Propane (40%)
Rhodium, kg	24	24
Ligands, ton	0.75	0.75
Operation Temperature / °C	90	90
Operation Pressure / MPa	1.5	2.5
Conversion % (propylene)	95	95
Chemo-selectivity, %	99	100
Regio-selectivity, %	97	96

4.2.3 Economic analysis

Comparative economic analyses are performed by estimating total capital investment (TCI) and total production cost (TPC) for each process. The consumption of utilities and chemicals was estimated from the process simulations. The capital investment is estimated following the percentage of purchased-equipment cost method. The purchased equipment costs are estimated based on attributes such as equipment size, the material of construction, weight or surface area.[189] Other direct and indirect costs are estimated by multiplying the purchased equipment cost by a weighting factor. The costs associated with utilities, raw materials and labor are obtained from current reference sources.[190-192] All the costs are adjusted to February 2017 figures using the

Chemical Engineering Plant Cost Index (CEPCI).[193] Further, the impact of single-pass propylene conversion in PXL process on the operating costs is analyzed through a sensitivity analysis.

4.2.4 Life Cycle Analysis

The environmental impacts of the conventional and PXL process are identified by economic input−output life cycle assessment (EIO-LCA) method.[194-196] It is a life cycle assessment tool that estimates the material and energy resources required for, and associated environmental emissions resulting from, activities in our economy.[197-198] The use of input-output models is advantageous since they take into account the entire supply chain for a product (including indirect suppliers), allowing for tracing of the full range of inputs to a process, and consequently providing a complete system boundary.[199]

In this work, the online EIO-LCA tool developed by Green Design Institute at Carnegie Mellon University is used to perform the analysis.[200]. The greenhouse gas emissions, air pollutants emission and toxics release associated with both the conventional and PXL processes are calculated and compared.

4.3 Results and discussion

4.3.1 Economic analysis

4.3.1.1 Total capital investment (TCI)

Figure 4-5 shows the purchased costs of major equipment in both processes. Table 4-2 compares the capital investments for both conventional and PXL processes. Details of the contribution of each component to the TCI is listed in Appendix I.

Table 4-2 Comparison of capital costs for both conventional and PXL processes

	Conventional process ($ million)	PXL process ($ million)
Purchased equipment costs	49.6	38.3
Direct installation costs (1.3 of purchased cost)	64.4	49.8
Direct costs(others) (0.55 of purchased cost)	27.3	21.1
Total direct costs	141.3	109.1
Indirect costs (0.7 of direct cost)	98.9	76.4
Fixed capital investment (FCI) (direct + indirect cost)	240.1	185.5
Working capital (10% of FCI)	24.0	18.5
Total capital investment (FCI + working capital)	264.1	204.0

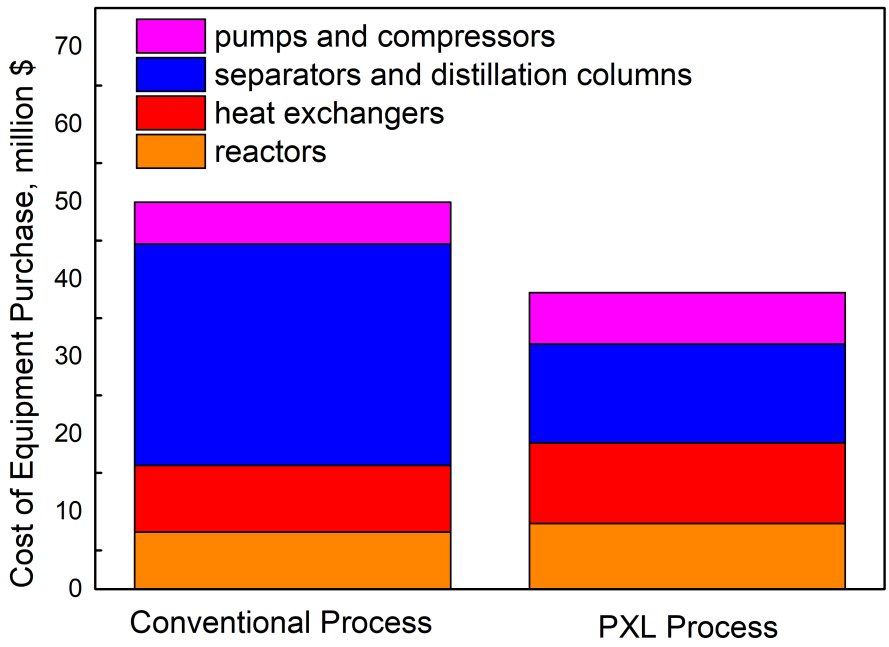

Figure 4-5 Comparison of purchased equipment costs for conventional and PXL processes.

The estimated purchased equipment cost associated with the conventional process is 30% greater than the PXL process. Because of the use of relatively large propane/propylene distillation columns (diameter = 10m, height = 80 m, number = 2), the separation equipment contributes to

more than 50% of the total equipment cost in the conventional process and is three times greater than that in the PXL process.

4.3.1.2 Total production cost

The annual total production cost (TPC), and the contributors are shown in Table 4-3.

Table 4-3 Itemized annual total production cost conventional and PXL Processes*

	Conventional process ($ million)	PXL process ($ million)
Raw chemicals	84.5	84.4
Utilities	5.5	4.3
Labor	1.1	1.1
Other production costs	17.9	13.8
Fixed charges	5.0	3.9
Plant overhead cost	2.1	1.8
General expense	53.9	18.5
Total annual production cost	140.1	127.7

*Raw material and utility unit costs are provided in appendix J

The details of each production category are listed in Appendix K. The raw material cost is identical and contributes more than 60% of the total cost of both processes. The utility costs for both processes and their components are shown in Figure 4-6. High-pressure (HP) steam and electricity account for a major part of the utility costs. Note that the estimated costs of HP steam in the PXL process (without the need for C_3 distillation columns) is ~50% less than the conventional process, resulting in a ~22% cost savings in utility costs.

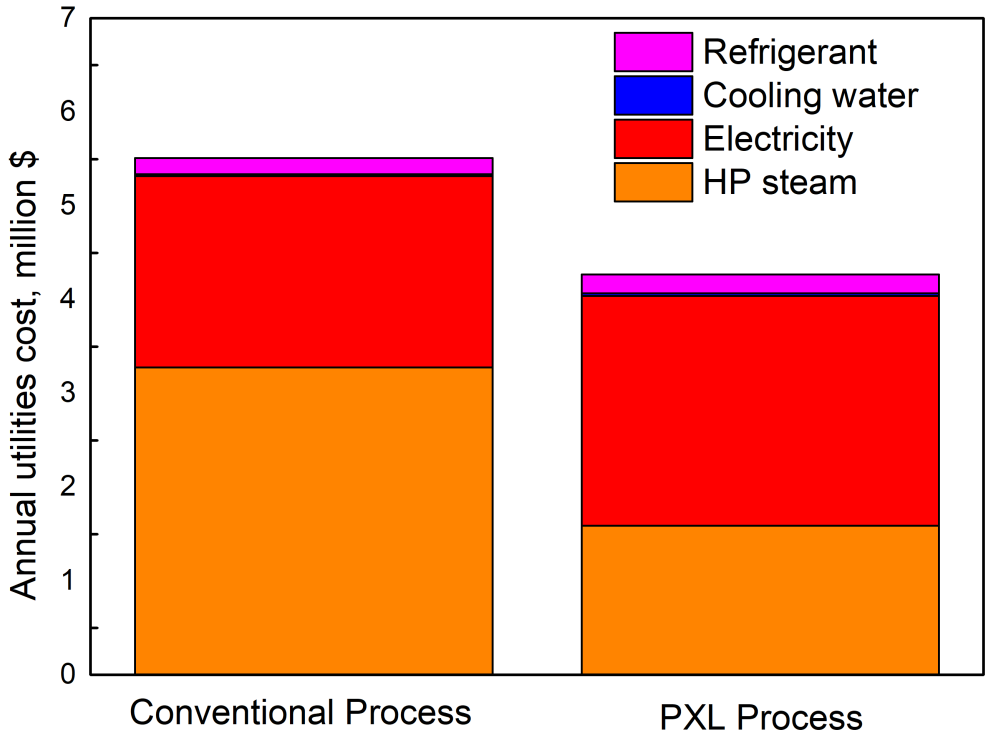

Figure 4-6 Comparison of annual utility costs for conventional and PXL processes

4.3.1.3 Effect of single-pass propylene conversion on TPC of the PXL Process

A sensitivity analysis on TPC was performed with various single-pass propylene conversion in PXL process at fixed chemoselectivity. As expected, higher single-pass conversions increase cost savings (Figure 4-7) as less of the unreacted propylene is recycled back to the PDH reactor resulting in decreased materials consumption and operating costs. Note that the TPC of the PXL process is lower than the conventional process even when the single-pass propylene conversion is ~89%.

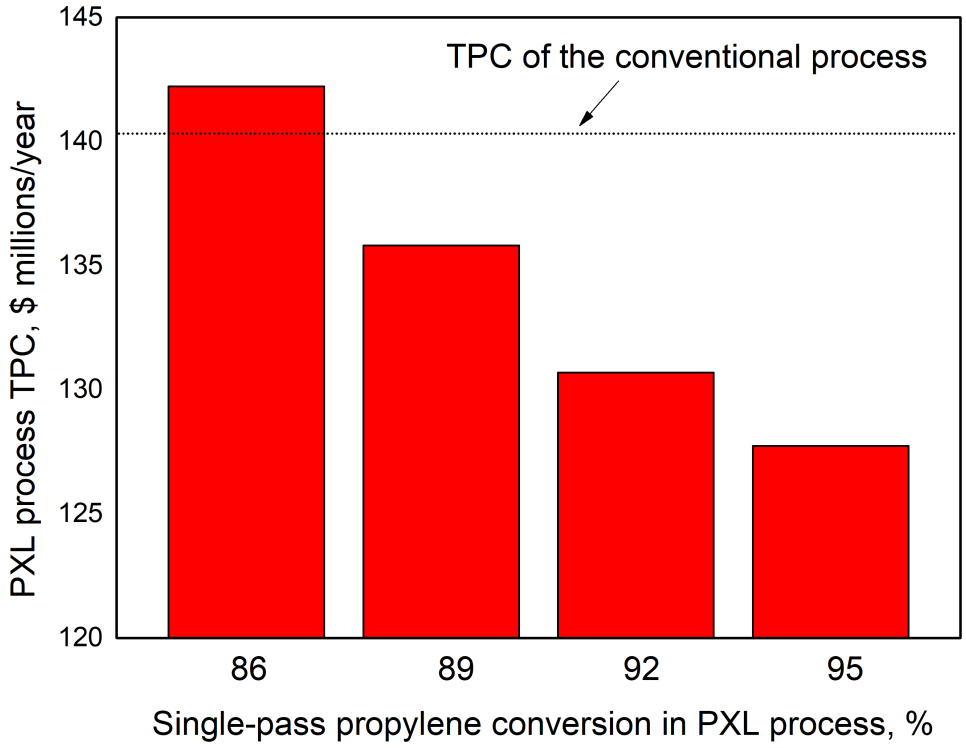

Figure 4-7 Single-pass HXF conversion sensitivity analysis in PXL process

4.3.2 Environmental impact analysis

The estimates of greenhouse gas emissions, air pollutants emission and toxic release associated the capital investments are summarized in Figure 4-8 to Figure 4-10. The details for each environmental impact category are listed in Table 4-4 to Table 4-6. The EIO sectors used for assessing the major categories of the capital and production costs are detailed in Appendix L. The category of greenhouse gas emissions is composed of CO_2, methane, N_2O and high global warming potentials (GWP) gases such as hydrofluorocarbon and perfluorocarbon. The total CO_2 equivalent emissions (i.e., CO_2 emissions from fossil fuel combustion sources and those from sources other than fossil fuel combustion) from the conventional process is ~ 20% greater compared to PXL process.

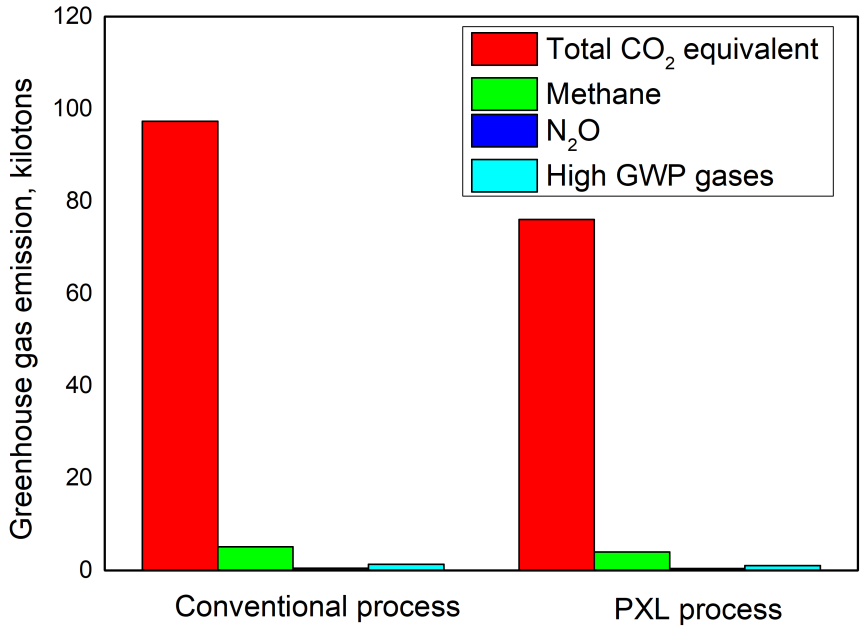

Figure 4-8 Comparison of EIO-LCA estimated greenhouse gas emission with major capital investment items for both processes

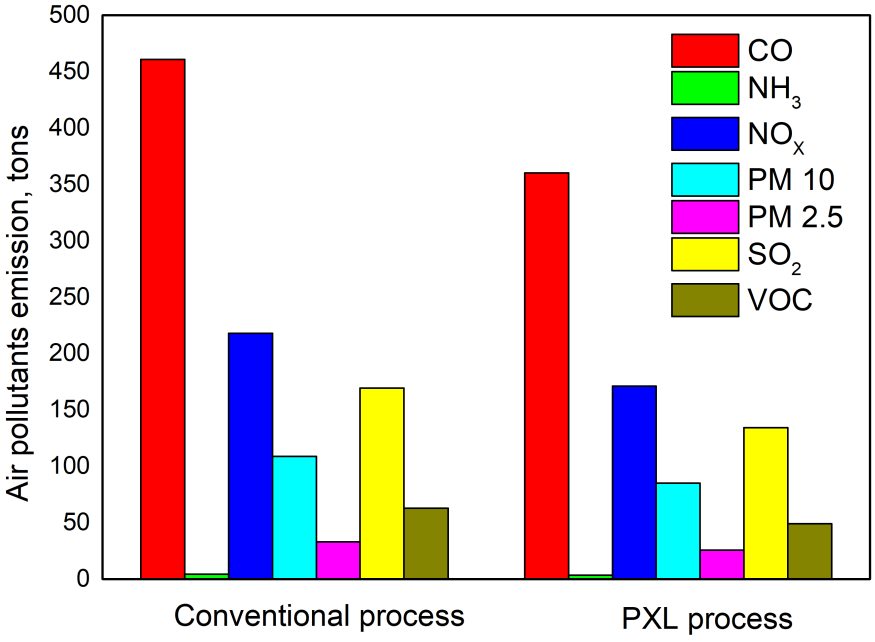

Figure 4-9 Comparison of EIO-LCA estimated air pollutants emission with major capital investment items for both processes (PM 10 means particulate matter 10 μm or less in diameter)

The air pollutants are attributed to CO, NH_3, NO_x, PM 10 (particulate matter 10 μm or less in diameter), PM 2.5 (particulate matter 2.5 μm or less in diameter), SO_2 and VOC emissions. The CO emission is the primary source of air contamination for both processes. The potential release of toxic to air, surface water, groundwater, land and off-site transfer are shown in Figure 4-10. The most significant impacts arise from the manufacturing of the metal tanks (reactor, distillation columns) and piping. Compared to the conventional process, the adverse environmental impacts associated with the PXL process are significantly lower which is a reflection of its much lower consumption of material and energy.

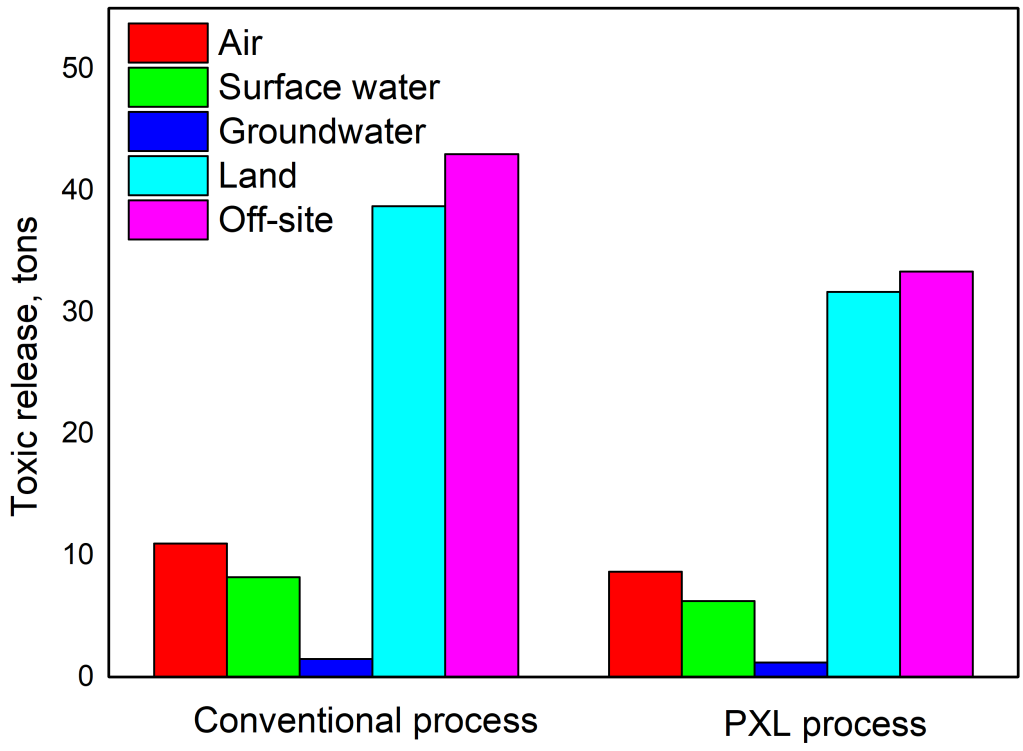

Figure 4-10 Comparison of EIO-LCA estimated toxic release in conventional and PXL processes

Table 4-4 EIO-LCA estimates of greenhouse gas emissions associated with major capital investment items

Item	Conventional process, metric tons				PXL process, metric tons			
	Total CO_2 equivalent	Methane	N_2O	High GWP gases	Total CO_2 equivalent	Methane	N_2O	High-GWP gases
Reactors	5100.0	278.0	24.7	87.8	5860.0	320.0	28.3	101.0
Separators and distillation columns	19700.0	1080.0	95.4	339.0	10900.0	595.0	52.7	187.0
Heat exchangers	4920.0	277.0	28.6	111.0	5960.0	336.0	34.6	135.0
Pump and compressors	2220.0	130.0	18.0	60.9	2710.0	159.0	22.0	74.4
Equipment delivery	5040.0	240.0	9.7	10.8	3920.0	187.0	7.5	8.4
Piping	43900.0	2190.0	128.0	593.0	33900.0	1690.0	99.1	459.0
Concrete foundations	4490.0	158.0	19.2	27.3	3490.0	123.0	14.9	21.2
Electrical service	560.0	45.8	11.8	8.2	435.0	35.6	9.2	6.3
Building constructions	8980.0	522.0	141.0	81.5	6980.0	406.0	109.0	63.3
Engineering cost	1160.0	107.0	41.0	28.1	902.0	83.6	31.9	21.8
Research and development	1260.0	99.4	21.5	14.3	1040.0	82.0	17.7	11.8
Total	97330.0	5127.2	538.9	1361.9	76097.0	4017.2	426.9	1089.2

Table 4-5 EIO-LCA estimates of air pollutant emissions associated with major capital investment items

Item	Conventional process, metric tons							PXL process, metric tons						
	CO	NH_3	NO_x	PM 10	PM 2.5	SO_2	VOC	CO	NH_3	NO_x	PM 10	PM 2.5	SO_2	VOC
Reactors	22.8	0.2	9.9	2.7	1.4	9.9	3.8	26.2	0.2	11.3	3.1	1.6	11.4	4.3
Separators and distillation columns	88.1	0.8	38.2	10.6	5.4	38.3	14.5	48.7	0.5	21.1	5.8	3.0	21.1	8.0
Heat exchangers	21.6	0.2	10.0	2.8	1.4	11.6	3.3	26.2	0.3	12.1	3.4	1.7	14.1	4.0
Pump and compressors	9.8	0.1	5.2	1.8	0.8	6.1	2.0	12.0	0.2	6.4	2.1	1.0	7.4	2.4
Equipment delivery	36.2	0.2	39.1	10.2	2.0	3.3	5.2	28.2	0.1	30.4	7.9	1.6	2.5	4.1
Piping	217.0	1.4	73.9	19.6	11.1	68.8	17.1	168.0	1.1	57.2	15.2	8.6	53.2	13.2
Concrete foundations	12.3	0.2	12.0	4.0	1.5	10.8	1.7	9.6	0.1	9.4	3.2	1.2	8.4	1.3
Electrical service	2.1	0.1	1.6	0.5	0.2	1.5	0.6	1.6	0.1	1.2	0.4	0.1	1.2	0.4
Building constructions	41.8	1.0	22.3	54.2	8.4	13.2	12.6	32.5	0.7	17.3	42.1	6.5	10.2	9.8
Engineering cost	5.0	0.2	2.9	1.4	0.5	2.8	1.4	3.9	0.1	2.2	1.1	0.4	2.2	1.1
Research and development	4.2	0.2	3.0	1.1	0.4	3.3	0.9	3.5	0.2	2.5	0.9	0.3	2.7	0.7
Total	461.0	4.6	218.0	108.9	33.0	169.4	63.0	360.4	3.6	171.1	85.3	25.9	134.3	49.3

Table 4-6 EIO-LCA estimates of toxic release with major capital investment items

Item	Conventional process, kg					PXL process, metric kg				
	Total Air	Surface Water	Ground Water	Land	Off-site	Total Air	Surface Water	Ground Water	Land	Off-site
Reactors	733	573	70	1500	2340	841	658	80	1720	2690
Separators and distillation columns	2830	2220	269	5790	9050	1560	1220	149	3200	5000
Heat exchangers	679	305	126	4490	1920	824	369	153	5450	2320
Pump and compressors	482	98	56	1020	727	589	120	69	1250	889
Equipment delivery	135	25	20	186	74	105	19	16	145	58
Piping	4080	4660	510	22400	27600	3160	3610	394	17300	21400
Concrete foundations	458	82	42	608	436	356	64	33	473	339
Electrical service	106	13	16	119	35	82	10	13	93	27
Building constructions	864	137	139	1600	613	671	106	108	1240	476
Engineering cost	465	71	201	618	136	362	55	156	481	106
Research and development	149	20	24	409	78	123	17	20	338	65
Total	10981	8205	1473	38740	43010	8673	6249	1189	31690	33370

The comparisons of environmental impacts associated with the production of the raw materials and the products in the conventional and PXL processes are shown in Figure 4-11 - Figure 4-13. The quantitative estimates of each environmental impact category are listed in Table 4-7 - Table 4-9. Compared to the conventional process, there is no significant difference with CO_2 emission equivalents (primary contributor to greenhouse gas emissions category), SO_2 emission (primary contributor to air pollutants emission category) and toxic release to land (primary contributor to air toxic release) for PXL process. This is because the manufacture of the raw materials (propylene, syngas, and catalysts) is the primary contributor to all the environmental impact category and the raw material usage is identical for both processes.

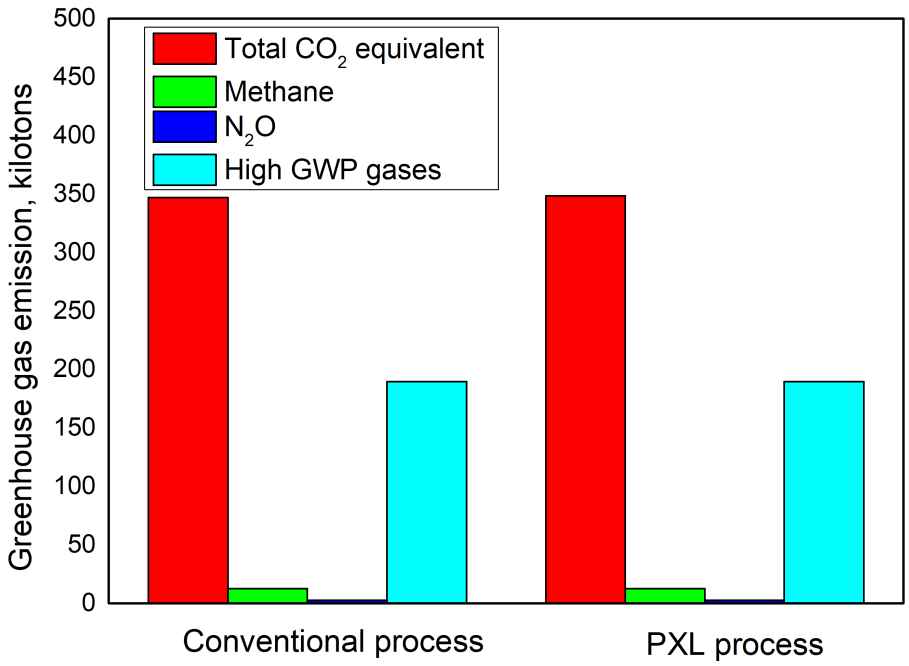

Figure 4-11 Comparison of EIO-LCA estimated greenhouse gas emissions associated with major production categories

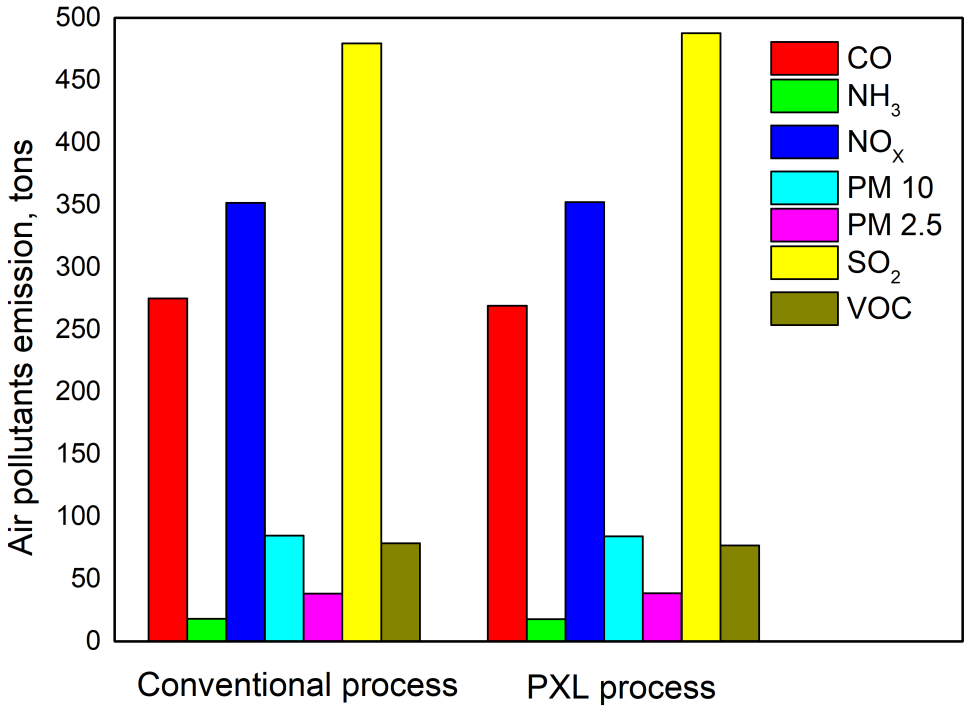

\

Figure 4-12 Comparison of EIO-LCA estimated air pollutant emissions associated with major production categories

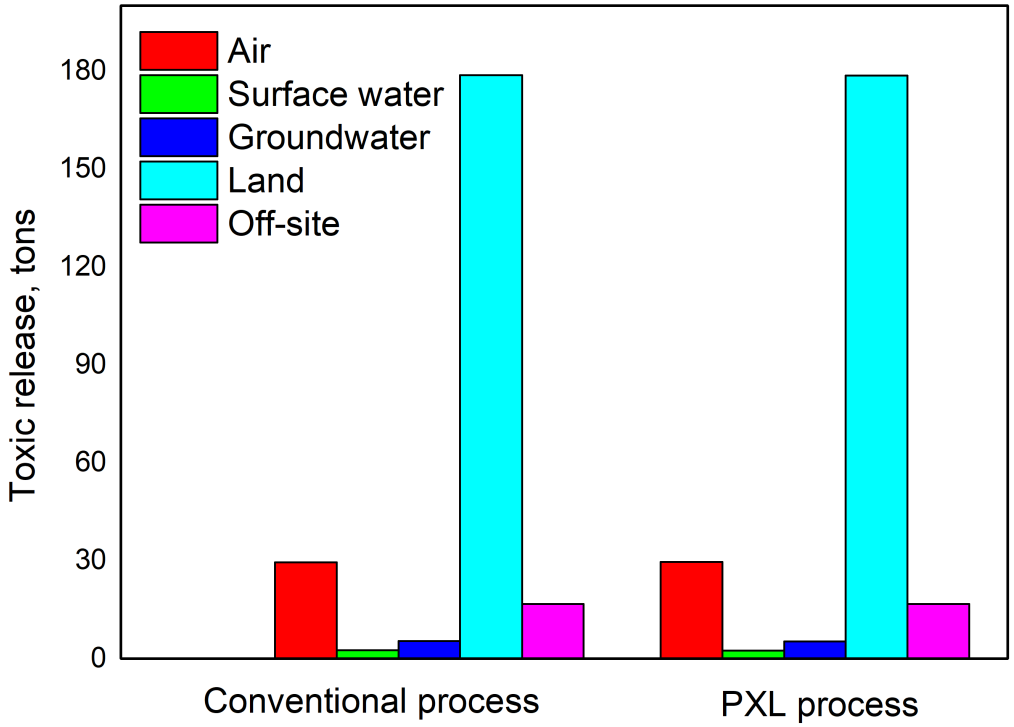

Figure 4-13 Comparison of EIO-LCA estimated toxic release associated with major production categories

Table 4-7 EIO-LCA estimates of greenhouse gas emission with major production categories

Item	Conventional process, metric tons				PXL process, metric tons			
	Total CO_2 equivalent	Methane	N_2O	High GWP gases	Total CO_2 equivalent	Methane	N_2O	High GWP gases
Propane	270000.0	9570.0	1990.0	158000.0	270000.0	9570.0	1990.0	158000.0
Syngas	49500.0	1750.0	365.0	29000.0	49500.0	1750.0	365.0	29000.0
Solvent	926.0	73.5	69.0	22.5	708.0	56.2	52.8	17.2
Catalysts	7760.0	220.0	23.5	2380.0	7760.0	220.0	23.5	2380.0
Electricity	14000.0	515.0	83.8	85.6	16800.0	618.0	101.0	103.0
Cooling water	17.8	6.0	1.0	0.1	35.6	12.1	2.0	0.2
Refrigerant	93.1	5.7	1.2	2.2	116.0	7.1	1.5	2.7
Direct labor	95.0	8.2	1.4	0.8	95.0	8.2	1.4	0.8
Maintenance	601.0	51.7	8.0	14.7	464.0	39.9	6.2	11.4
Engineering cost	2190.0	167.0	27.6	21.1	1690.0	129.0	21.3	16.3
Research and development	1970.0	170.0	57.7	19.2	1520.0	131.0	44.5	14.8
Total	347152.9	12537.1	2628.3	189546.2	348688.6	12541.5	2609.2	189546.4

Table 4-8 EIO-LCA estimates of air pollutants emission with major production categories

Item	Conventional process, metric tons							PXL process, metric tons						
	CO	NH_3	NO_x	PM 10	PM 2.5	SO_2	VOC	CO	NH_3	NO_x	PM 10	PM 2.5	SO_2	VOC
Propane	165.0	13.3	244.0	57.5	25.9	287.0	56.4	165.0	13.3	244.0	57.5	25.9	287.0	56.4
Syngas	30.3	2.4	44.7	10.5	4.8	52.5	10.3	30.3	2.4	44.7	10.5	4.8	52.5	10.3
Solvent	2.1	0.2	1.9	0.7	0.3	1.8	1.0	1.6	0.2	1.5	0.6	0.2	1.4	0.7
Catalysts	40.7	1.1	13.8	5.9	2.6	71.5	2.4	40.7	1.1	13.8	5.9	2.6	71.5	2.4
Electricity	6.0	0.2	27.0	4.0	3.0	54.8	1.2	7.2	0.2	32.5	4.8	3.6	65.9	1.4
Cooling water	0.0	0.0	0.0	0.0	0.0	0.0	0.0	0.1	0.0	0.1	0.0	0.0	0.1	0.1
Refrigerant	0.4	0.0	0.2	0.1	0.0	0.2	0.2	0.5	0.0	0.3	0.1	0.0	0.3	0.3
Direct labor	0.4	0.0	0.3	0.1	0.0	0.2	0.1	0.4	0.0	0.3	0.1	0.0	0.2	0.1
Maintenance	6.2	0.1	1.6	0.4	0.2	1.6	0.6	4.8	0.0	1.2	0.3	0.1	1.2	0.5
Engineering cost	13.0	0.2	12.1	3.3	0.9	5.0	4.7	10.0	0.2	9.3	2.5	0.7	3.9	3.7
Research and development	11.2	0.6	6.4	2.4	0.8	5.1	1.7	8.7	0.4	4.9	1.8	0.6	3.9	1.3
Total	275.2	18.1	351.9	84.9	38.4	479.7	78.7	269.2	17.9	352.5	84.2	38.6	487.8	77.1

Table 4-9 EIO-LCA estimates of toxic release with major production categories

Item	Conventional process, kg					PXL process, metric kg				
	Total Air	Surface Water	Ground Water	Land	Off-site	Total Air	Surface Water	Ground Water	Land	Off-site
Propane	16200	1280	3630	87300	3580	16200	1280	3630	87300	3580
Syngas	2960	234	665	16000	655	2960	234	665	16000	655
Solvent	289	102	255	126	53	221	78	195	96	40
Catalysts	7680	865	750	73300	12000	7680	865	750	73300	12000
Electricity	1690	13	4	844	206	2040	16	5	1010	248
Cooling water	1	0	0	1	0	2	0	0	3	1
Refrigerant	47	5	5	44	28	59	7	6	55	35
Direct labor	14	1	1	22	5	14	1	1	22	5
Maintenance	97	17	20	239	84	75	13	16	185	65
Distribution and marketing	289	28	33	369	98	223	22	25	285	75
Research and development	192	28	37	441	98	148	22	28	340	76
Total	29459	2573	5400	178687	16806	29622	2537	5322	178596	16780

4.4 Conclusion

Comparative economic analyses of the integrated propane dehydrogenation and propylene hydroformylation process show a more than 30% lower capital investment for the PXL process compared to the conventional process that includes energy-intensive distillation to obtain polymer-grade propylene from propane/propylene mixtures. Without the need for C_3 distillation columns, the annual utility cost in the PXL process is ~20% less than the conventional process, resulting in ~8% annual savings in production cost. This translates to a savings of $0.04/kg of propylene produced or an annual savings of $12.4 Million in the 300 kt/yr plant. Comparative environmental impact analyses performed by the EIO-LCA method show that the potential gate-to-gate environmental impacts (greenhouse gas emission, air pollutant emissions and toxic release) associated with the PXL process are significantly lower than the conventional process for its much lower material and energy consumption. However, when considering cradle-to-gate emissions, the environmental impacts are almost similar. This is a reflection of the fact that processes involving the production of the raw materials (whose consumption in both processes is similar) impose the dominant environmental burden.

Chapter 5: Hydroformylation of 1-Octene in n-butane expanded solvents with Co-based Complexes

5.1 Introduction

Hydroformylation involves the addition of a formyl group (CHO) to a carbon-carbon double bond. The most commonly used hydroformylation catalysts are either unmodified or modified rhodium and cobalt complexes. Rhodium-based catalysts are widely used in the lower olefin (C<5) hydroformylations. However, they are not well suited for higher olefin hydroformylation because the Rh complexes are unstable at typical temperatures required for product separation/distillation. Hence, the less expensive cobalt-based catalysts are used for industrial higher olefin hydroformylation, even though harsh reaction temperatures (~180°C) and pressures (~20 MPa) are needed to activate and maintain the catalyst complex.[16, 172, 201-202]

Gas-expanded liquids (GXLs) are generated by dissolving compressible gases such as CO_2 and light olefins in an organic solvent. The liquid phase volumetrically expands upon dissolution of the compressed gas.[121, 203] Compared to traditional organic solvent, GXLs provide both process and environmental advantages while allowing operation at much lower pressures than supercritical fluids.[118, 120, 204] Previously, several groups including ours have clearly demonstrated that for phosphine modified rhodium catalyzed 1-octene hydroformylation reaction, turnover frequency (TOF) and regioselectivity (*n/i*) are significantly enhanced as well as pressure tunable in CO_2-based media.[14, 131, 141-142] In the case of carbon dioxide-expanded liquids (CXLs), the observed beneficial effects on hydroformylation activity and selectivity are attributed to the favorable tunability of H_2/CO ratio in the CXL phase.[13]

Besides CO_2, the use of other gases as expansion media to create GXLs has also been reported.[126, 205] In comparison to CO_2 (T_c = 31.0 °C; P_c = 7.38 MPa), propane (T_c = 96.6 °C; P_c =

4.25 MPa) and *n*-butane (T_c = 152.0 °C; P_c = 3.70 MPa) possess higher critical temperatures but lower critical pressures. Consequently, propane and *n*-butane can expand organic solvents at higher temperatures and lower pressures compared to CO_2. Previously, we demonstrated that the solubilities of H_2 and CO in either propane-expanded or propylene-expanded phase are greater than those in the neat organic solvents, by as high as 78% at 70 °C and 1.5 MPa.[163] For rhodium/triphenylphosphine catalyzed propylene hydroformylation performed in the 70-100 °C range and pressures up to 2.0 MPa, the *n/i* aldehyde ratio is increased by up to 45% in propane-expanded liquids (PXLs). This is attributed to the increased H_2/CO ratio in the GXL phase. Like propane, reaction media expanded by *n*-butane, whose critical temperature is close to typical reaction temperatures (160-180°C) for Co-based hydroformylation, has the potential to enhance activity and selectivity at milder pressures.

In this chapter we experimentally quantify the volumetric expansion of typical hydroformylation mixtures by *n*-butane, including the solubility of the Co catalyst complexes in such BXLs. The activity and selectivity of Co-catalyzed hydroformylation of 1-octene were compared in neat solvent media and BXLs. The experimental results reveal that the TOF was enhanced more than 20% in BXL media with a 20% reduction in organic solvent usage. The increased TOF in BXLs is attributed to the improved syngas availability in the BXL phase compared to neat solvent.

5.2 Experimental

5.2.1 Materials

The purchased materials are listed in Table 5-1. All organic compounds were used as is unless otherwise noted.

Table 5-1 Materials used in this work

Material	Purity	Company
1-Octene	98%	Sigma-Aldrich, In
Toluene	anhydrous, 99.8%	Sigma-Aldrich, In
Decane	anhydrous, ≥99%	Sigma-Aldrich, In
1-Octanol	99%	Sigma-Aldrich, In
Triphenylphosphine (TPP)	99%	Sigma-Aldrich, In
Cobalt(III) acetylacetonate	99.99%	Sigma-Aldrich, In
Hydrogen	99.99%	Matheson Tri-Gas Co.
Syngas	49.5% H_2 with balance being CO	Matheson Tri-Gas Co.
n-Butane	99.9%	Matheson Tri-Gas Co.
Nitrogen	99.9%	Matheson Tri-Gas Co.

5.2.2 Apparatus and methods

5.2.2.1 Volumetric Expansion and Catalyst Solubilities Experiments:

The experimental setup for investigating catalyst solubilities and solvent expansion with *n*-butane is illustrated in Figure 5-1. It consists of a ~80 cm^3 Jerguson® Series 20™ liquid level gage (Clark-Reliance Corp.), thermocouples (Omega Engineering, Inc., type T, ±1.0 °C), pressure transducer (Omega Engineering Model PX835-2KSI, 0-13.79 MPa ±0.5%) and an oven (from a Applied Separations Model 7700 Speed® SFE unit, <240 °C). A Mitutoyo Digimatic® height gage with Titan® cathetometer is used to measure the expanded liquid volume (each mm division corresponds to a volume of 0.54 cm^3). The liquid level gage is located in the oven, and the gage will henceforth be referred to as the 'view cell'.

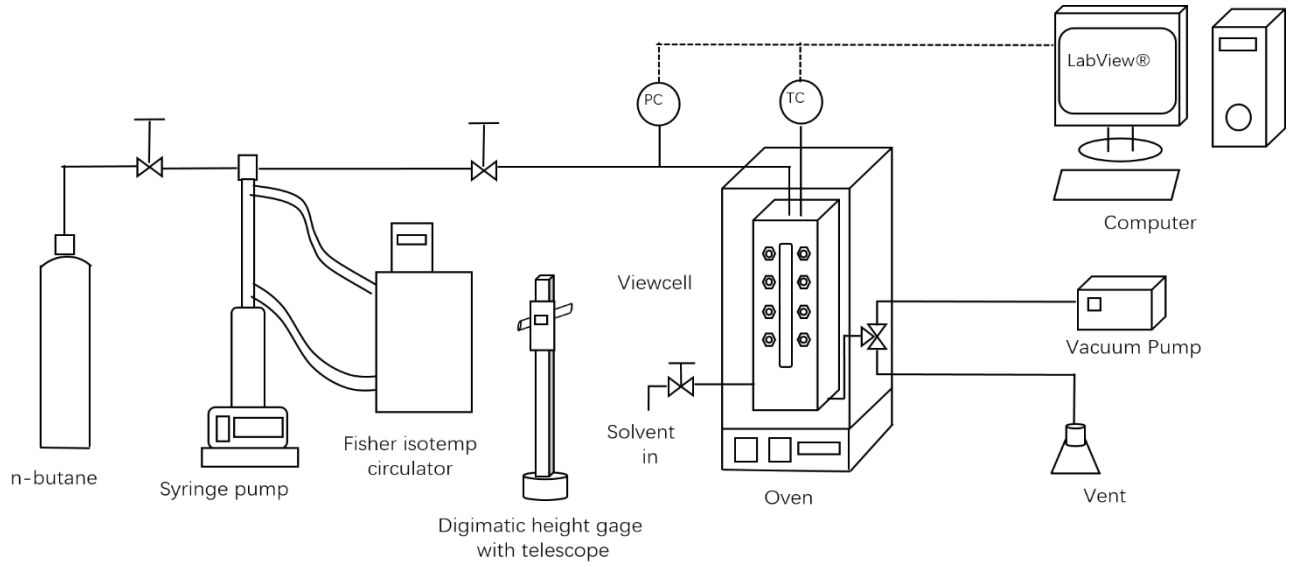

Figure 5-1 Schematic of setup for volumetric expansion and catalyst solubility study

In a typical run, the system was evacuated with a vacuum pump, and the resulting vacuum was used to pull a known amount of organic liquid into the view cell through a port located in the bottom of the cell. The liquid consists of either pure solvent or a mixture of solvents and reactants at various compositions representative of typical hydroformylation reaction mixtures. Enough liquid was introduced into the system such that the meniscus in the view cell was visible using the cathetometer, looking through a round window located in the oven door. The mixture was then brought to the desired temperature, and the level recorded. Known amounts of *n*-butane were gradually introduced using a syringe pump. The gas was bubbled through a 2-micron frit immersed in the liquid, at the end of a vertical 1/16" stainless steel tube introduced into the view cell through a side port at the top of the cell. The expansion of the organic liquid by *n*-butane was recorded in terms of the relative increase in the liquid volume from the initial state (*n*-butane-free, equilibrated pressure, P_0) to the final state (*n*-butane expanded, equilibrated pressure, P) at the same temperature. The volumetric expansion ratio was calculated using Equation 5-1.

$$\frac{V}{V_0} = \frac{V(T,P)}{V(T,P_0)} \quad (5\text{-}1)$$

The volumetric expansion data are also predicted by Peng-Robinson equation of state (PR-EoS) with van der Waals' mixing rules embedded in the Aspen Plus® software.[165-166] This simulation method has been previously demonstrated to satisfactorily predict the volumetric expansion as well as VLE data for CO_2- and propane-expanded solvent systems.[14, 125, 163]

The cloud point pressure at which the dissolved Co catalyst complex precipitates was also measured during the expansion study. Operating pressures below the cloud point are used for performing homogeneous hydroformylation in BXLs, whereas pressures above the cloud point may be exploited for catalyst precipitation post-reaction.

5.2.2.2 Hydroformylation experiments:

The hydroformylation reaction was performed in a 50 cm^3 high-pressure autoclave reactor in a semi-batch mode. The equipment description and procedures are described elsewhere.[13] In a typical run, a known amount of liquid solution containing substrate, dissolved catalyst and organic solvent are first introduced into the reactor. The reactor head space was flushed with nitrogen at ambient conditions to remove air. The reactor was then heated to the desired temperature with stirring. Following this step, *n*-butane was pumped into the reactor to attain the desired operating pressure for performing homogeneous catalysis in BXLs, as determined from the volumetric expansion study. The system was allowed to sit for approximately 30 minutes to equilibrate. Stirring was then temporarily halted and premixed syngas stored in the external gas reservoir was then introduced into the reactor to a predetermined syngas partial pressure. The stirrer was then set to 1000 rpm to start the reaction. For investigating the effects of different H_2/CO ratios, the reactor was pressurized initially with CO and H_2 to achieve the desired initial H_2/CO ratio while feeding syngas with a molar H_2/CO ratio of 2 from the external reservoir. During the experiments,

the temperature and pressure in the syngas reservoir as well as the reactor were monitored and recorded by LabView® data acquisition system. At the end of the reaction period, the autoclave was placed in an ice-bath to quench the reaction and contents carefully transferred into another container for immediate chromatographic analysis. Figure 5-2 (corresponding to Table 5-3, Entry #3,) shows typical pressure and temperature profiles during the batch experiments.

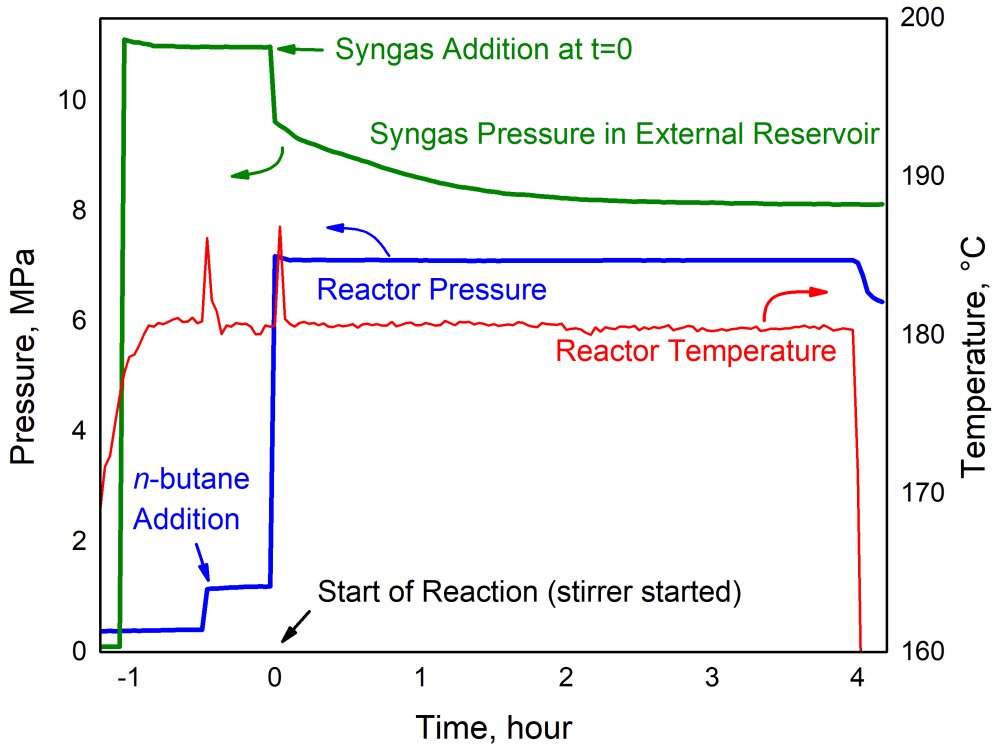

Figure 5-2 Pressure and temperature as a function of time during the hydroformylation in n-butane expanded solvents (Table 4, Entry #3).

The TOF was calculated from the linear portion of the syngas consumption profile corresponding to low (<20%) 1-octene conversion. The syngas consumed from the reactor gas phase due to reaction is continuously replenished from an external reservoir to maintain a constant reactor pressure. Thus, the moles of syngas consumed in the reaction is estimated from the measured pressure drop in the external reservoir at a constant temperature. Further, if the desired

product is nonanol, each mole of 1-octene should react with two moles of hydrogen and one mole of carbon monoxide.

$$\text{TOF}\ (\text{hour}^{-1}) = \frac{\text{Moles of syngas consumed at low } (< 20\%) \text{ octene conversion}}{(\text{moles of Co})(\text{batch time})} \quad (5\text{-}2)$$

$S_{nonanol}$, $S_{aldehyde}$ and S_{octane} are defined as the number of moles of nonanol, aldehyde and octane formed respectively, relative to the total number of moles of reaction products formed at the end of the batch run. The *regio*-selectivity (*n/i*) was estimated as the molar ratio of the linear to branched alcohols in the product. The carbon and hydrogen balances are estimated by calculating the moles of syngas consumed (from the observed pressure drop in the syngas reservoir) and comparing the value with the moles of hydrogen and carbon added in the products. Sample calculations are shown in the Appendix M and Table M1. The combined deficit for molar carbon and hydrogen balances is less than 5% in all the runs reported here (as seen in Table M2).

5.3 Results and discussion

5.3.1 Volumetric Expansion and Catalyst Solubility studies:

The purpose of conducting *n*-butane-expansion and catalyst solubility studies was to determine the operating conditions for performing homogeneous hydroformylation. Figure 5-3 shows the volumetric expansions of 1-octene by *n*-butane measured at pressures ranging from 0 to 2.4 MPa at 170 °C and 180 °C. As seen from Figure 3, the liquid phase containing only 1-octene was increased exponentially upon *n*-butane pressurization (by up to two-fold at 2.2 MPa, 170 °C and 2.4 MPa at 180 °C). As expected, the volumetric expansion is greater and more sensitive to pressure at the lower temperature (170 °C) as compared to the higher temperatures (180 °C). The experimental data are predicted reasonably well by simulations performed using Aspen Plus® software employing the Peng–Robinson equation of state (PR-EOS).

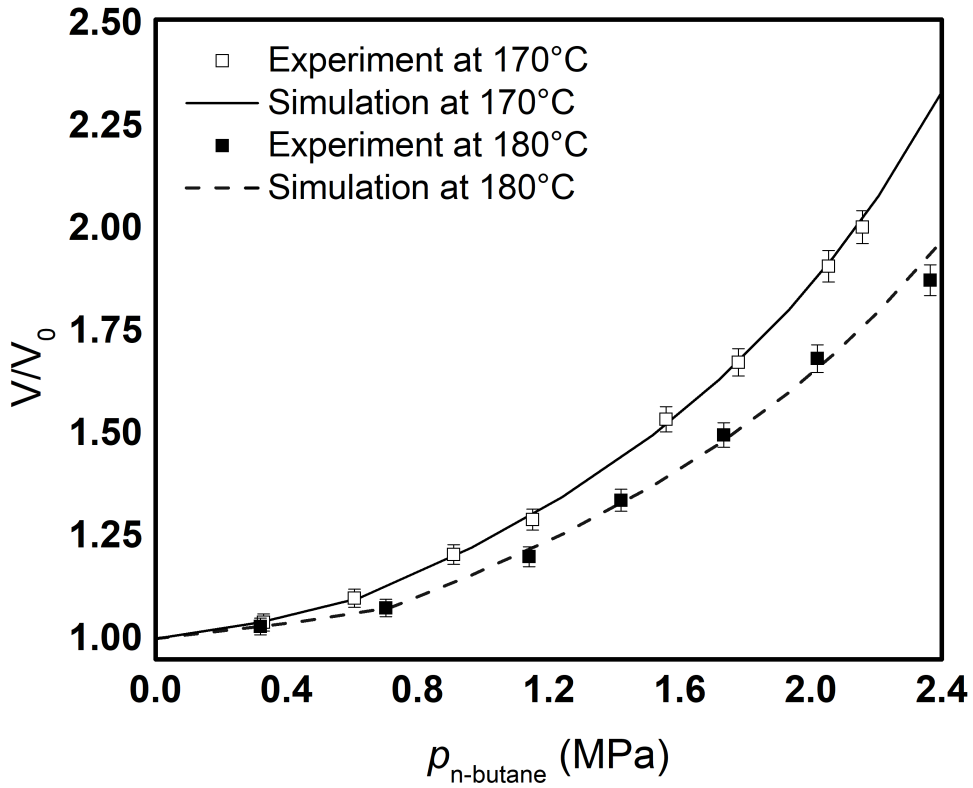

Figure 5-3 Volumetric expansion of 1-octene by n-butane at 170 °C and 180 °C

Figure 5-4 shows the expansion of model hydroformylation reaction mixtures representing different conversion levels (0%, 30%, 70%) by *n*-butane at 180 °C. Knowledge of the volume expansion of typical reaction mixtures by *n*-butane as well as catalyst solubility in the expanded phase guide the choice of operating conditions (*P*, *T*, and composition) for the reaction studies. These include the extent of volumetric expansion at various *n*-butane pressures and the range of pressures where 1-octene hydroformylation in BXLs can be performed homogeneously. As seen in Figure 4, all the tested hydroformylation solvents demonstrate good miscibility with *n*-butane at mild pressures. Nearly 50% expansion was noticed as butane partial pressure is increased to 1.8 MPa. The measured expansion ratios were almost identical for the various reaction mixtures with an initial volume of 20 mL. However, catalyst precipitation was observed in *n*-butane expanded

solvents around 1.3 MPa. The presence of polar nonanol slightly increases the cloud point pressure suggesting improved catalyst solubility in such mixtures. The observation of catalyst precipitation demonstrates the potential of exploiting *n*-butane as an antisolvent for catalyst recovery post reaction.

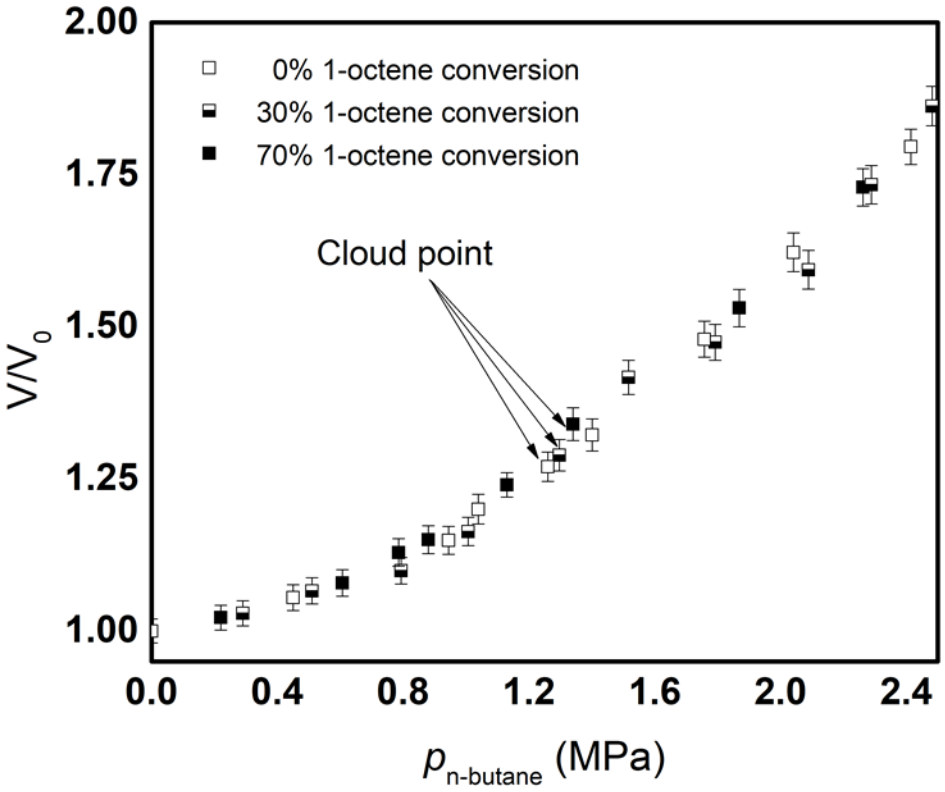

Figure 5-4 Volumetric expansion of model hydroformylation reaction mixtures containing dissolved cobalt catalyst representing different 1-octene conversion (0%: 7ml toluene + 12ml 1-octene + 1ml decane; 30%: 7ml toluene + 8.4ml 1-octene +3.6ml octanol + 1ml decane; 70%: 7ml toluene + 3.6ml octanol +7.4ml 1-octene + 1ml decane) at 180 °C. The cloud point indicates the catalyst precipitation. Catalyst: 0.0676g cobalt acetylacetonate + 0.69g triphenylphosphine.

Volumetric expansion studies were also performed at different starting volumes (15, 20 and 25 ml) at 180°C with and without 6.0 MPa syngas (H_2/CO ratio = 2) in the gas phase (Figure 5-5). The observed expansion behavior was almost identical for the different starting volumes. Further, the presence of 6.0 MPa syngas did not have a significant effect on the overall expansion (which is dominated by *n*-butane dissolution) even though the syngas solubility should increase at

higher *n*-butane pressure based on such observation with other gas-expanded liquids.[13, 122-123, 163] The simulation results also confirm that the V/V_0 values are 1.01 and 1.02 for H_2/1-octene and CO/1-octene systems, respectively, at 6.0MPa and 180°C.[125] This is to be expected as CO (-138.7°C) and H_2 (−239.95°C) are far removed from their critical temperatures at the expansion conditions.[203]

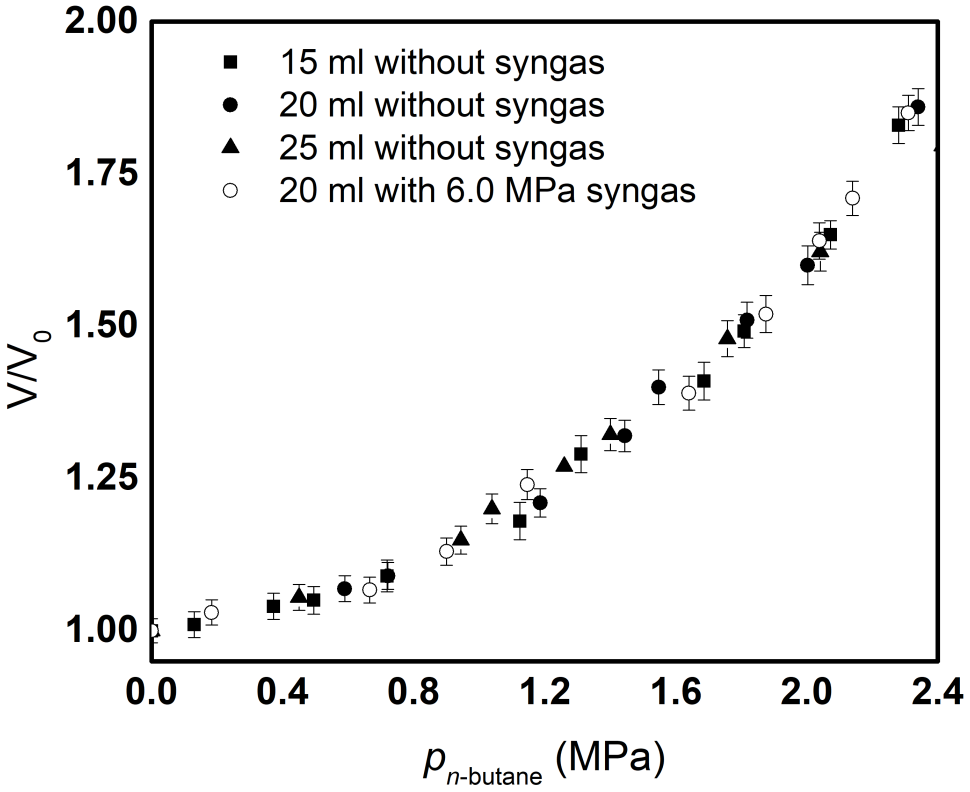

Figure 5-5 Volumetric expansion of model hydroformylation reaction at different staring volume (15, 20 and 25 ml) with and without 6.0 MPa syngas (H_2/CO ratio = 2) in the gas phase at 180 °C. volumetric 1-octene/toluene/decane = 12/7/1.

5.3.2 Reaction in neat organic solvents.

The benchmark reaction for Co-catalyzed hydroformylation of 1-octene was carried out at 180°C in a batch reactor with a syngas partial pressure of 6.0 MPa. As inferred from Table 5-2,

more than 85% nonanol yield (*n/i* ~2) with negligible aldehyde formation is obtained in neat organic solvent, which matches well with the literature.[206]

Table 5-2 Benchmark reaction for Co-catalyzed hydroformylation of 1-octene

	X, %	*n/i*	$S_{nonanol}$ %	S_{octane} %
Benchmark	88.7	1.9	86.1	13.9
Literature	90.3	2.2	86.5	13.5

T = 180°C, P = 6.0 MPa, H_2/CO = 2:1; [Co] = 1000 ppm, 1-octene/toluene = 3/2 (V/V), Catalyst: cobalt acetylacetonate; P/Co (molar) = 10; Ligands: triphenylphosphine; t = 8 h; X refers to 1-octene conversion; n/i refers to nonanol isomers.

The influence of operating conditions was first investigated in neat organic solvent to determine suitable conditions for testing the reaction in BXLs. Activity data on Co/TPP at various temperatures, pressures, H_2/CO ratios and catalyst concentrations are summarized in Table 5-3. The reaction temperature was varied at syngas pressures of 6.0 MPa (Entries# 1-3), the syngas pressure was varied at 180 °C using identical cobalt concentration (Entries# 4-6), the H_2/CO ratio was varied from 1:1 to 3:1 at syngas pressures of 6.0 MPa (Entries# 7-8) and the catalyst concentration was varied from 250 ppm to 2000 ppm at 6.0 MPa syngas and 180 °C (Entries# 9-11). As inferred from Table 3, the reaction rate (TOF) as well as nonanol yield are reduced at lower temperatures with increased selectivity towards aldehydes, hydrogenation and isomerization products. In general, both the TOF as well as the yield of the desired nonanol (> 85%) are favored at the higher temperatures.

An increase in the syngas pressure resulted in higher TOFs and *n/i* ratios (Table 5-3, Entries #3-6). However, at the highest syngas pressure (8 MPa), side reactions including 1-octene hydrogenation and isomerization also occur decreasing the nonanol selectivity. At identical syngas pressures, while a H_2/CO ratio of 2 is optimum for maximizing the reaction rate, alcohol yield and *n/i* ratio, a higher (H_2/CO ratio of 3) favors the formation of the hydrogenation product (Table 5-3, Entries 7-8).

Table 5-3 Co-catalyzed hydroformylation of 1-octene in neat organic solvent

No.	T, °C	P, MPa	H_2/CO	[Co], ppm	X, %	*n/i*	TOF, h^{-1}	$S_{nonanol}$, %	$S_{nonanal}$, %	S_{octane}, %	$S_{inter\text{-}octene}$, %
1	160	6.0	2:1	1000	93.2	3.26	17.2	11.2	19.8	30.1	38.9
2	170	6.0	2:1	1000	91.9	2.08	76.3	80.4	1.9	15.0	2.6
3	180	6.0	2:1	1000	89.0	1.85	95.0	86.3	Trace	12.9	0.8
4	180	3.0	2:1	1000	64.6	1.52	51.6	80.3	trace	16.8	2.3
5	180	5.0	2:1	1000	82.0	1.77	77.7	83.1	trace	14.4	3.5
6	180	8.0	2:1	1000	93.6	2.03	135.2	81.4	trace	15.6	3.0
7	180	6.0	1:1	1000	90.2	1.72	81.7	32.3	24.0	26.3	17.4
8	180	6.0	3:1	1000	92.1	1.98	129.2	80.5	trace	19.5	trace
9	180	6.0	2:1	250	76.5	1.52	111.4	75.9	4.1	16.4	3.6
10	180	6.0	2:1	500	87.7	1.69	83.6	86.3	trace	13.7	trace
11	180	6.0	2:1	2000	91.2	1.87	74.6	86.4	trace	13.6	trace

Catalyst: cobalt acetylacetonate; Ligand: triphenylphosphine; t = 4 h; volumetric 1-octene/toluene/decane (internal standard) = 12/7/1; P/Co (molar) = 10; (H_2/CO) refers to intial molar ratio in the reactor (molar H_2/CO in external reservoir = 2 in all cases); X refers to 1-octene conversion; n/i refers to nonanol isomers.

Figure 5-7 compares the syngas conversion as a function of time at different catalyst concentrations. It is shown that increasing catalyst concentration clearly increases the syngas consumption rate while enhancing the linear alcohol yield (Table 3, Entries# 9-11). However, the TOF (defined in eq. #2) decreases at higher catalyst concentrations with diminishing effect beyond 1000 ppm.

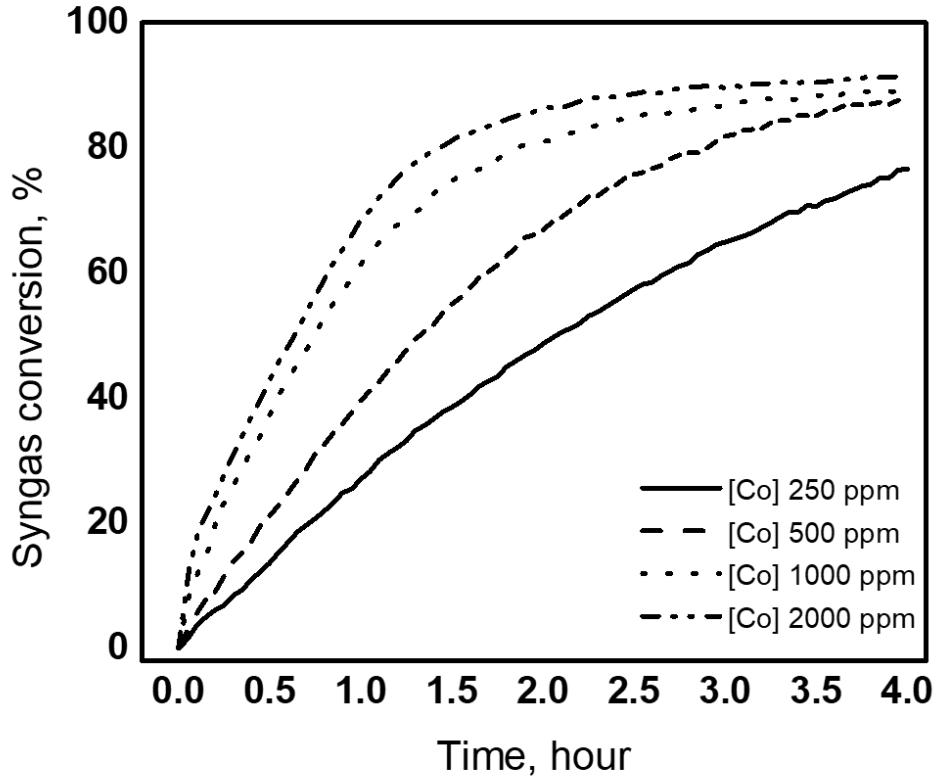

Figure 5-6 Temporal syngas conversion profiles for 1-octene hydroformylation at different catalyst precursor concentrations. The initial moles of syngas: 0.229 mol. Other reaction conditions are as given in Table 5-3.

The mechanisms for phosphine modified Co-catalyzed hydroformylation have been well studied.[20, 207-209] Figure 5-7 is a schematic for the well accepted catalytic mechanism for Co-catalyzed hydroformylation reactions. The active species is a 16-electron hydride complex, $[HCo(CO)_2L]$ (L=CO or phosphine), in equilibrium with the 18-electron tricarbonyl $[HCo(CO)_3L]$ complex. Co-ordination of alkene and insertion into the Co–H bond generates a cobalt–alkyl complex which is followed by CO-insertion to give an acyl species. Hydrogenation of the acyl liberates the aldehyde and regenerates the active hydride species. The alcohol is then formed by the hydrogenation of aldehyde. It has been reported that for Co-catalyzed hydroformylation reaction, sufficiently high CO partial pressures are required to stabilize the carbonyl complexes and that the rate-limiting step is the hydrogenation of the acyl intermediate.[209-211] On the other

hand, lower CO pressure would be beneficial for shifting the equilibrium toward the active species $HCo(CO)_2L$, implying the requirement of an optimum CO concentration in the reaction phase. Therefore, an optimum H_2/CO ratio in the reaction phase is required to maximize the reaction rate. However, as discussed earlier, progressively higher H_2/CO ratios favor the hydrogenation product adversely affecting the linear alcohol selectivity. A H_2/CO ratio of 2 is typically used industrially. Given that H_2/CO may be easily tuned in gas-expanded liquids with syngas of a fixed composition,[13, 163] we chose to investigate *n*-butane expanded reaction media for optimizing Co-catalyzed hydroformylation.

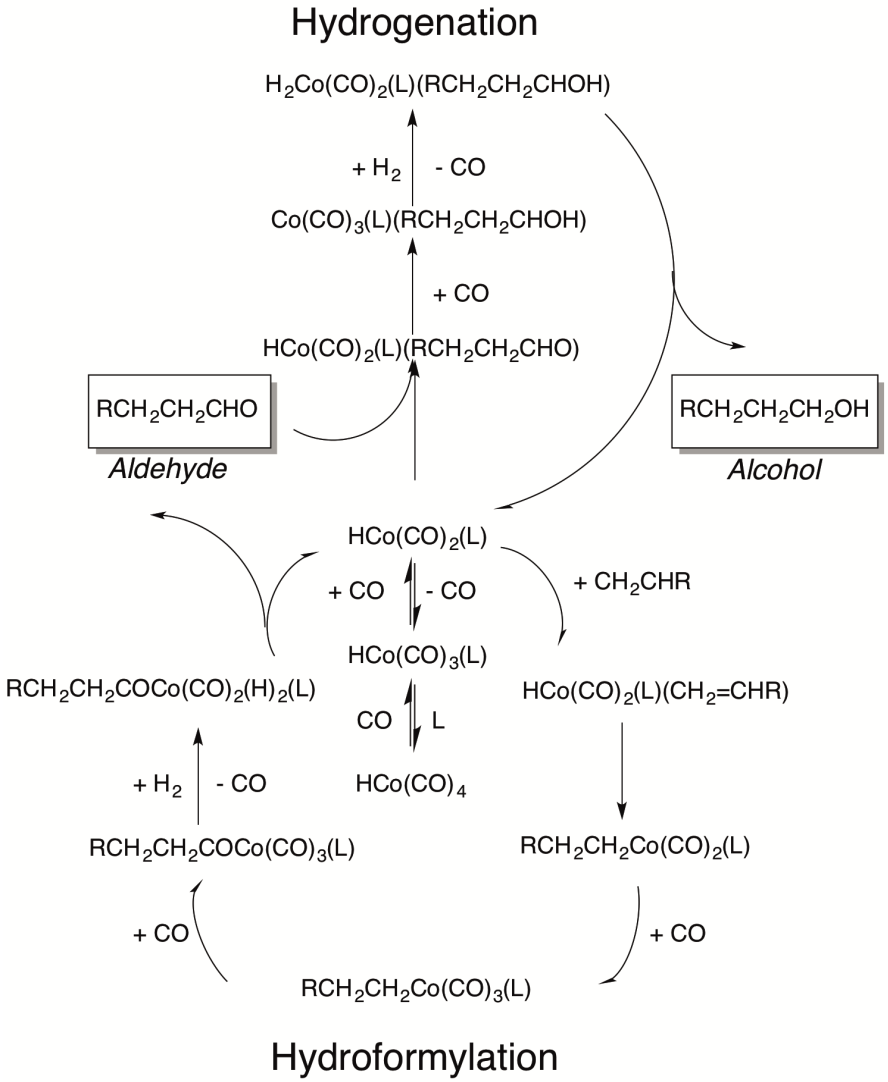

Figure 5-7 Simplified mechanism for Co-catalyzed hydroformylation and hydrogenation

5.3.3 Reaction in n-butane expanded solvents:

For the 1-octene hydroformylation runs in *n*-butane-expanded media, volumetric expansion ratios from 1.0 to 1.2 were investigated to maintain homogeneous reaction conditions. The syngas partial pressure was fixed at 6.0 MPa, while system pressure was increased with *n*-butane addition to create BXLs. To eliminate the dilution effect caused by *n*-butane dissolution, the amount of pure organic solvent was reduced (guided by the volumetric expansion data) to maintain an identical initial liquid volume in all the runs. In this way, the initial catalyst and reactant concentrations are kept nearly constant in the various runs.

Table 5-4 Co-catalyzed hydroformylation of 1-octene in BXL-toluene

No.	$P_{n\text{-butane}}$, MPa	V/V_0	X, %	*n/i*	TOF, h^{-1}	$S_{nonanol}$, %	$S_{nonanal}$, %	S_{octane}, %	$S_{inter\text{-}octene}$, %
1	0.4	1.05	90.2	1.93	101.2	85.8	Trace	13.3	0.9
2	0.7	1.10	91.2	1.88	104.5	86.5	Trace	12.3	1.2
3	1.1	1.20	91.8	1.85	116.3	87.1	Trace	11.8	1.1
4	1.3	1.40	84.2	2.03	41.6	60.2	4.5	22.8	12.5

T = 180°C, P_{syngas} = 6.0 MPa, Initial H_2/CO in reactor and H_2/CO in external reservoir (molar) = 2:1; Catalyst: cobalt acetylacetonate; Ligand: triphenylphosphine; t = 4 h; P/Co (molar) = 10; Initial liquid phase volume: 20 mL; X refers to 1-octene conversion; *n/i* refers to nonanol isomers.

As seen in Table 5-4, at homogeneous reaction conditions (*n*-butane partial pressure < 1.2 MPa), the TOFs were up to 22% greater in the BXL phase compared to neat toluene (Table 5-3, entry 3). However, *n*-butane addition has less of an effect on the *n*/*i* ratio. The enhanced TOF in the BXL phase is attributed to increased syngas solubility in that phase. As expected, catalyst precipitation occurs when *n*-butane partial pressure was increased beyond 1.3 MPa (Figure 5-4), causing a significant reduction in the TOF and nonanol yield (Table 5-4, Entry #4).

To further clarify the effect of *n*-butane addition, the reactions were run with different solvents and gases to replace the butane in the liquid and vapor phases while maintaining identical

initial concentrations of the substrate (1-octene) and catalyst in the liquid phases. The comparison experiments were designed as follows: (1) an expanded toluene mixture (V/V_0=1.2) is subjected to a total pressure of 7.1 MPa, with the partial pressures of syngas and *n*-butane being 6.0 and 1.1 MPa, respectively; (2) an expanded 1-octanol mixture (V/V_0=1.2) at otherwise identical conditions as run 1; (3) replacing *n*-butane with *n*-hexane (with polarity similar to *n*-butane) in the liquid phase maintaining the same initial volume as in other runs but under a total pressure of 6.0 MPa syngas alone; (4) toluene alone as solvent (as in run 1) but using pure syngas (7.1 MPa) in the vapor phase; (5) toluene alone as solvent (as in run 1) but replacing n-butane in the vapor phase with N_2 by using a mixture of syngas (6.0 MPa) and N_2 (1.1 MPa).

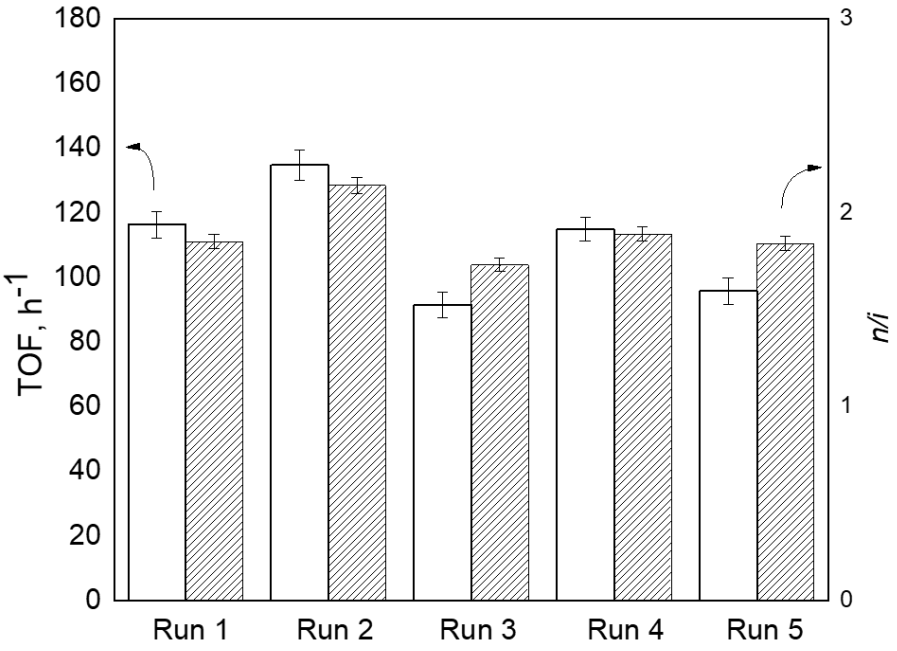

Figure 5-8 Comparison of 1-octene hydroformylation in different media. Run 1: BXL-toluene (6.0 MPa syngas + 1.1 MPa n-butane); Run 2: BXL-octanol (6.0 MPa syngas + 1.1 MPa n-butane); Run 3: toluene + hexane (6.0 MPa syngas); Run 4: toluene (7.1 MPa syngas); Run 5: toluene (6.0 MPa syngas + 1.1 MPa N_2); Other reaction conditions are as given in Table 5-4.

As shown in Figure 5-8, the TOF in *n*-butane-expanded toluene (run 1) is 30% greater than that in *n*-hexane at (Run 3) with similar *n/i* ratios observed in both runs. Compared to reaction in the toluene-BXL system, higher TOF and *n/i* are observed in 1-octanol-BXL system indicating beneficial effects of the polar product. Higher syngas partial pressures (7.1 MPa, Run 4) with neat solvent (toluene) are needed to match the TOF and *n/i* observed with toluene-BXL system that uses lower syngas partial pressure (6.0 MPa, Run 1), indicating enhanced syngas availability in the BXL phase. However, when a syngas partial pressure of 6.0 MPa and a N_2 partial pressure of 1.1 MPa were used with toluene as solvent (Run 5), a decrease in the TOF is observed. These results provide clear evidence that the beneficial effects of BXLs on the observed TOF and *n/i* ratio during Co-catalyzed 1-octene hydroformylation are due to *n*-butane dissolution in the liquid phase.

Table 5-5 summarizes results of Co-catalyzed 1-octene hydroformylation performed in *n*-butane expanded octanol. As inferred from Table 5, TOFs are generally enhanced at increased butane partial pressures at constant initial volumes (i.e., constant initial 1-octene and catalyst concentrations) as long as homogenous reaction conditions without catalyst precipitation are maintained. At a *n*-butane partial pressure of 1.3 MPa (Table 5, Entry #4), the TOF is 25% higher than in neat octanol (Table 5, entry 1). At higher partial pressure of 1.5 MPa (Table 5, Entry #5), the TOF markedly decreases, attributed to catalyst precipitation induced by increased dissolution of *n*-butane. However, the cloud point pressure that induces catalyst precipitation is greater (1.5 MPa) in 1-octanol-BXL (1.5 MPa) than in toluene-BXL system (1.3 MPa). In other words, the polar octanol as an effective co-solvent favoring enhanced catalyst solubility.

These results clearly show that the addition of *n*-butane has a beneficial effect on the TOF for Co-catalyzed 1-octene hydroformylation. However, the strong anti-solvent effect of *n*-butane

results in catalyst precipitation and limits its application to relatively low *n*-butane partial pressures. The potential benefits of BXLs may be maximized by designing catalysts that show improved solubility in the reaction mixture. In this context, premising candidates include Co complexes containing fluorophosphines that have been reported to exhibit high solubility in *sc*CO_2 and enhanced performance for 1-octene hydroformylation.[212-213]

Table 5-5 Co-catalyzed hydroformylation of 1-octene in BXL-octanol

No.	$P_{n\text{-butane}}$, MPa	V/V_0	X, %	*n/i*	TOF, h^{-1}	$S_{nonanol}$, %	$S_{nonanal}$, %	S_{octane}, %	$S_{inter\text{-}octene}$, %
1	0	1.00	99.5	2.06	111.6	85.2	0.5	12.9	1.4
2	0.7	1.10	99.3	2.08	127.2	86.4	0.5	12.3	0.8
3	1.1	1.20	98.8	2.14	134.7	85.3	Trace	13.3	1.4
4	1.3	1.30	99.2	2.13	141.6	84.3	Trace	14.5	1.2
5	1.5	1.40	98.4	2.20	67.5	68.6	3.0	18.3	10.1

T = 180°C, P_{syngas} = 6.0 MPa, Initial H_2/CO in reactor and H_2/CO in external reservoir (molar) = 2:1; Catalyst: cobalt acetylacetonate; Ligand: triphenylphosphine; t = 4h; P/Co (molar) = 10; Initial liquid phase volume: 20 mL; X refers to 1-octene conversion; *n/i* refers to nonanol isomers.

5.4 Conclusion

The application of *n*-butane expanded liquids (BXLs) as reaction media for Co-catalyzed 1-octene hydroformylation was successfully demonstrated. Volumetric expansion studies show that *n*-butane can significantly expand the volume of 1-octene and typical hydroformylation mixtures, by up to 50% at 1.8 MPa and 180 °C. For Co-catalyzed 1-octene hydroformylation at 180°C, enhanced TOFs (~ 20%) are observed in BXLs compared to neat solvent at relatively mild pressures. However, increased *n*-butane dissolution in toluene at higher pressures (1.3 MPa) induces catalyst precipitation, decreasing TOFs and nonanol yield. These first results clearly point out the need for designing Co complexes with improved solubility in BXL media and thereby better exploit these promising reaction media in industrial hydroformylation.

Chapter 6: Performance of supported ionic liquid phase (SILP) catalysts for hydroformylation reactions

6.1 Introduction

The concept of supported ionic liquid phase (SILP) catalysis presents new opportunities for combining the advantages of homogeneous and heterogeneous catalysis such as high activity and selectivity, good catalyst stability and simple catalyst recycling with ease of product separation.[91, 214] While SILP catalysts show promise for gas phase reaction, their application for liquid phase reactions is challenged by the problem of leaching.[90] During extended runs with a liquid phase, the IL film along with the dissolved catalyst complex has a tendency to gradually leach from the support. It has been previously reported that for an economically viable 1-octene hydroformylation process, the Rh make up rate should less than 0.94% of the initial Rh content in the reactor.[8] To meet this criterion, a robust SILP systems in which the IL phase is virtually insoluble in the reaction mixture and has good stability for continuous operation must be developed.

We hypothesize that the presence of a gas such as dense CO_2 in the liquid phase helps regulate the polarity of the reaction mixture. Thus, it may be possible to minimize, if not totally eliminate, leaching with optimal design of the IL phase and propane or CO_2-expanded liquid phase.

In this chapter, in collaboration with researchers in Friedrich-Alexander University Erlangen-Nürnberg (Erlangen, Germany), the preliminary results of SILP catalysts for hydroformylation reactions are reported. The work is aimed at extending the application of SILP catalyst for hydroformylation of higher olefins that are typically performed in a liquid phase. Specifically, we investigate (a) metal leaching from Rh-based SILP catalysts in organic solvent,

supercritical CO_2, liquid propylene, and (b) the catalyst performance for 1-octene, propylene and butadiene hydroformylation reaction.

6.2 Experimental

6.2.1 SILP catalysts

The SILP catalysts are received from FAU researchers (prepared with different ligands) and identified as follows. The details of catalysts preparation were described previously.[82] The catalysts received were stored under argon until further use.

The SILP catalysts received from FAU researchers (prepared with different ligands) are shown in Figure 6-1. Details of preparation of these catalysts were described previously.[91] The catalysts received from FAU were stored under argon until use. The syngas (49.5% H_2 with balance being CO), propane (99.9%), and CO_2 (99.9%) are purchased from Matheson Tri-Gas Co., 1-octene (98%), toluene (anhydrous, 99.8%) and 1,3-butadiene solution (20 wt.% in toluene) are purchased from Sigma-Aldrich, In. All organic compounds were used as is unless otherwise noted.

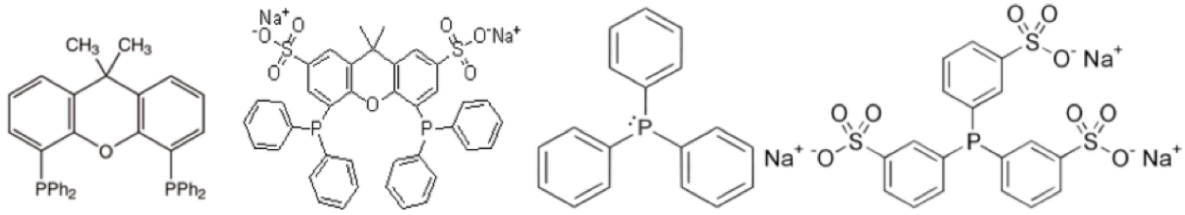

Figure 6-1 SILP catalysts received and studied in this work

6.2.2 Metal leaching and reaction study

Both the catalyst metal leaching and reaction studies were performed in a 50 mL Parr reactor equipped with a 6-port valve for periodic sampling of reactor contents, the photo of the reactor is shown in Figure 6-2.

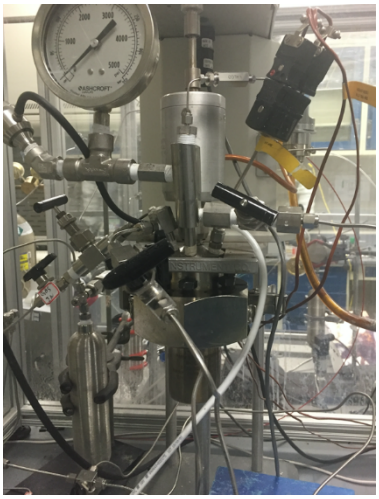

Figure 6-2 The photo of Parr reactor for SILP catalysts test

For metal leaching study, a known amount of SILP catalysts were first introduced into the reactor. The reactor head space was flushed with the test gas (CO_2 or propane) at ambient conditions to remove air. The reactor was then heated to the desired temperature (90 ºC). Following this step, liquified CO_2 or propane was pumped into the reactor with an ISCO pump at -6 °C to attain the desired operating pressure. After sitting for approximately 5 minutes to equilibrate the system, the stirrer was then set to 1000 rpm to start the test.

For hydroformylation reaction study, a known amount of SILP catalysts were first placed in 20 mL 1-octene (for 1-octene hydroformylation) or butadiene solution (20 wt. % in toluene) (for butadiene hydroformylation) introduced into the reactor. The reactor head space was then flushed with the N_2 at ambient conditions to remove air. The reactor was then heated to the desired temperature with stirring. The system was allowed to sit for approximately 5 minutes to equilibrate.

Stirring was then temporarily halted and premixed syngas stored in the external gas reservoir was then introduced into the reactor to a predetermined syngas partial pressure. The stirrer was then set to the desired rpm to start the reaction. During the experiments, the temperature and pressure in the syngas reservoir as well as the reactor were monitored and recorded by LabView® data acquisition system. At the end of the reaction period, the autoclave was placed in an ice-bath to quench the reaction and contents carefully transferred into another container for analysis.

The Rh concentration in the SILP catalyst is determined using X-ray Fluorescence (XRF) (PANalytical Zetium) instrument before and after reaction. The Rh concentration in the liquid phase product mixture following reaction is analyzed by inductively coupled plasma atomic emission spectroscopy (ICP-AES) (Horiba J-Y 2000). The concentrations of the various reactants and products in the reaction mixture is analyzed by gas chromatographic (GC) (Agilent Technologies 7890A)

6.3 Results and discussion

6.3.1 Hydroformylation of 1-octene by SILP catalyst

Hydroformylation of 1-octene with SILP catalysts (containing mono-phosphine ligands) have been reported previously in continuous fixed bed reactor.[90] The diffusion of syngas into the SILP layer is an important step that can be potentially rate limiting. In the present study, SILP catalysts with four different ligands are tested in a batch reactor at similar operating conditions as in our previous report (same 1-octene/ Rh ratio).[13] The reaction conditions and results are summarized in Table 6-1.

Table 6-1 Hydroformylation of 1-octene at 60 ºC

Catalyst	P/Rh	Catalyst, g	1-Octene, g	Toluene, g	Yield of nonanal, %	TOF, h^{-1}	n/i
Xantphos	10	2.41	4.50	13.66	39.1	131.4	7.59
Sulfxantphos	9.74	2.37	4.40	13.79	5.4	8.2	3.48
TPP	9.63	2.35	4.44	13.73	14.7	32.1	2.78
TPPTS	4.95	2.36	4.35	13.85	12.4	33.2	2.78
Homo Cat. /TPP	205	-	-	-	81.6	140	3.9

Reaction time: 4 h, 1-Octene/Rh mole ratio: 988, P_{syngas}: 0.2 MPa; rpm: 1000

The P/Rh ratio in SILP catalyst is based on the relative amounts used during SILP preparation. Among the four catalysts tested, the Xantphos-based Rh complex shows the best performance. However, for all SILP catalysts, the product yields and TOF are lower than the homogeneous Rh/TPP complexes. We believe this to be partly due to the low P/Rh ratio in the SILP catalysts. Further, XRF and ICP results (Table 6-2) confirm significant Rh leaching from the SILPs during the reaction.

Table 6-2 Characterization of catalysts before and after 1-octene hydroformylation reaction*

		XRF analysis of SILPs			ICP analysis
		Based on fresh SILP	Characterized	After reaction	Spent reaction mixture
Xantphos	Rh,	0.169 %	0.175 %	0.124 %	50.1 ppm
Sulfxantphos	Rh,	0.170 %	0.191 %	0.125 %	48.2 ppm
TPP	Rh,	0.174 %	0.180 %	0.058 %	150.3 ppm
TPPTS	Rh,	0.170 %	0.193 %	0.091 %	90.5 ppm

The color change of the SILP catalysts before and after reaction are shown in the Figure 6-3. The color fading was observed after reaction which further confirm the Rh leaching.

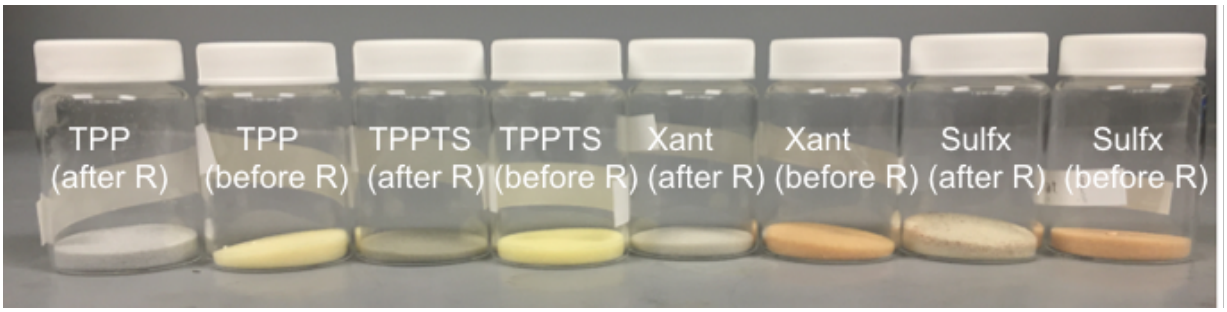

Figure 6-3 Color change of SILP catalysts before and after reactions

6.3.2 Hydroformylation of propylene in PXLs by SILP catalyst

Hydroformylation of propylene with SILP catalyst has been reported before in fixed bed reactor.[152,170] ere, the reaction is performed in neat toluene and propane-expanded toluene (PXL) with SILP-Sulfxantphos catalyst. The results are shown in Table 6-3. The Rh catalyzed propylene hydroformylation with homogeneous biphephos ligand were also listed for comparison. To minimize possible physical damage and leaching of the SILP layer, a lower stirrer rpm of 100 was also investigated. With the bidentate ligand, the SILP-sulfxantphos catalyst performs impressively in both neat toluene and propane-expanded toluene.

Table 6-3 Hydroformylation of propylene at 90 ºC

Catalyst	Solvent	$P_{propylene}$, MPa	$P_{propane}$, MPa	rpm	V/V_0	TOF, h^{-1}	*n/i*
SILP-Sulfxantphos	Toluene	1.00	0	100	1.1	5.1	11.25
SILP-Sulfxantphos	PXL	1.15	0.35	100	1.4	5.4	12.12
Homo-Biphephos	Toluene	1.00	0	1000	1.1	61.2	23.3
Homo-Biphephos	PXL	1.15	0.35	1000	1.4	59.0	30.1

Reaction time: 0.5 h, Initial liquid phase volume: 20 ml

As can be seen from Table 6-4, the Rh leaching is much reduced at low rpm. With bidentate ligand, the SILP-sulfxantphos catalyst performs impressively in both pure toluene and propane-expanded toluene. The results indicate that SILP catalyst has potential for C_3 mixture hydroformylation in liquid phase.

Table 6-4 Characterization of catalyst before and after propylene hydroformylation reaction*

		XRF analysis			ICP analysis
		Theoretical	Characterized	After reaction	After reaction
SILP-Sulfxantphos in toluene	Rh	0.170 %	0.191 %	0.166 %	7.2 ppm
SILP-Sulfxantphos in PXLs				0.155 %	9.1 ppm

*Propylene hydroformylation reaction condition: T: 90 ℃, reaction time: 0.5 h, P_{syngas}: 1.0 MPa; $P_{propane}$:1.15 for reaction in PXLs; rpm: 100,

6.3.3 Hydroformylation of butadiene by SILP catalyst

Adipic acid is an important large volume commodity product used as an intermediate for producing nylon 6,6. The current commercial process for adipic acid manufacture involves a two-step process: oxidation of cyclohexane to a mixture of cyclohexanol and cyclohexanone, which is oxidized to adipic acid using HNO_3 and H_2SO_4as reagents. The generation of large quantities of inorganic salts and the release of nitrous oxide emissions pose serious environmental concerns, providing a strong motivation to develop cleaner and atom-economical alternative routes for adipic acid.

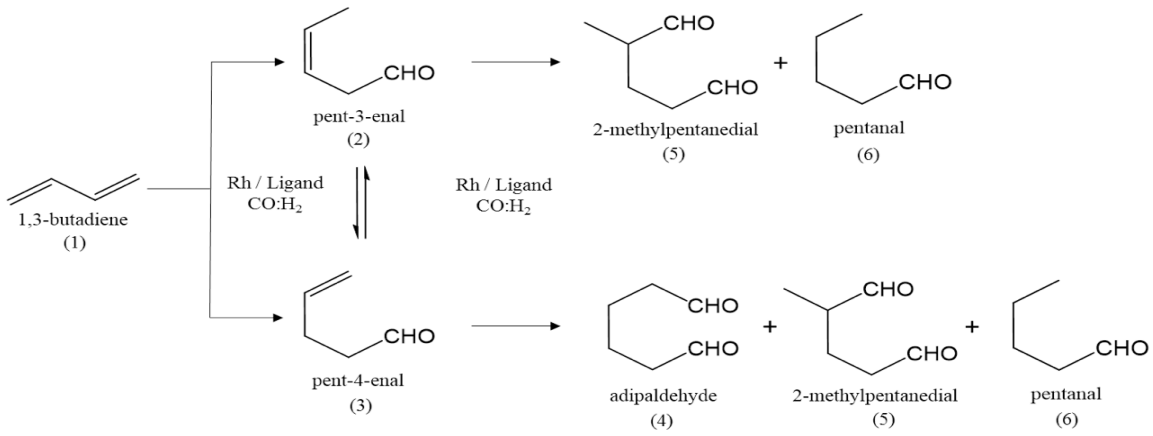

Figure 6-4 Reaction pathway of 1,3 butadiene hydroformylation

The hydroformylation of 1,3 butadiene provides such a route, in which one of the terminal olefin groups is first converted to the isomeric unsaturated mono-aldehydes (pent-4-enal and pent-3-enal) followed by hydroformylation of pent-4-enal to adipaldehyde (see Table 6-5)

Here, the hydroformylation of butadiene is performed in pure toluene with SILP-xantphos catalyst and compared with homogeneous xantphos ligands. The reaction condition and results are shown in the Table 6-5.

Table 6-5 Hydroformylation of butadiene at 90 ºC

Catalyst	rpm	$S_{pentanal}$, %	$S_{trans\text{-}3\text{-}pentenal}$,%	$S_{cis\text{-}3\text{-}pentenal}$,%	$S_{2\text{-}methylpentadial}$, %	$S_{4\text{-}pentenal}$, %	$S_{adipaldehyde}$, %
SILP-xantphos	100	22.61	40.72	11.08	0.74	19.70	5.15
Homo-xantphos	1000	10.08	58.20	23.06	0.99	1.17	6.49

Reaction time: 8 h; rpm: 100; P_{syngas} :1.38 MPa

As can be seen from Table 6-5, SILP catalyst performs as well as the homogeneous system with xantphos-based complexes. This suggests that the system merits further study aimed at enhancing adipaldehyde yield.

6.3.4 Metal leaching test in sub- and super-critical solvents.

The leaching of the catalyst layer within the SILP catalysts was also investigated in neat toluene, supercritical CO_2 (***sc*CO_2**) and liquefied propylene. The test conditions and results are shown in Table 6-6.

Even though Rh leaching is observed in all cases observed, the metal leaching in liquefied propylene and supercritical CO_2 are much less than in neat toluene. Since the tests are also performed in high rpm, the strong shear force may be "damaging" the absorbed ionic liquid layer on the support. Compared to TPP, the modified ligand (TPPTS) with higher polarity shows better leach-resistance in *sc*CO_2 and liquefied propylene medium.

Table 6-6 Metal leaching test in neat toluene, supercritical CO_2 and liquefied propylene by XRF analysis

		Theoretical	Characterized	Toluene*	Propylene**	*sc*CO_2***
Xantphos	Rh, %	0.169	0.175	0.133	0.159	0.158
Sulfxantphos	Rh, %	0.170	0.191	0.131	0.162	0.159
TPP	Rh, %	0.174	0.180	0.064	0.141	0.126
TPPTS	Rh, %	0.170	0.193	0.098	0.158	0.173

* Condition for neat toluene: T: 90 ºC, rpm:1000, test time: 4h
** Condition for liquefied propylene: T: 90 ºC, P: 2.5 MPa, rpm:1000, test time: 4h
*** Condition for supercritical CO_2: T: 90 ºC, P: 8.0 MPa, rpm:1000, test time: 4h

6.4 Conclusion

In preliminary work, we have investigated the leaching of SILP catalysts in neat organic solvent, *sc*CO_2 and liquefied propylene. We also tested the performance of SILPs for 1-octene, propylene and butadiene hydroformylation reactions. The SILP catalyst (with sulfxantphos ligand) works well for the hydroformylation of propane/propylene mixtures. The *n/i* ratio and TOF obtained are comparable with pure propylene as feedstock. The hydroformylation of butadiene was also demonstrated with SILP-xantphos catalyst for the first time. The target product yield is comparable with that obtained with a homogeneous complex tested at similar conditions implying that the SILP formulation has potential for further optimization. For all cases tested, the SILP catalyst is more stable (i.e., more leach resistant) in supercritical CO_2 and liquefied propylene than in organic solvents.

Chapter 7: Conclusions and recommendations

7.1 Conclusions

This dissertation research has successfully extended the concept of gas-expanded liquids (GXLs) to perform hydroformylation of olefins in solvent media expanded by light alkanes. Specifically, alternate hydroformylation reaction media that admit the principles of green chemistry and green engineering while also providing potential economic benefits have been demonstrated. The main contributions of this dissertation are as follows:

- A clear understanding of the enhancement of hydrogen and carbon monoxide solubilities in propane- and propylene- expanded solvents with increased H_2/CO ratios in the GXL phase that benefit propylene hydroformylation in terms of enhancing *regio*-selectivity toward linear aldehydes with Rh/TPP catalyst complexes.
- Demonstration that refinery-grade propane/propylene mixtures (i.e., without the need for purification to obtain polymer-grade propylene) can be used directly for propylene hydroformylation at typical industrial conditions using Rh/biphephos catalysts without compromising on activity and selectivity. The hydroformylation reactor in effect serves to enrich propane which is then recycled back to the propane dehydrogenation reactor to make refinery grade propane/propylene feed mixtures.
- Comparative economic and environmental analyses of the integrated propane dehydrogenation and propylene hydroformylation process shows lower capital investment (by ~30%) and utility costs (~20%) for the PXL process compared to the conventional process with propane/propylene separation by distillation. The savings in production costs is 4 cents/lb or annually 12.1 $ millions for a 300kt/y plant.

- Use of *n*-butane expanded liquids (BXLs) as reaction media for Co-catalyzed hydroformylation of 1-octene was demonstrated. The presence of *n*-butane enhanced the TOF within the homogeneous reaction region while preserving the regioselectivity towards the linear alcohols and reducing organic solvent usage by ~20 vol %.
- Supported ionic liquid phase (SILP) catalysts used for hydroformylation reactions are more stable (i.e., more metal leach-resistant) in supercritical CO_2 and liquefied propylene than in organic solvents.

These accomplishments are summarized in the following paragraphs.

This dissertation has conclusively shown that the solubility of hydrogen and carbon monoxide could be enhanced in propane- and propylene expanded solvents. we investigated the vapor-liquid equilibrium (VLE) data of the following ternary systems in a variable-volume view cell at temperatures ranging from 70 to 90 °C and pressures up to 1.5 MPa: propane/H_2/toluene, propane/CO/toluene, propylene/H_2/toluene, propylene/CO/toluene, propane/H_2/NX-795, propane/CO/NX-795, propylene/H_2/NX-795 and propylene/CO/NX-795. The measured solubilities of H_2 and CO in conventional solvents were consistent with literature values. At identical H_2 or CO fugacities in the vapor phase, the solubilities of H_2 and CO in either propane- or propylene-expanded solvents are greater than those in the corresponding neat solvents by as high as 76% at 70 °C and 1.5 MPa. Whereas the H_2/CO ratio in the neat solvent at a given temperature is constant at *all* syngas partial pressures, it is enhanced in gas-expanded liquid phase with increased propane or propylene partial pressures. By modelling the vapor and the gas-expanded liquid phases as pseudo-binary systems, the Peng-Robenson equation of state (PR-EoS) with van der Waals' mixing rules and binary interaction parameters predict the experimental VLE data very well.

Refinery-grade propane/propylene mixtures were demonstrated can be used directly for propylene hydroformylation without the need for purification to obtain polymer-grade propylene. Because the hydroformylation of propylene in the mixed stream is selective, an enriched propane stream that may be recycled for producing more propylene results. In addition to the energy savings and resulting economic/environmental benefits, the mixed propylene/propane feed also provides reaction benefits by volumetrically expanding the reaction mixture to yield the so-called gas-expanded liquids (GXLs). Unlike conventional reaction media, the H_2/CO ratio in GXL media can be enhanced by simply increasing the partial pressure of propane. For rhodium/triphenylphosphine catalyzed propylene hydroformylation performed between 343.15 K to 363.15 K and pressured up to 2.0 MPa, the *n/i* aldehyde ratio in GXL media is increased by up to 45% compared to conventional media. The increased H_2/CO ratio in the GXL phase favors the reaction pathway responsible for producing the linear aldehyde.

Comparative economic analyses of the integrated propane dehydrogenation and propylene hydroformylation process shows a more than 30% lower capital investment for the PXL process compared to the conventional process with propane/propylene separation by distillation. Without the use of high energy consuming C3 distillation columns, the annual utility cost in PXL process is 20% less than the conventional process, resulting in total 8% annual production cost saving. The comparative environmental impact analysis by EIO-LCA method shows the adverse environmental impacts (greenhouse gas emission, air pollutants emission, and toxic release) associated with the PXL process are significantly lower than the conventional process for its much less material and energy consumption.

The use of *n*-butane expanded liquids (BXLs) as reaction media for Co-catalyzed hydroformylation of 1-octene at 180°C was demonstrated for the first time. The volume of liquid

phase 1-octene as well as typical hydroformylation mixtures could be increased significantly with the addition of *n*-butane even at high temperature (up to 50% increase at 1.8 MPa of *n*-butane at 180 °C). Co-catalyzed 1-octene hydroformylation with triphenylphosphine ligand in neat solvent media (without *n*-butane addition) and *n*-butane expanded media was compared at identical concentrations of the substrate (1-octene), catalyst and the batch run time. The reaction results show that the TOF was enhanced more than 20% within the homogeneous reaction region in BXL system at a 20% reduction in the organic solvent usage. The higher TOF in BXLs is attributed to the improved syngas availability in the liquid phase compared to neat solvent.

Metal leaching from supported ionic liquid phase (SILP) catalysts in neat organic solvent, *sc*CO_2 and liquefied propylene as well as during hydroformylation of olefins (1-octene, propylene and butadiene) were investigated. The SILP catalyst (Rh with sulfxantphos ligand) works well for the hydroformylation of propane/propylene mixtures. The *n/i* ratio and TOF obtained are comparable with pure propylene as feedstock. The hydroformylation of butadiene was also demonstrated with SILP-xantphos catalyst for the first time. The target product yield is comparable with a homogeneous complex tested at similar conditions implying that the SILP formulation has the potential for further study. For all the cases tested, the SILP catalyst is more stable (i.e., more leach resistant) in supercritical CO_2 and liquefied propylene than in organic solvents.

7.2 Recommendations

- The current study has shown that refinery-grade propane/propylene mixtures can be used directly for propylene hydroformylation under semi-batch operation without the need for further purification. Development and validation of a continuous process is important to verify its operational statue.

- In order to broaden the applications of the gas-expanded liquids (GXLs) based hydroformylation, it will be extremely beneficial to develop a mathematical model of GXL-based reactor. Rational design and scale-up will be facilitated by such a mathematical model. Detailed kinetic studies of the PXL process are also necessary for better understanding of the reaction mechanism.
- Catalyst precipitation was observed in Co/TPP system around 1.3 MPa in *n*-butane expanded solvents mixtures. In this situation, significant reductions in the reaction rate and nonanol yield are observed. To take advantage of all the benefits of gas-expanded solvents, catalyst systems with high solubility in GXL should be developed. Promising candidates include Co complexes containing fluorophosphines that have been reported to exhibit high solubility in $scCO_2$ and enhanced performance for 1-octene hydroformylation
- The idea of using gas-expanded liquids to tune H_2/CO ratio may also find application in Ir and Ru catalyzed hydroformylation reactions. It will be extremely interesting to see if enhanced TOF and *n*/*i* can also attainable with other metal-catalyzed reactions, considering lower activity and selectivity for Ir[64] and Ru[58] catalyzed hydroformylation.
- Preliminary results show that SILP catalysts (Rh/Sulfxantphos) are active for hydroformylation of propane/propylene mixtures in a semi-batch reactor. Further studies including continuous gas-phase hydroformylation in fixed bed reactor are needed to demonstrate its advantages.
- The SILP concept has been successfully applied to gas-phase hydroformylation[92] but its application to liquid phase reaction is limited by significant metal leaching. Here, we demonstrate the SILP catalyst is more stable (i.e., more leach resistant) in supercritical CO_2 and liquefied propylene than in organic solvents. The application of sub- or super- critical

solvents as reaction medium may be a promising solution to improve its stability and even activity for liquid phase hydroformylation reactions.

- The utilization of carbon dioxide as a nontoxic and inexpensive C-1 building block is of widespread interest. Previous work has demonstrated that olefins could be converted to aldehyde or alcohol under a tandem reverse water-gas shift (RWGS)-hydroformylation reaction with Ru, Rd or Fe based catalyst using CO_2 and H_2 as feedstock.[61, 215-216] The concept of CO_2-expanded liquid may also work for this system to enhance the reaction rate and suppress the side reaction.

References

1. Sheldon, R. A., Engineering a more sustainable world through catalysis and green chemistry. *Journal of The Royal Society Interface* **2016,** *13* (116), 20160087.

2. García-Serna, J.; Pérez-Barrigón, L.; Cocero, M., New trends for design towards sustainability in chemical engineering: Green engineering. *Chemical Engineering Journal* **2007,** *133* (1-3), 7-30.

3. Tang, S. L.; Smith, R. L.; Poliakoff, M., Principles of green chemistry: PRODUCTIVELY. *Green Chemistry* **2005,** *7* (11), 761-762.

4. Lee, H.-J.; Ghanta, M.; Busch, D. H.; Subramaniam, B., Toward a CO2-free ethylene oxide process: Homogeneous ethylene oxide in gas-expanded liquids. *Chemical Engineering Science* **2010,** *65* (1), 128-134.

5. Li, M.; Niu, F.; Zuo, X.; Metelski, P. D.; Busch, D. H.; Subramaniam, B., A spray reactor concept for catalytic oxidation of p-xylene to produce high-purity terephthalic acid. *Chemical Engineering Science* **2013,** *104*, 93-102.

6. Yan, W.; Ramanathan, A.; Patel, P. D.; Maiti, S. K.; Laird, B. B.; Thompson, W. H.; Subramaniam, B., Mechanistic insights for enhancing activity and stability of Nb-incorporated silicates for selective ethylene epoxidation. *Journal of Catalysis* **2016,** *336*, 75-84.

7. Jin, H.; Subramaniam, B., Homogeneous catalytic hydroformylation of 1-octene in CO2-expanded solvent media. *Chemical engineering science* **2004,** *59* (22-23), 4887-4893.

8. Xie, Z.; Subramaniam, B., Development of a Greener Hydroformylation Process Guided by Quantitative Sustainability Assessments. *ACS Sustainable Chemistry & Engineering* **2014,** *2* (12), 2748-2757.

9. Wu, J.-F.; Ramanathan, A.; Subramaniam, B., Novel tungsten-incorporated mesoporous silicates synthesized via evaporation-induced self-assembly: Enhanced metathesis performance. *Journal of Catalysis* **2017,** *350*, 182-188.

10. Ramanathan, A.; Wu, J.-F.; Maheswari, R.; Hu, Y.; Subramaniam, B., Synthesis of molybdenum-incorporated mesoporous silicates by evaporation-induced self-assembly: Insights into surface oxide species and corresponding olefin metathesis activity. *Microporous and Mesoporous Materials* **2017,** *245*, 118-125.

11. Chaudhari, R. V.; Torres, A.; Jin, X.; Subramaniam, B., Multiphase catalytic hydrogenolysis/hydrodeoxygenation processes for chemicals from renewable feedstocks: kinetics, mechanism, and reaction engineering. *Industrial & Engineering Chemistry Research* **2013,** *52* (44), 15226-15243.

12. Jin, X.; Shen, J.; Yan, W.; Zhao, M.; Thapa, P. S.; Subramaniam, B.; Chaudhari, R. V., Sorbitol hydrogenolysis over hybrid Cu/CaO-Al2O3 catalysts: tunable activity and selectivity with solid base incorporation. *ACS Catalysis* **2015,** *5* (11), 6545-6558.

13. Xie, Z.; Fang, J.; Subramaniam, B.; Maiti, S. K.; Snavely, W.; Tunge, J. A., Enhanced hydroformylation by carbon dioxide-expanded media with soluble Rh complexes in nanofiltration membrane reactors. *AIChE Journal* **2013,** *59* (11), 4287-4296.

14. Jin, H.; Subramaniam, B., Homogeneous catalytic hydroformylation of 1-octene in CO 2-expanded solvent media. *Chemical engineering science* **2004,** *59* (22), 4887-4893.

15. Van Leeuwen, P. W.; Claver, C., *Rhodium catalyzed hydroformylation*. Springer Science & Business Media: 2002; Vol. 22.

16. Franke, R.; Selent, D.; Börner, A., Applied hydroformylation. *Chemical reviews* **2012,** *112* (11), 5675-5732.

17. Eilbracht, P.; Schmidt, A. M., Synthetic applications of tandem reaction sequences involving hydroformylation. In *Catalytic Carbonylation Reactions*, Springer: 2006; pp 65-95.

18. ALDEHYDE MARKET IS EXPECTED TO REACH USD 5.7 BILLION BY 2022. (accessed 0228).

19. Adkins, H.; Krsek, G., Hydroformylation of unsaturated compounds with a cobalt carbonyl catalyst. *Journal of the American Chemical Society* **1949,** *71* (9), 3051-3055.

20. Slaugh, L. H.; Mullineaux, R. D., Novel hydroformylation catalysts. *Journal of Organometallic Chemistry* **1968,** *13* (2), 469-477.

21. Gorbunov, D.; Volkov, A.; Kardasheva, Y. S.; Maksimov, A.; Karakhanov, E., Hydroformylation in petroleum chemistry and organic synthesis: Implementation of the process and solving the problem of recycling homogeneous catalysts. *Petroleum Chemistry* **2015,** *55* (8), 587-603.

22. Pruett, R. L.; Smith, J. A., Low-pressure system for producing normal aldehydes by hydroformylation of. alpha.-olefins. *The Journal of Organic Chemistry* **1969,** *34* (2), 327-330.

23. Evans, D.; Yagupsky, G.; Wilkinson, G., The reaction of hydridocarbonyltris (triphenylphosphine) rhodium with carbon monoxide, and of the reaction products, hydridodicarbonylbis (triphenylphosphine) rhodium and dimeric species, with hydrogen. *Journal of the Chemical Society A: Inorganic, Physical, Theoretical* **1968**, 2660-2665.

24. Evans, D.; Osborn, J.; Wilkinson, G., Hydroformylation of alkenes by use of rhodium complex catalysts. *Journal of the Chemical Society A: Inorganic, Physical, Theoretical* **1968**, 3133-3142.

25. Bohnen, H.-W.; Cornils, B., Hydroformylation of alkenes: An industrial view of the status and importance. **2002**.

26. Beller, M.; Cornils, B.; Frohning, C. D.; Kohlpaintner, C. W., Progress in hydroformylation and carbonylation. *Journal of Molecular Catalysis A: Chemical* **1995,** *104* (1), 17-85.

27. Tudor, R.; Ashley, M., Enhancement of industrial hydroformylation processes by the adoption of rhodium-based catalyst: Part I. *Platinum Metals Review* **2007,** *51* (3), 116-126.

28. Tudor, B. R.; Ashley, M., Enhancement of industrial hydroformylation processes by the adoption of rhodium-based catalyst: part II. *Platinum Metals Review* **2007,** *51* (4), 164-171.

29. Rhodium price. (accessed 0305).

30. Cobalt Price. (accessed 0305).

31. Kohlpaintner, C. W.; Fischer, R. W.; Cornils, B., Aqueous biphasic catalysis: Ruhrchemie/Rhône-Poulenc oxo process. *Applied Catalysis A: General* **2001,** *221* (1-2), 219-225.

32. Cornils, B.; Kuntz, E. G., Introducing TPPTS and related ligands for industrial biphasic processes. *Journal of organometallic chemistry* **1995,** *502* (1-2), 177-186.

33. Li, C.; Yan, L.; Lu, L.; Xiong, K.; Wang, W.; Jiang, M.; Liu, J.; Song, X.; Zhan, Z.; Jiang, Z., Single atom dispersed Rh-biphephos&PPh 3@ porous organic copolymers: highly efficient catalysts for continuous fixed-bed hydroformylation of propene. *Green Chemistry* **2016,** *18* (10), 2995-3005.

34. Weiß, A.; Munoz, M.; Haas, A.; Rietzler, F.; Steinrück, H.-P.; Haumann, M.; Wasserscheid, P.; Etzold, B. J., Boosting the Activity in Supported Ionic Liquid-Phase-Catalyzed Hydroformylation via Surface Functionalization of the Carbon Support. *ACS Catalysis* **2016,** *6* (4), 2280-2286.

35. Hou, C.; Zhao, G.; Ji, Y.; Niu, Z.; Wang, D.; Li, Y., Hydroformylation of alkenes over rhodium supported on the metal-organic framework ZIF-8. *Nano Research* **2014,** *7* (9), 1364-1369.

36. Fang, J.; Jana, R.; Tunge, J. A.; Subramaniam, B., Continuous homogeneous hydroformylation with bulky rhodium catalyst complexes retained by nano-filtration membranes. *Applied Catalysis A: General* **2011,** *393* (1-2), 294-301.

37. Dreimann, J. M.; Skiborowski, M.; Behr, A.; Vorholt, A. J., Recycling homogeneous catalysts simply by organic solvent nanofiltration: new ways to efficient catalysis. *ChemCatChem* **2016,** *8* (21), 3330-3333.

38. Janssen, M.; Wilting, J.; Müller, C.; Vogt, D., Continuous Rhodium-Catalyzed Hydroformylation of 1-Octene with Polyhedral Oligomeric Silsesquioxanes (POSS) Enlarged Triphenylphosphine. *Angewandte Chemie International Edition* **2010,** *49* (42), 7738-7741.

39. Hamerla, T.; Rost, A.; Kasaka, Y.; Schomäcker, R., Hydroformylation of 1-Dodecene with Water-Soluble Rhodium Catalysts with Bidentate Ligands in Multiphase Systems. *ChemCatChem* **2013,** *5* (7), 1854-1862.

40. Rost, A.; Müller, M.; Hamerla, T.; Kasaka, Y.; Wozny, G.; Schomäcker, R., Development of a continuous process for the hydroformylation of long-chain olefins in aqueous multiphase systems. *Chemical Engineering and Processing: Process Intensification* **2013,** *67*, 130-135.

41. Pogrzeba, T.; Müller, D.; Hamerla, T.; Esche, E.; Paul, N.; Wozny, G. n.; Schomäcker, R., Rhodium-catalyzed hydroformylation of long-chain olefins in aqueous multiphase systems in a continuously operated miniplant. *Industrial & Engineering Chemistry Research* **2015,** *54* (48), 11953-11960.

42. Chikkali, S. H.; van der Vlugt, J. I.; Reek, J. N., Hybrid diphosphorus ligands in rhodium catalysed asymmetric hydroformylation. *Coordination chemistry reviews* **2014,** *262*, 1-15.

43. Mon, I.; Jose, D. A.; Vidal-Ferran, A., Bis (phosphite) Ligands with Distal Regulation: Application in Rhodium-mediated Asymmetric Hydroformylations. *Chemistry-A European Journal* **2013,** *19* (8), 2720-2725.

44. Allmendinger, S.; Kinuta, H.; Breit, B., Easily Accessible TADDOL-Derived Bisphosphonite Ligands: Synthesis and Application in the Asymmetric Hydroformylation of Vinylarenes. *Advanced Synthesis & Catalysis* **2015,** *357* (1), 41-45.

45. Kämper, A.; Kucmierczyk, P.; Seidensticker, T.; Vorholt, A. J.; Franke, R.; Behr, A., Ruthenium-catalyzed hydroformylation: from laboratory to continuous miniplant scale. *Catalysis Science & Technology* **2016,** *6* (22), 8072-8079.

46. Rieger, B.; Plikhta, A.; Castillo-Molina, D. A., Ionic Liquids in Transition Metal-Catalyzed Hydroformylation Reactions. In *Ionic Liquids (ILs) in Organometallic Catalysis*, Springer: 2014; pp 95-144.

47. Ramalho, H. F.; di Ferreira, K. M.; Machado, P. M.; Oliveira, R. S.; Silva, L. P.; Prauchner, M. J.; Suarez, P. A., Biphasic hydroformylation of soybean biodiesel using a rhodium complex dissolved in ionic liquid. *Industrial Crops and Products* **2014,** *52*, 211-218.

48. Koeken, A. C.; Smeets, N. M., A bulky phosphite modified rhodium catalyst for efficient hydroformylation of disubstituted alkenes and macromonomers in supercritical carbon dioxide. *Catalysis Science & Technology* **2013,** *3* (4), 1036-1045.

49. Pospech, J.; Fleischer, I.; Franke, R.; Buchholz, S.; Beller, M., Alternative metals for homogeneous catalyzed hydroformylation reactions. *Angewandte Chemie International Edition* **2013,** *52* (10), 2852-2872.

50. Fox, D. J.; Duckett, S. B.; Flaschenriem, C.; Brennessel, W. W.; Schneider, J.; Gunay, A.; Eisenberg, R., A model iridium hydroformylation system with the large bite angle ligand xantphos: Reactivity with parahydrogen and implications for hydroformylation catalysis. *Inorganic chemistry* **2006,** *45* (18), 7197-7209.

51. Ren, W.; Chang, W.; Dai, J.; Shi, Y.; Li, J.; Shi, Y., An Effective Pd-Catalyzed Regioselective Hydroformylation of Olefins with Formic Acid. *Journal of the American Chemical Society* **2016,** *138* (45), 14864-14867.

52. Chuang, S. S., Sulfided group VIII metals for hydroformylation. *Applied catalysis* **1990,** *66* (1), L1-L6.

53. Takahashi, N.; Tobise, T.; Mogi, I.; Sasaki, M.; Mijin, A.; Fujimoto, T.; Ichikawa, M., Effects of Pd Dispersion on the Catalytic Activity of Pd/SiO2 for Ethylene Hydroformylation. *Bulletin of the Chemical Society of Japan* **1992,** *65* (9), 2565-2567.

54. Pruchnik, F. P., *Organometallic chemistry of the transition elements*. Springer Science & Business Media: 2013.

55. Evans, D.; Osborn, J.; Jardine, F.; Wilkinson, G., Homogeneous hydrogenation and hydroformylation using ruthenium complexes. *Nature* **1965,** *208* (5016), 1203.

56. Takahashi, K.; Yamashita, M.; Tanaka, Y.; Nozaki, K., Ruthenium/C5Me5/Bisphosphine-or Bisphosphite-Based Catalysts for normal-Selective Hydroformylation. *Angewandte Chemie* **2012,** *124* (18), 4459-4463.

57. Fleischer, I.; Wu, L.; Profir, I.; Jackstell, R.; Franke, R.; Beller, M., Towards the Development of a Selective Ruthenium-Catalyzed Hydroformylation of Olefins. *Chemistry-A European Journal* **2013,** *19* (32), 10589-10594.

58. Wu, L.; Fleischer, I.; Jackstell, R.; Profir, I.; Franke, R.; Beller, M., Ruthenium-catalyzed hydroformylation/reduction of olefins to alcohols: extending the scope to internal alkenes. *Journal of the American Chemical Society* **2013,** *135* (38), 14306-14312.

59. Tominaga, K.-i.; Sasaki, Y., Ruthenium complex-catalyzed hydroformylation of alkenes with carbon dioxide. *Catalysis Communications* **2000,** *1* (1-4), 1-3.

60. Tominaga, K.-i.; Sasaki, Y., Ruthenium-catalyzed one-pot hydroformylation of alkenes using carbon dioxide as a reactant. *Journal of Molecular Catalysis A: Chemical* **2004,** *220* (2), 159-165.

61. Liu, Q.; Wu, L.; Fleischer, I.; Selent, D.; Franke, R.; Jackstell, R.; Beller, M., Development of a ruthenium/phosphite catalyst system for domino hydroformylation–reduction of olefins with carbon dioxide. *Chemistry-A European Journal* **2014,** *20* (23), 6888-6894.

62. Piras, I.; Jennerjahn, R.; Jackstell, R.; Spannenberg, A.; Franke, R.; Beller, M., A General and Efficient Iridium-Catalyzed Hydroformylation of Olefins. *Angewandte Chemie* **2011,** *123* (1), 294-298.

63. Behr, A.; Kämper, A.; Nickel, M.; Franke, R., Crucial role of additives in iridium-catalyzed hydroformylation. *Applied Catalysis A: General* **2015,** *505*, 243-248.

64. Kämper, A.; Warrelmann, S. J.; Reiswich, K.; Kuhlmann, R.; Franke, R.; Behr, A., First iridium-catalyzed hydroformylation in a continuously operated miniplant. *Chemical Engineering Science* **2016,** *144*, 364-371.

65. Barbaro, P.; Liguori, F., *Heterogenized homogeneous catalysts for fine chemicals production: materials and processes*. Springer Science & Business Media: 2010; Vol. 33.

66. Neves, Â. C.; Calvete, M. J.; Pinho e Melo, T. M.; Pereira, M. M., Immobilized catalysts for hydroformylation reactions: A versatile tool for aldehyde synthesis. *European Journal of Organic Chemistry* **2012,** *2012* (32), 6309-6320.

67. Li, X.; Ding, Y.; Jiao, G.; Li, J.; Ya, L.; Zhu, H., Hydroformylation of methyl-3-pentenoate over a phosphite ligand modified Rh/SiO2 catalyst. *Journal of Natural Gas Chemistry* **2008,** *17* (4), 351-354.

68. Li, X.; Ding, Y.; Jiao, G.; Li, J.; Lin, R.; Gong, L.; Yan, L.; Zhu, H., A new concept of tethered ligand-modified Rh/SiO2 catalyst for hydroformylation with high stability. *Applied Catalysis A: General* **2009,** *353* (2), 266-270.

69. He, Y.; Chen, G.; Kawi, S.; Wong, S., Catalytic study of MCM-41 immobilized RhCl 3 for the hydroformylation of styrene. *Journal of Porous Materials* **2009,** *16* (6), 721.

70. Bae, J. A.; Song, K.-C.; Jeon, J.-K.; Ko, Y. S.; Park, Y.-K.; Yim, J.-H., Effect of pore structure of amine-functionalized mesoporous silica-supported rhodium catalysts on 1-octene hydroformylation. *Microporous and Mesoporous Materials* **2009,** *123* (1-3), 289-297.

71. Zhou, W.; He, D., A facile method for promoting activities of ordered mesoporous silica-anchored Rh–P complex catalysts in 1-octene hydroformylation. *Green Chemistry* **2009,** *11* (8), 1146-1154.

72. Sharma, S. K.; Parikh, P. A.; Jasra, R. V., Hydroformylation of alkenes using heterogeneous catalyst prepared by intercalation of HRh (CO)(TPPTS) 3 complex in hydrotalcite. *Journal of Molecular Catalysis A: Chemical* **2010,** *316* (1-2), 153-162.

73. Mukhopadhyay, K.; Mandale, A. B.; Chaudhari, R. V., Encapsulated HRh (CO)(PPh3) 3 in microporous and mesoporous supports: novel heterogeneous catalysts for hydroformylation. *Chemistry of materials* **2003,** *15* (9), 1766-1777.

74. Li, B.; Li, X.; Asami, K.; Fujimoto, K., Hydroformylation of 1-hexene over rhodium supported on active carbon catalyst. *Chemistry letters* **2003,** *32* (4), 378-379.

75. Wang, F.; Mielby, J.; Richter, F. H.; Wang, G.; Prieto, G.; Kasama, T.; Weidenthaler, C.; Bongard, H. J.; Kegnæs, S.; Fürstner, A., A polyphenylene support for Pd catalysts with exceptional catalytic activity. *Angewandte Chemie International Edition* **2014,** *53* (33), 8645-8648.

76. Kim, J. Y.; Park, J. H.; Jung, O.-S.; Chung, Y. K.; Park, K. H., Heterogenized Catalysts Containing Cobalt–Rhodium Heterobimetallic Nanoparticles for Olefin Hydroformylation. *Catalysis letters* **2009,** *128* (3-4), 483-486.

77. Sun, Q.; Dai, Z.; Liu, X.; Sheng, N.; Deng, F.; Meng, X.; Xiao, F.-S., Highly efficient heterogeneous hydroformylation over Rh-metalated porous organic polymers: synergistic effect of high ligand concentration and flexible framework. *Journal of the American Chemical Society* **2015,** *137* (15), 5204-5209.

78. Lang, R.; Li, T.; Matsumura, D.; Miao, S.; Ren, Y.; Cui, Y. T.; Tan, Y.; Qiao, B.; Li, L.; Wang, A., Hydroformylation of Olefins by a Rhodium Single-Atom Catalyst with Activity Comparable to RhCl (PPh3) 3. *Angewandte Chemie International Edition* **2016,** *55* (52), 16054-16058.

79. Rogers, R. D.; Seddon, K. R., Ionic liquids--solvents of the future? *Science* **2003,** *302* (5646), 792-793.

80. Amarasekara, A. S., Acidic ionic liquids. *Chemical reviews* **2016,** *116* (10), 6133-6183.

81. Vekariya, R. L., A review of ionic liquids: applications towards catalytic organic transformations. *Journal of Molecular Liquids* **2017,** *227*, 44-60.

82. Chauvin, Y.; Mussmann, L.; Olivier, H., A novel class of versatile solvents for two-phase catalysis: hydrogenation, isomerization, and hydroformylation of alkenes catalyzed by rhodium complexes in liquid 1, 3-dialkylimidazolium salts. *Angewandte Chemie International Edition* **1996,** *34* (23-24), 2698-2700.

83. Brauer, D. J.; Kottsieper, K. W.; Liek, C.; Stelzer, O.; Waffenschmidt, H.; Wasserscheid, P., Phosphines with 2-imidazolium and para-phenyl-2-imidazolium moieties—synthesis and application in two-phase catalysis. *Journal of Organometallic Chemistry* **2001,** *630* (2), 177-184.

84. Sheldon, R., Catalytic reactions in ionic liquids. *Chemical Communications* **2001,** (23), 2399-2407.

85. Bronger, R. P.; Silva, S. M.; Kamer, P. C.; van Leeuwen, P. W., A novel dicationic phenoxaphosphino-modified Xantphos-type ligand—a unique ligand specifically designed for a high activity, selectivity and recyclability. *Chemical Communications* **2002,** (24), 3044-3045.

86. Haumann, M.; Riisager, A., Hydroformylation in room temperature ionic liquids (RTILs): catalyst and process developments. *Chemical reviews* **2008,** *108* (4), 1474-1497.

87. Lin, Q.; Jiang, W.; Fu, H.; Chen, H.; Li, X., Hydroformylation of higher olefin in halogen-free ionic liquids catalyzed by water-soluble rhodium–phosphine complexes. *Applied Catalysis A: General* **2007,** *328* (1), 83-87.

88. Mehnert, C. P.; Mozeleski, E. J.; Cook, R. A., Supported ionic liquid catalysis investigated for hydrogenation reactions. *Chemical Communications* **2002,** (24), 3010-3011.

89. Mehnert, C. P.; Cook, R. A.; Dispenziere, N. C.; Afeworki, M., Supported ionic liquid catalysis− A new concept for homogeneous hydroformylation catalysis. *Journal of the American Chemical Society* **2002,** *124* (44), 12932-12933.

90. Riisager, A.; Eriksen, K. M.; Wasserscheid, P.; Fehrmann, R., Propene and 1-octene hydroformylation with silica-supported, ionic liquid-phase (SILP) Rh-phosphine catalysts in continuous fixed-bed mode. *Catalysis Letters* **2003,** *90* (3-4), 149-153.

91. Riisager, A.; Wasserscheid, P.; van Hal, R.; Fehrmann, R., Continuous fixed-bed gas-phase hydroformylation using supported ionic liquid-phase (SILP) Rh catalysts. *Journal of Catalysis* **2003,** *219* (2), 452-455.

92. Haumann, M.; Dentler, K.; Joni, J.; Riisager, A.; Wasserscheid, P., Continuous Gas-Phase Hydroformylation of 1-Butene using Supported Ionic Liquid Phase (SILP) Catalysts. *Advanced Synthesis & Catalysis* **2007,** *349* (3), 425-431.

93. Haumann, M.; Jakuttis, M.; Franke, R.; Schönweiz, A.; Wasserscheid, P., Continuous Gas-Phase Hydroformylation of a Highly Diluted Technical C4 Feed using Supported Ionic Liquid Phase Catalysts. *ChemCatChem* **2011,** *3* (11), 1822-1827.

94. Mehnert, C. P., Supported ionic liquid catalysis. *Chemistry-A European Journal* **2005,** *11* (1), 50-56.

95. Olmos, A.; Asensio, G.; Pérez, P. J., Homogeneous metal-based catalysis in supercritical carbon dioxide as reaction medium. *ACS Catalysis* **2016,** *6* (7), 4265-4280.

96. Rathke, J.; Klingler, R.; Krause, T., Propylene hydroformylation in supercritical carbon dioxide. *Organometallics* **1991,** *10* (5), 1350-1355.

97. Guo, Y.; Akgerman, A., Hydroformylation of propylene in supercritical carbon dioxide. *Industrial & engineering chemistry research* **1997,** *36* (11), 4581-4585.

98. Jessop, P. G.; Ikariya, T.; Noyori, R., Homogeneous catalysis in supercritical fluids. *Chemical Reviews* **1999,** *99* (2), 475-494.

99. Fujita, S.-i.; Fujisawa, S.; Bhanage, B. M.; Ikushima, Y.; Arai, M., Hydroformylation of 1-hexene catalyzed with rhodium fluorinated phosphine complexes in supercritical carbon dioxide and in conventional organic solvents: effects of ligands and pressures. *New Journal of Chemistry* **2002,** *26* (10), 1479-1484.

100. Palo, D. R.; Erkey, C., Homogeneous catalytic hydroformylation of 1-octene in supercritical carbon dioxide using a novel rhodium catalyst with fluorinated arylphosphine ligands. *Industrial & engineering chemistry research* **1998,** *37* (10), 4203-4206.

101. Davis, T.; Erkey, C., Hydroformylation of Higher Olefins in Supercritical Carbon Dioxide with HRh (CO)[P (3, 5-(CF3) 2− C6H3) 3] 3. *Industrial & engineering chemistry research* **2000,** *39* (10), 3671-3678.

102. Palo, D. R.; Erkey, C., Homogeneous hydroformylation of 1-octene in supercritical carbon dioxide with [RhH (CO)(P (p-CF3C6H4) 3) 3]. *Industrial & engineering chemistry research* **1999,** *38* (5), 2163-2165.

103. Palo, D. R.; Erkey, C., Kinetics of the homogeneous catalytic hydroformylation of 1-octene in supercritical carbon dioxide with HRh (CO)[P (p-CF3C6H4) 3] 3. *Industrial & engineering chemistry research* **1999,** *38* (10), 3786-3792.

104. Sellin, M. F.; Webb, P. B.; Cole-Hamilton, D. J., Continuous flow homogeneous catalysis: hydroformylation of alkenes in supercritical fluid–ionic liquid biphasic mixtures. *Chemical Communications* **2001,** (8), 781-782.

105. Sellin, M. F.; Cole-Hamilton, D. J., Hydroformylation reactions in supercritical carbon dioxide using insoluble metal complexes. *Journal of the Chemical Society, Dalton Transactions* **2000,** (11), 1681-1683.

106. Scurto, A. M.; Aki, S. N.; Brennecke, J. F., CO2 as a separation switch for ionic liquid/organic mixtures. *Journal of the American Chemical Society* **2002,** *124* (35), 10276-10277.

107. Ahosseini, A.; Ren, W.; Scurto, A. M., Understanding biphasic ionic liquid/CO2 systems for homogeneous catalysis: hydroformylation. *Industrial & Engineering Chemistry Research* **2009,** *48* (9), 4254-4265.

108. Hintermair, U.; Gong, Z.; Serbanovic, A.; Muldoon, M. J.; Santini, C. C.; Cole-Hamilton, D. J., Continuous flow hydroformylation using supported ionic liquid phase catalysts with carbon dioxide as a carrier. *Dalton transactions* **2010,** *39* (36), 8501-8510.

109. Hintermair, U.; Zhao, G.; Santini, C. C.; Muldoon, M. J.; Cole-Hamilton, D. J., Supported ionic liquid phase catalysis with supercritical flow. *Chemical Communications* **2007,** (14), 1462-1464.

110. Cole-Hamilton, D. J., Homogeneous catalysis--new approaches to catalyst separation, recovery, and recycling. *Science* **2003,** *299* (5613), 1702-1706.

111. Vogl, C.; Paetzold, E.; Fischer, C.; Kragl, U., Highly selective hydroformylation of internal and terminal olefins to terminal aldehydes using a rhodium-BIPHEPHOS-catalyst system. *Journal of Molecular Catalysis A: Chemical* **2005,** *232* (1-2), 41-44.

112. Sandee, A. J.; van der Veen, L. A.; Reek, J. N.; Kamer, P. C.; Lutz, M.; Spek, A. L.; van Leeuwen, P. W., A robust, environmentally benign catalyst for highly selective hydroformylation. *Angewandte Chemie International Edition* **1999,** *38* (21), 3231-3235.

113. Horváth, I. T.; Kiss, G.; Cook, R. A.; Bond, J. E.; Stevens, P. A.; Rábai, J.; Mozeleski, E. J., Molecular engineering in homogeneous catalysis: One-phase catalysis coupled with biphase catalyst separation. The fluorous-soluble HRh (CO){P [CH2CH2 (CF2) 5CF3] 3} 3 hydroformylation system. *Journal of the American Chemical Society* **1998,** *120* (13), 3133-3143.

114. Shaharun, M. S.; Dutta, B. K.; Mukhtar, H.; Maitra, S., Hydroformylation of 1-octene using rhodium–phosphite catalyst in a thermomorphic solvent system. *Chemical Engineering Science* **2010,** *65* (1), 273-281.

115. Koch, D.; Leitner, W., Rhodium-catalyzed hydroformylation in supercritical carbon dioxide. *Journal of the American Chemical Society* **1998,** *120* (51), 13398-13404.

116. Wasserscheid, P.; van Hal, R.; Bösmann, A., 1-n-Butyl-3-methylimidazolium ([bmim]) octylsulfate—an even 'greener'ionic liquid. *Green Chemistry* **2002,** *4* (4), 400-404.

117. Webb, P. B.; Kunene, T. E.; Cole-Hamilton, D. J., Continuous flow homogeneous hydroformylation of alkenes using supercritical fluids. *Green Chemistry* **2005,** *7* (5), 373-379.

118. Subramaniam, B.; Chaudhari, R. V.; Chaudhari, A. S.; Akien, G. R.; Xie, Z., Supercritical fluids and gas-expanded liquids as tunable media for multiphase catalytic reactions. *Chemical Engineering Science* **2014,** *115*, 3-18.

119. Akien, G. R.; Poliakoff, M., A critical look at reactions in class I and II gas-expanded liquids using CO2 and other gases. *Green Chemistry* **2009,** *11* (8), 1083-1100.

120. Subramaniam, B., Exploiting neoteric solvents for sustainable catalysis and reaction engineering: opportunities and challenges. *Industrial & Engineering Chemistry Research* **2010,** *49* (21), 10218-10229.

121. Jessop, P. G.; Subramaniam, B., Gas-expanded liquids. *Chemical reviews* **2007,** *107* (6), 2666-2694.

122. Lopez-Castillo, Z. K.; Aki, S. N.; Stadtherr, M. A.; Brennecke, J. F., Enhanced solubility of hydrogen in CO2-expanded liquids. *Industrial & Engineering Chemistry Research* **2008,** *47* (3), 570-576.

123. Lopez-Castillo, Z. K.; Aki, S. N.; Stadtherr, M. A.; Brennecke, J. F., Enhanced solubility of oxygen and carbon monoxide in CO2-expanded liquids. *Industrial & engineering chemistry research* **2006,** *45* (15), 5351-5360.

124. Xie, Z.; Snavely, W. K.; Scurto, A. M.; Subramaniam, B., Solubilities of CO and H2 in neat and CO2-expanded hydroformylation reaction mixtures containing 1-Octene and nonanal up to 353.15 K and 9 MPa. *Journal of Chemical & Engineering Data* **2009,** *54* (5), 1633-1642.

125. Ye, K.; Freund, H.; Xie, Z.; Subramaniam, B.; Sundmacher, K., Prediction of multicomponent phase behavior of CO2-expanded liquids using CEoS/GE models and comparison with experimental data. *The Journal of Supercritical Fluids* **2012,** *67*, 41-52.

126. Lee, H.-J.; Ghanta, M.; Busch, D. H.; Subramaniam, B., Toward a CO 2-free ethylene oxide process: homogeneous ethylene oxide in gas-expanded liquids. *Chemical Engineering Science* **2010,** *65* (1), 128-134.

127. Subramaniam, B.; Akien, G. R., Sustainable catalytic reaction engineering with gas-expanded liquids. *Current Opinion in Chemical Engineering* **2012,** *1* (3), 336-341.

128. Takegami, Y.; Watanabe, Y.; Masada, H.; Mitsudo, T., Studies of the Organic Reactions of Metal Carbonyls. XVI. Solvent Effects on the Hydroformylation of Propylene and on the Reaction of Cobalt Hydrocarbonyl with 1-Pentene. *Bulletin of the Chemical Society of Japan* **1969,** *42* (1), 206-210.

129. Craddock, J.; Hershman, A.; Paulik, F.; Roth, J., Hydroformylation Catalysis by Arylphosphine Complexes of Rhodium. *Industrial & Engineering Chemistry Product Research and Development* **1969,** *8* (3), 291-297.

130. Purwanto; Deshpande, R.; Chaudhari, R.; Delmas, H., Solubility of hydrogen, carbon monoxide, and 1-octene in various solvents and solvent mixtures. *Journal of Chemical & Engineering Data* **1996,** *41* (6), 1414-1417.

131. Jin, H.; Subramaniam, B.; Ghosh, A.; Tunge, J., Intensification of catalytic olefin hydroformylation in CO2-expanded media. *AIChE journal* **2006,** *52* (7), 2575-2581.

132. Fang, J.; Jin, H.; Ruddy, T.; Pennybaker, K.; Fahey, D.; Subramaniam, B., Economic and environmental impact analyses of catalytic olefin hydroformylation in CO2-expanded liquid (CXL) media. *Industrial & Engineering Chemistry Research* **2007,** *46* (25), 8687-8692.

133. Hallett, J. P.; Ford, J. W.; Jones, R. S.; Pollet, P.; Thomas, C. A.; Liotta, C. L.; Eckert, C. A., Hydroformylation catalyst recycle with gas-expanded liquids. *Industrial & Engineering Chemistry Research* **2008,** *47* (8), 2585-2589.

134. Musie, G.; Wei, M.; Subramaniam, B.; Busch, D. H., Catalytic oxidations in carbon dioxide-based reaction media, including novel CO2-expanded phases. *Coordination Chemistry Reviews* **2001,** *219*, 789-820.

135. Wei, M.; Musie, G. T.; Busch, D. H.; Subramaniam, B., CO2-expanded solvents: unique and versatile media for performing homogeneous catalytic oxidations. *Journal of the American Chemical Society* **2002,** *124* (11), 2513-2517.

136. Zuo, X.; Niu, F.; Snavely, K.; Subramaniam, B.; Busch, D. H., Liquid phase oxidation of p-xylene to terephthalic acid at medium-high temperatures: multiple benefits of CO 2-expanded liquids. *Green Chemistry* **2010,** *12* (2), 260-267.

137. Fujita, S.-i.; Akihara, S.; Zhao, F.; Liu, R.; Hasegawa, M.; Arai, M., Selective hydrogenation of cinnamaldehyde using ruthenium–phosphine complex catalysts with multiphase reaction systems in and under pressurized carbon dioxide: significance of pressurization and interfaces for the control of selectivity. *Journal of Catalysis* **2005,** *236* (1), 101-111.

138. Xie, X.; Liotta, C. L.; Eckert, C. A., CO2-protected amine formation from nitrile and imine hydrogenation in gas-expanded liquids. *Industrial & engineering chemistry research* **2004,** *43* (24), 7907-7911.

139. Fujita, S.-i.; Onodera, Y.; Yoshida, H.; Arai, M., Selective hydrogenation of acetophenone with supported Pd and Rh catalysts in water, organic solvents, and CO 2-dissolved expanded liquids. *Green chemistry* **2016,** *18* (18), 4934-4940.

140. Zhao, B.-H.; Chen, J.-G.; Liu, X.; Liu, Z.-W.; Hao, Z.; Xiao, J.; Liu, Z.-T., Selective hydrogenation of cinnamaldehyde over Pt and Pd supported on multiwalled carbon nanotubes in a CO2-expanded alcoholic medium. *Industrial & Engineering Chemistry Research* **2012,** *51* (34), 11112-11121.

141. Koeken, A. C.; Benes, N. E.; van den Broeke, L. J.; Keurentjes, J. T., Efficient hydroformylation in dense carbon dioxide using phosphorus ligands without perfluoroalkyl substituents. *Advanced Synthesis & Catalysis* **2009,** *351* (9), 1442-1450.

142. Frisch, A. C.; Webb, P. B.; Zhao, G.; Muldoon, M. J.; Pogorzelec, P. J.; Cole-Hamilton, D. J., "Solventless" continuous flow homogeneous hydroformylation of 1-octene. *Dalton Transactions* **2007,** (47), 5531-5538.

143. Yoshida, H.; Kato, K.; Wang, J.; Meng, X.; Narisawa, S.; Fujita, S.-i.; Wu, Z.; Zhao, F.; Arai, M., Hydrogenation of nitrostyrene with a Pt/TiO2 catalyst in CO2-dissolved expanded polar and nonpolar organic liquids: their macroscopic and microscopic features. *The Journal of Physical Chemistry C* **2011,** *115* (5), 2257-2267.

144. Fujita, S.-i.; Yamada, T.; Akiyama, Y.; Cheng, H.; Zhao, F.; Arai, M., Hydrogenation of phenol with supported Rh catalysts in the presence of compressed CO2: Its effects on reaction rate, product selectivity and catalyst life. *The Journal of Supercritical Fluids* **2010,** *54* (2), 190-201.

145. Krokoszinski R, H. U., Todd K Method for producing propylene hydroformylation products and acrylic acid and/or acrolein. 2005.

146. Still, C.; Salmi, T.; Mäki-Arvela, P.; Eränen, K.; Murzin, D. Y.; Lehtonen, J., Solubility of gases in a hydroformylation solvent. *Chemical engineering science* **2006,** *61* (11), 3698-3704.

147. Bernas, A.; Mäki-Arvela, P. i.; Lehtonen, J.; Salmi, T.; Murzin, D. Y., Kinetic modeling of propene hydroformylation with Rh/TPP and Rh/CHDPP catalysts. *Industrial & Engineering Chemistry Research* **2008,** *47* (13), 4317-4324.

148. Xie, Z. SOLUBILITIES OF CO AND H2 IN NEAT AND CO2-EXPANDED HYDROFORMYLATION REACTION MIXTURES CONTAINING 1-OCTENE AND NONANAL UP TO 80° C AND 90 BARS. University of Kansas, 2009.

149. Shen, V.; Siderius, D.; Krekelberg, W.; Hatch, H., NIST Standard Reference Simulation Website, NIST Standard Reference Database Number 173, National Institute of Standards and Technology, Gaithersburg, MD, 20899. 2017.

150. Bakeev, K. A., *Process analytical technology: spectroscopic tools and implementation strategies for the chemical and pharmaceutical industries*. John Wiley & Sons: 2010.

151. Widdoes, L. C.; Katz, D. L., Vapor-liquid equilibrium constants for carbon monoxide. *Industrial & Engineering Chemistry* **1948,** *40* (9), 1742-1746.

152. Trust, D.; Kurata, F., Vapor-liquid and liquid-liquid vapor phase behavior of the carbon monoxide-propane and the carbon monoxide-ethane systems. *AIChE Journal* **1971,** *17* (2), 415-419.

153. Burriss, W.; Hsu, N.; Reamer, H.; Sage, B., Phase behavior of the hydrogen-propane system. *Industrial & Engineering Chemistry* **1953,** *45* (1), 210-213.

154. SAGARA, H.; MIHARA, S.; ARAI, Y.; SAITO, S., VAPOR-LIQUID EQUILIBRIA AND HENRY"S CON-STANTS FOR TERNARY SYSTEMS CONTAINING HYDROGEN AND LIGHT HYDROCARBONS. *Journal of Chemical Engineering of Japan* **1975,** *8* (2), 98-104.

155. Jáuregui-Haza, U.; Pardillo-Fontdevila, E.; Wilhelm, A.; Delmas, H., Solubility of hidrogen and carbon monoxide in water and some organic solvents. *Latin American applied research* **2004,** *34* (2), 71-74.

156. Yin, J.-Z.; Tan, C.-S., Solubility of hydrogen in toluene for the ternary system H 2+ CO 2+ toluene from 305 to 343K and 1.2 to 10.5 MPa. *Fluid phase equilibria* **2006,** *242* (2), 111-117.

157. Nair, V. S.; Mathew, S. P.; Chaudhari, R. V., Kinetics of hydroformylation of styrene using homogeneous rhodium complex catalyst. *Journal of Molecular Catalysis A: Chemical* **1999,** *143* (1-3), 99-110.

158. Castillón, S.; Fernandez, E., Rhodium Catalyzed Hydroformylation. *Catalysis by Metal Complexes* **2000,** *22*.

159. Riisager, A.; Fehrmann, R.; Haumann, M.; Gorle, B. S.; Wasserscheid, P., Stability and kinetic studies of supported ionic liquid phase catalysts for hydroformylation of propene. *Industrial & engineering chemistry research* **2005,** *44* (26), 9853-9859.

160. Bahrmann, H.; Bach, H.; Frohning, C.; Kleiner, H.; Lappe, P.; Peters, D.; Regnat, D.; Herrmann, W., BINAS: A new ligand with outstanding properties in the hydroformylation of propylene. *ChemInform* **1997,** *28* (20).

161. Natta, G.; Ercoli, R.; Castellano, S.; Barbieri, F., The influence of hydrogen and carbon monoxide partial pressures on the rate of the hydroformylation reaction. *Journal of the American Chemical Society* **1954,** *76* (15), 4049-4050.

162. Tucci, E. R., Hydroformylating Terminal Olefins. *Industrial & Engineering Chemistry Product Research and Development* **1970,** *9* (4), 516-521.

163. Liu, D.; Chaudhari, R. V.; Subramaniam, B., Enhanced solubility of hydrogen and carbon monoxide in propane-and propylene-expanded liquids. *AIChE Journal* **2017**.

164. Liu, D.; Chaudhari, R. V.; Subramaniam, B., Enhanced solubility of hydrogen and carbon monoxide in propane-and propylene-expanded liquids. *AIChE Journal* **2018,** *64* (3), 970-980.

165. Xu, Z.; Sandler, S. I., Application to mixtures of the Peng-Robinson equation of state with fluid-specific parameters. *Industrial & engineering chemistry research* **1987,** *26* (6), 1234-1238.

166. Tester, J. W.; Modell, M., *Thermodynamics and its Applications*. Prentice Hall PTR: 1997.

167. Ford, J. W.; Janakat, M. E.; Lu, J.; Liotta, C. L.; Eckert, C. A., Local polarity in CO2-expanded acetonitrile: a nucleophilic substitution reaction and solvatochromic probes. *The Journal of organic chemistry* **2008,** *73* (9), 3364-3368.

168. Wiese, K.-D.; Obst, D., Hydroformylation. In *Catalytic Carbonylation Reactions*, Springer: 2006; pp 1-33.

169. Pruett, R. L., Hydroformylation. In *Advances in Organometallic Chemistry*, Elsevier: 1979; Vol. 17, pp 1-60.

170. Xie, Z.; Akien, G. R.; Sarkar, B. R.; Subramaniam, B.; Chaudhari, R. V., Continuous hydroformylation with phosphine-functionalized polydimethylsiloxane rhodium complexes as nanofilterable homogeneous catalysts. *Industrial & Engineering Chemistry Research* **2015,** *54* (43), 10656-10660.

171. Liu, D.; Xie, Z.; Snavely, W. K.; Chaudhari, R. V.; Subramaniam, B., Enhanced hydroformylation of 1-octene in n-butane expanded solvents with Co-based Complexes. *Reaction Chemistry & Engineering* **2018**.

172. Wiese, K.-D.; Obst, D., Hydroformylation. *Catalytic Carbonylation Reactions* **2006**, 1-33.

173. Eisenschmid, T. C.; Mokhtarzadeh, M.; Smith III, C. R.; Becker, M. C.; Phillips, G. R.; Brammer, M. A.; Miller, G. A.; Watson, R. B.; Cox, I. B.; Lord, E. A., Hydroformylation process. Google Patents: 2017.

174. Cornils, B.; Herrmann, W. A.; Beller, M.; Paciello, R., *Applied Homogeneous Catalysis with Organometallic Compounds: A Comprehensive Handbook in Four Volumes*. John Wiley & Sons: 2018; Vol. 4.

175. Torres, G. M.; Frauenlob, R.; Franke, R.; Börner, A., Production of alcohols via hydroformylation. *Catalysis Science & Technology* **2015,** *5* (1), 34-54.

176. Frey, G. D., 75 Years of oxo synthesis–The success story of a discovery at the OXEA Site Ruhrchemie. *Journal of Organometallic Chemistry* **2014,** *754*, 5-7.

177. Tudor, R.; Shah, A., Industrial Low Pressure Hydroformylation: Forty-Five Years of Progress for the LP OxoSM Process. *Johnson Matthey Technology Review* **2017,** *61* (3), 246-256.

178. Armin, B.; Franke, R., *Hydroformylation: fundamentals, processes, and applications in organic synthesis*. John Wiley & Sons: 2016.

179. Caers, R. F.; Van Driessche, E. T. A., Process for hydroformylation of propylene. Google Patents: 2011.

180. Krokoszinski, R.; Hammon, U.; Todd, K., Method for producing propylene hydroformylation products and acrylic acid and/or acrolein. Google Patents: 2005.

181. OUTLOOK '18: US propylene production set to expand in 2018. https://www.icis.com/resources/news/2018/01/03/10179497/outlook-18-us-propylene-production-set-to-expand-in-2018/

182. Ghanta, M.; Fahey, D. R.; Busch, D. H.; Subramaniam, B., Comparative economic and environmental assessments of H2O2-based and tertiary butyl hydroperoxide-based propylene oxide technologies. *ACS Sustainable Chemistry & Engineering* **2013,** *1* (2), 268-277.

183. Li, M.; Ruddy, T.; Fahey, D.; Busch, D. H.; Subramaniam, B., Terephthalic acid production via greener spray process: comparative economic and environmental impact assessments with mid-century process. *ACS Sustainable Chemistry & Engineering* **2014,** *2* (4), 823-835.

184. Gong, K.; Chafin, S.; Pennybaker, K.; Fahey, D.; Subramaniam, B., Economic and environmental impact analyses of solid acid catalyzed isoparaffin/olefin alkylation in supercritical carbon dioxide. *Industrial & Engineering Chemistry Research* **2008,** *47* (23), 9072-9080.

185. Arora, V., Propylene via CATOFIN propane dehydrogenation technology. *Handbook of petrochemicals production processes* **2004**, 10.43-10.49.

186. Seo, S.-T.; Lee, K. S. In *Repetitive control of CATOFIN process*, SICE-ICASE, 2006. International Joint Conference, IEEE: 2006; pp 3314-3319.

187. Maher, J. M.; Babin, J. E.; Billig, E.; Bryant, D. R.; Leung, T. W., Hydroformylation process. Google Patents: 1994.

188. Argyropoulos, J. N.; Bryant, D. R.; Tulchinsky, M. L.; Kanel, J. S.; Foley, P.; Fish, B. B., Metal-ligand complex catalyzed processes. Google Patents: 2001.

189. Peters, M. S.; Timmerhaus, K. D.; West, R. E.; Timmerhaus, K.; West, R., *Plant design and economics for chemical engineers*. McGraw-Hill New York: 1968; Vol. 4.

190. Bureau of Labor Statistics. https://www.bls.gov/.

191. U.S. Energy Information Administration (EIA). https://www.eia.gov/.

192. Engelhard Industrial Bullion (EIB) Prices: https://apps.catalysts.basf.com/apps/eibprices/mp/.

193. Economic indicators. https://www.scribd.com/document/352561651/CEPCI-June-2017-Issue.

194. Tatari, O.; Kucukvar, M.; Onat, N. C. In *Towards a triple bottom line life cycle sustainability assessment of buildings*, Science for Sustainable Construction and Manufacturing Workshop Volume I. Position Papers and Findings, 2015; p 226.

195. Luo, X. L.; Zou, A. Q.; Quan, C. G. In *A Study on the Carbon Emissions Calculation Model of Iron and Steel Products Based on EIO-LCA*, Applied Mechanics and Materials, Trans Tech Publ: 2015; pp 2970-2974.

196. Simonen, K.; Huang, M.; Aicher, C.; Morris, P., Embodied Carbon as a Proxy for the Environmental Impact of Earthquake Damage Repair. *Energy and Buildings* **2018**.

197. Finnveden, G.; Hauschild, M. Z.; Ekvall, T.; Guinée, J.; Heijungs, R.; Hellweg, S.; Koehler, A.; Pennington, D.; Suh, S., Recent developments in life cycle assessment. *Journal of environmental management* **2009,** *91* (1), 1-21.

198. Hendrickson, C. T.; Lave, L. B.; Matthews, H. S., *Environmental life cycle assessment of goods and services: an input-output approach*. Resources for the Future: 2006.

199. Ferrao, P.; Nhambiu, J., A comparison between conventional LCA and hybrid EIO-LCA: Analyzing crystal giftware contribution to global warming potential. In *Handbook of input-output economics in industrial ecology*, Springer: 2009; pp 219-230.

200. Economic Input-Output Life Cycle Assessment. http://www.eiolca.net/.

201. Pruett, R. L., Hydroformylation. *Advances in Organometallic Chemistry* **1979,** *17*, 1-60.

202. Kamer, P. C.; Reek, J. N.; van Leeuwen, P. W., Rhodium Catalyzed Hydroformylation. *Mechanisms in Homogeneous Catalysis: A Spectroscopic Approach* **2005**, 231-269.

203. Hutchenson, K. W.; Scurto, A. M.; Subramaniam, B., *Gas-expanded Liquids and Near-critical Media: Green Chemistry and Engineering*. ACS Publications: 2009.

204. Subramaniam, B., Gas-expanded liquids for sustainable catalysis and novel materials: Recent advances. *Coordination Chemistry Reviews* **2010,** *254* (15), 1843-1853.

205. Ghanta, M.; Subramaniam, B.; Lee, H. J.; Busch, D. H., Highly selective homogeneous ethylene epoxidation in gas (ethylene)-expanded liquid: Transport and kinetic studies. *AIChE Journal* **2013,** *59* (1), 180-187.

206. Bungu, P. N.; Otto, S., Evaluation of ligand effects in the modified cobalt hydroformylation of 1-octene. Crystal structures of [Co (L)(CO) 3] 2 (L= PA–C 5, PCy 3 and PCyp 3). *Dalton Transactions* **2011,** *40* (36), 9238-9249.

207. Kégl, T., Computational aspects of hydroformylation. *RSC Advances* **2015,** *5* (6), 4304-4327.

208. Rush, L. E.; Pringle, P. G.; Harvey, J. N., Computational Kinetics of Cobalt-Catalyzed Alkene Hydroformylation. *Angewandte Chemie International Edition* **2014,** *53* (33), 8672-8676.

209. Damoense, L.; Datt, M.; Green, M.; Steenkamp, C., Recent advances in high-pressure infrared and NMR techniques for the determination of catalytically active species in rhodium-and cobalt-catalysed hydroformylation reactions. *Coordination chemistry reviews* **2004,** *248* (21), 2393-2407.

210. Mirbach, M. F., On the mechanism of the Co2 (CO) 8 catalyzed hydroformylation of olefins in hydrocarbon solvents. A high pressure UV and IR study. *Journal of organometallic chemistry* **1984,** *265* (2), 205-213.

211. Whyman, R., The hydroformylation of olefins catalysed by cobalt carbonyls: a high pressure infrared spectral study. *Journal of Organometallic Chemistry* **1974,** *81* (1), 97-106.

212. Chen, M. J.; Klingler, R. J.; Rathke, J. W.; Kramarz, K. W., In situ high-pressure NMR studies of Co2 (CO) 6 [P (p-CF3C6H4) 3] 2 in supercritical carbon dioxide: ligand

substitution, hydrogenation, and hydroformylation reactions. *Organometallics* **2004,** *23* (11), 2701-2707.

213. Patcas, F.; Maniut, C.; Ionescu, C.; Pitter, S.; Dinjus, E., Supercritical carbon dioxide as an alternative reaction medium for hydroformylation with integrated catalyst recycling. *Applied Catalysis B: Environmental* **2007,** *70* (1-4), 630-636.

214. Riisager, A.; Jørgensen, B.; Wasserscheid, P.; Fehrmann, R., First application of supported ionic liquid phase (SILP) catalysis for continuous methanol carbonylation. *Chemical Communications* **2006,** (9), 994-996.

215. Ren, X.; Zheng, Z.; Zhang, L.; Wang, Z.; Xia, C.; Ding, K., Rhodium-Complex-Catalyzed Hydroformylation of Olefins with CO2 and Hydrosilane. *Angewandte Chemie International Edition* **2017,** *56* (1), 310-313.

216. Federsel, C.; Boddien, A.; Jackstell, R.; Jennerjahn, R.; Dyson, P. J.; Scopelliti, R.; Laurenczy, G.; Beller, M., A Well-Defined Iron Catalyst for the Reduction of Bicarbonates and Carbon Dioxide to Formates, Alkyl Formates, and Formamides. *Angewandte Chemie International Edition* **2010,** *49* (50), 9777-9780.

Appendix A. Calibrations for liquid and vapor phase components in Chapter 2

External standardization method was applied for on-line gas chromatographic (GC) analysis of liquid and vapor phase samples. A standard of known composition is analyzed on the GC to generate linear calibration curves for each of the components in the systems being investigated. An identical volume of the sample with unknown composition is analyzed. The concentration of a given component is then estimated from the GC peak areas of that component corresponding to the calibration sample and the measured sample.

Calibration curves of gaseous components were generated using the vacuum calibration method using an experimental unit shown below (Figure A.1).

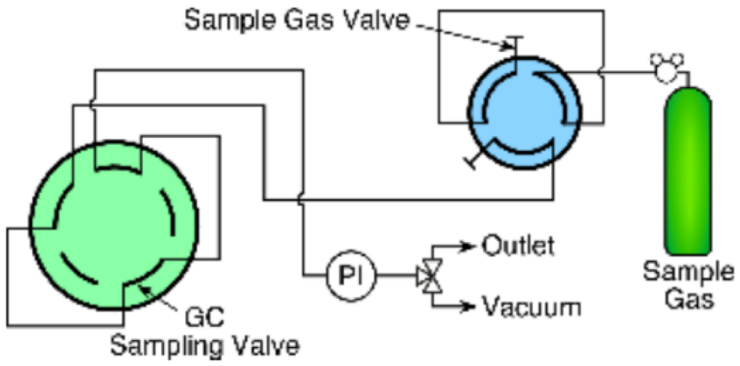

Figure A1. Schematic of vacuum calibration method

The calibration procedure involves evacuating a gas sampling valve by a vacuum pump to -0.098 MPa prior to each injection. The sample loop was then filled with the sample with a known composition to a predetermined pressure (less than atmospheric pressure). Because the vapor phase was sampled at atmospheric pressure during the VLE experiments (using atmospheric balancing technique), the concentrations obtained here were normalized to atmosphere pressure 0.101 MPa). In other words,

$$x = \frac{P}{P_{atm}} x'$$

where x = normalized concentration of the sample being analyzed (mol%)

P = pressure in the sample loop (MPa)

Patm = atmospheric pressure (MPa)

x’ = concentration in the calibration sample (mole%)

A range of pressures was chosen to produce concentrations that bracket the feed and expected product concentrations. Three repeat injections were made for each pressure (i.e., concentration). Concentration versus peak area curves was thus generated for each gaseous component.

Calibration curves for the liquid samples were obtained by manual injections. A series of liquid samples with known concentrations was first prepared and then manually injected into the GC using microliter syringes. At least three repeat injections were made for each concentration to check for reproducibility. Concentrations versus peak area curves were thus generated. The calibration data are shown in Figure A2.

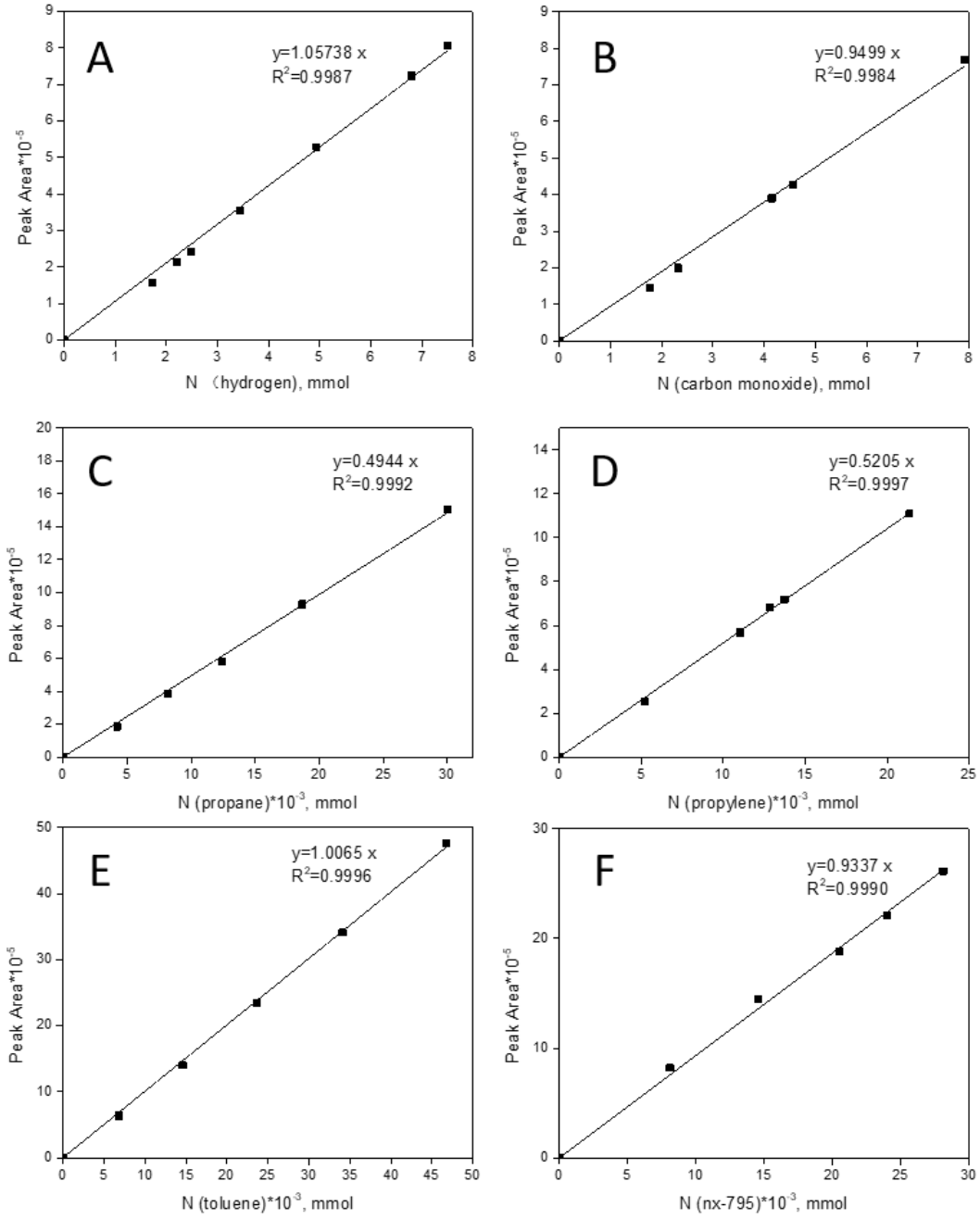

Figure A2. Calibration curves for hydrogen(A), carbon monoxide(B), propane(C), propylene(D), toluene(E), NX-795(F)

Appendix B. Calculation of solute gas mole fraction in the neat solvent in Chapter 2

The following sample calculation is based on entry 12 in Table 5 [T = 90 °C, P_{total} = 1.5 MPa, f_{H2} = 1.092 MPa]. The mole fraction of the solute gas in the neat solvent at a given gas-phase solute fugacity is estimated using Henry's law constants obtained from Table 4. At 90 °C, K_H = 26.2 (MPa*m^3/kmol), $M_{toluene}$ = 92.14 g/mol, $\rho_{toluene}$ = 799 kg/m^3. *

$$K_H = \frac{MPa}{\frac{kmol}{m^3}} = \frac{f_{H_2}}{c_{H_2}}$$

$$x_{H_2} = \frac{c_{H_2}}{c_{toluene} + c_{H_2}}$$

$$x_{toluene} = 1 - x_{H_2}$$

$$\frac{n_{H_2}}{n_{toluene}} = \frac{x_{H_2}}{1 - x_{H_2}}$$

Assuming the volume of hydrogen in the liquid phase is negligible compared to toluene,

$$n_{toluene} = (V_{sample} * \rho_{toluene})/M_{toluene}$$

$$n_{H_2} = \frac{(V_{sample} * \rho_{toluene})}{M_{toluene}} * \frac{x_{H_2}}{1 - x_{H_2}}$$

$$c_{H_2} = \frac{n_{H_2}}{V_{sample}} = \frac{(V_{sample} * \rho_{toluene})}{M_{toluene}} * \frac{x_{H_2}}{1 - x_{H_2}} * \frac{1}{V_{sample}}$$

$$26.2 = \frac{1.092\ MPa}{\frac{799\ \frac{kg}{m^3} * x_{H_2}}{(1 - x_{H_2}) * 92.14\ kg/kmol}}$$

The foregoing equation is solved to obtain x_{H_2} = 0.0041. The equivalent mole fractions of either CO or H_2 in the neat solvent is denoted as $x_{i,\text{neat solvent}}$ in Tables 2.5 - 2.12 where *i* = CO or H_2.

*. Goodwin R D. Toluene thermophysical properties from 178 to 800 K at pressures to 1000 bar[J]. Journal of Physical and Chemical Reference Data, 1989, 18(4): 1565-1636.

Appendix C. Estimation of fugacity coefficient in chapter 2

$$\ln\widehat{\phi}_\iota = \frac{b_i}{b_{mix}}(Z^V_{mix}-1) - \ln\left(Z^V_{mix} - \frac{b_{mix}P}{RT}\right)$$

$$-\frac{a_{mix}}{2\sqrt{2}b_{mix}RT}\left[\frac{2\sum_j y_j a_{ij}}{a_{mix}} - \frac{b_i}{b_{mix}}\right]\ln\left[\frac{Z^V_{mix}+(1+\sqrt{2})\frac{b_{mix}P}{RT}}{Z^V_{mix}+(1-\sqrt{2})\frac{b_{mix}P}{RT}}\right]$$

$$= \frac{B_i}{B_{mix}}(Z^V_{mix}-1) - \ln(Z^V_{mix} - B_{mix})$$

$$-\frac{A_{mix}}{2\sqrt{2}B_{mix}}\left[\frac{2\sum_j y_j A_{ij}}{A_{mix}} - \frac{B_i}{B_{mix}}\right]\ln\left[\frac{Z^V_{mix}+(1+\sqrt{2})B_{mix}}{Z^V_{mix}+(1-\sqrt{2})B_{mix}}\right]$$

where Z^V is the compressibility factor for the mixture, A = a P/(RT)^2, B = b P/(RT), a and b are defined for pure components as follows:

$$a = [1 + (0.37464 + 1.54226\omega - 0.26993\omega^2)(1-\sqrt{T_r})]^2$$

$$b = 0.07779607R\frac{T_c}{P_c}$$

$$T_r = \frac{T}{T_c}$$

where T_c, P_c and ω represent the critical temperature, critical pressure and acentric factor, respectively. For mixtures, a and b are defined for pure components as follows:

$$a = \sum_i \sum_j x_i x_j a_{ij}$$

$$b = \sum_i x_i b_i$$

where $a_{ij} = \sqrt{a_i a_j}(1-k_{ij})$

and k_{ij} is the binary interaction parameter.

The compressibility factor needed to compute the fugacity of each specie is estimated using the Peng Robinson-Equation of State (PREOS).

Appendix D. Calculation of the average absolute relative deviation (AARD) for binary systems in chapter 2

The average absolute relative deviation (*AARD*) compares the experimental and predicted values in each phase at equilibrium, and is defined as follows for the individual phases.

$$AARD_x = \frac{1}{ND}\sum_1^{ND} \frac{|x_{cal}^i - x_{exp}^i|}{x_{exp}^i}$$

$$AARD_y = \frac{1}{ND}\sum_1^{ND} \frac{|y_{cal}^i - y_{exp}^i|}{y_{exp}^i}$$

where ND represents the number of data points, x_{exp}^i, y_{exp}^i and x_{cal}^i, y_{cal}^i represent the experimental and calculated mole fractions of each component in the liquid and vapor phases, respectively.

Table D1. AARD values for liquid phase (x) and gas phase (y) mole fractions for binary systems

System	*T* (°C)	*AARD, %*			
		x_1	x_2	y_1	y_2
Propane(1) + Toluene(2)	90	2.88	2.34	3.61	4.34
Propane(1) + Toluene(2)	80	2.50	2.89	2.01	1.97
Propane(1) + Toluene(2)	70	1.71	2.12	1.23	1.43
Propylene(1) + Toluene(2)	90	3.30	2.59	2.97	2.49
Propylene(1) + Toluene(2)	80	3.63	1.89	2.03	1.96
Propylene(1) + Toluene(2)	70	2.74	2.33	3.81	3.97
Propane(1) + NX-795(2)	90	3.14	2.62	3.60	2.77
Propylene(1) + NX-795(2)	90	2.12	3.22	2.77	3.76

Appendix E. Overall compositions for the ternary systems in Chapter 2

In a typical experiment, a predetermined amount of the liquid solvent (10 mL, 8.70 g) is syringed into the view cell. Either propane or propylene is introduced into the cell as liquid from an ISCO syringe pump followed by the addition of either H_2 or CO from a syngas reservoir to reach the final desired pressure. The moles of either propane or propylene inserted into the system are measured from the volume change in the pump reservoir and the pump temperature. The moles of either H_2 or CO added are calculated from knowing the pressure decrease in the external reservoir and the reservoir temperature. athe overall composition of a ternary system is shown below.

System: H_2(1) + propylene(2) + toluene(3); T = 90 °C; P_{total} = 1.5 MPa; as seen in Table 2.5, Entry 12)

Moles of toluene added

$$N_{toluene} = \frac{Mass}{Molecular\ weight} = \frac{8.70g}{92.14\ g/mol} = 0.0944 \text{ mol}$$

Moles of propylene added

The moles of either propane or propylene inserted into the system were measured from the pump volume change ($\Delta Volume$) and the pump temperature. The propylene exists as liquid in the ISCO syringe pump at 0°C and 6.0 MPa The density of propylene ($\rho_{propylene}$) at these conditions is 544.1 kg/m^3. *

$$N_{propylene} = \frac{\Delta Volume * \rho_{propylene}}{Molecular\ weight} = \frac{1.30\ ml * 0.5441\ g/ml}{42.08\ g/mol} = 0.0169 \text{ mol}$$

Moles of hydrogen added

The moles of H_2 added were calculated from the pressure decrease (ΔP) in the external reservoir and the reservoir temperature. The volume of the external reservoir (V_{res}) is 60 ml. The reservoir exists at room temperature (T_{res}). R is the gas constant.

$$N_{hydrogen} = \frac{\Delta P * V_{res}}{R * T_{res}} = \frac{101.65\ kPa * 0.06\ L}{8.314\ (L \cdot kPa \cdot K^{-1} \cdot mol^{-1}) * 293.15K} = 0.0025\ \text{mol}$$

The overall composition

For the ternary system H_2(1) + propane(2) + toluene(3), the overall composition of each component is estimated as follows:

H_2 (1): $$o_1 = \frac{0.0025}{0.0944 + 0.0169 + 0.0025} = 0.0220;$$

Propane (2) $$o_2 = \frac{0.0169}{0.0944 + 0.0169 + 0.0025} = 0.1485$$

Toluene (3) $$o_3 = \frac{0.0944}{0.0944 + 0.0169 + 0.0025} = 0.8295.$$

The overall compositions for the various ternary systems investigated in this work are summarized in Table E1.

*. http://www.thermopedia.com/content/1065/ (DOI: 10.1615/AtoZ.p.propylene).

Table E1. Overall compositions for the various ternary VLE measurements

System	P_{total} (MPa)	T (°C)	Overall composition	
			o_1	o_2
Table 2.5 in Main Text				
H_2(1) + Propane(2) + Toluene(3)	0.8	90	0.0206	0.0466
H_2(1) + Propane(2) + Toluene(3)	0.8	90	0.0180	0.0575
H_2(1) + Propane(2) + Toluene(3)	0.8	90	0.0154	0.1094
H_2(1) + Propane(2) + Toluene(3)	0.8	90	0.0120	0.1383
H_2(1) + Propane(2) + Toluene(3)	1.5	90	0.0377	0.1072
H_2(1) + Propane(2) + Toluene(3)	1.5	90	0.0313	0.1808
H_2(1) + Propane(2) + Toluene(3)	1.5	90	0.0267	0.2159
H_2(1) + Propane(2) + Toluene(3)	1.5	90	0.0127	0.2689
H_2(1) + Propane(2) + Toluene(3)	1.5	80	0.0374	0.1157
H_2(1) + Propane(2) + Toluene(3)	1.5	80	0.0165	0.2362
H_2(1) + Propane(2) + Toluene(3)	1.5	80	0.0122	0.2972
H_2(1) + Propane(2) + Toluene(3)	1.5	80	0.0056	0.3578
H_2(1) + Propane(2) + Toluene(3)	1.5	70	0.0220	0.1481
H_2(1) + Propane(2) + Toluene(3)	1.5	70	0.0199	0.2298
H_2(1) + Propane(2) + Toluene(3)	1.5	70	0.0117	0.3246
H_2(1) + Propane(2) + Toluene(3)	1.5	70	0.0036	0.4880
Table 2.6 in Main Text				
H_2(1) + propane(2) + NX-795(3)	1.5	90	0.0973	0.1314
H_2(1) + propane(2) + NX-795(3)	1.5	90	0.0790	0.2176
H_2(1) + propane(2) + NX-795(3)	1.5	90	0.0540	0.2919
H_2(1) + propane(2) + NX-795(3)	1.5	90	0.0318	0.3663
Table 2.7 in Main Text				
CO(1) + Propane(2) + Toluene(3)	1.5	90	0.0527	0.0950
CO(1) + Propane(2) + Toluene(3)	1.5	90	0.0365	0.1360
CO(1) + Propane(2) + Toluene(3)	1.5	90	0.0207	0.1975
CO(1) + Propane(2) + Toluene(3)	1.5	90	0.0065	0.2597
CO(1) + Propane(2) + Toluene(3)	1.5	80	0.0387	0.1347
CO(1) + Propane(2) + Toluene(3)	1.5	80	0.0176	0.2423
CO(1) + Propane(2) + Toluene(3)	1.5	80	0.0110	0.2970
CO(1) + Propane(2) + Toluene(3)	1.5	80	0.0055	0.3733
CO(1) + Propane(2) + Toluene(3)	1.5	70	0.0339	0.1974
CO(1) + Propane(2) + Toluene(3)	1.5	70	0.0089	0.3224
CO(1) + Propane(2) + Toluene(3)	1.5	70	0.0048	0.4460
CO(1) + Propane(2) + Toluene(3)	1.5	70	0.0043	0.4766
Table 2.8 in Main Text				
CO(1) + propane(2) + NX-795(3)	1.5	90	0.0946	0.1722
CO(1) + propane(2) + NX-795(3)	1.5	90	0.0769	0.2351
CO(1) + propane(2) + NX-795(3)	1.5	90	0.0526	0.3071
CO(1) + propane(2) + NX-795(3)	1.5	90	0.0314	0.3753

Table E2 (continued) Overall compositions for the various ternary VLE measurements

System	P_{total} (MPa)	T (°C)	Overall composition	
			o_1	o_2
Table 2.9 in Main Text				
H_2(1) + Propylene(2) + Toluene(3)	1.5	90	0.0464	0.0780
H_2(1) + Propylene(2) + Toluene(3)	1.5	90	0.0306	0.1029
H_2(1) + Propylene(2) + Toluene(3)	1.5	90	0.0175	0.1896
H_2(1) + Propylene(2) + Toluene(3)	1.5	90	0.0098	0.2517
H_2(1) + Propylene(2) + Toluene(3)	1.5	80	0.0366	0.1350
H_2(1) + Propylene(2) + Toluene(3)	1.5	80	0.0164	0.2426
H_2(1) + Propylene(2) + Toluene(3)	1.5	80	0.0092	0.2975
H_2(1) + Propylene(2) + Toluene(3)	1.5	80	0.0055	0.3733
H_2(1) + Propylene(2) + Toluene(3)	1.5	70	0.0426	0.1525
H_2(1) + Propylene(2) + Toluene(3)	1.5	70	0.0161	0.2524
H_2(1) + Propylene(2) + Toluene(3)	1.5	70	0.0090	0.3102
H_2(1) + Propylene(2) + Toluene(3)	1.5	70	0.0049	0.4350
Table 2.10 in Main Text				
H_2(1) + propylene(2) + NX-795(3)	1.5	90	0.0699	0.0563
H_2(1) + propylene(2) + NX-795(3)	1.5	90	0.0362	0.1990
H_2(1) + propylene(2) + NX-795(3)	1.5	90	0.0248	0.2595
H_2(1) + propylene(2) + NX-795(3)	1.5	90	0.0079	0.3502
Table 2.11 in Main Text				
CO(1) + Propylene(2) + Toluene(3)	1.5	90	0.0529	0.0907
CO(1) + Propylene(2) + Toluene(3)	1.5	90	0.0367	0.1321
CO(1) + Propylene(2) + Toluene(3)	1.5	90	0.0105	0.1961
CO(1) + Propylene(2) + Toluene(3)	1.5	90	0.0066	0.2495
CO(1) + Propylene(2) + Toluene(3)	1.5	80	0.0583	0.1165
CO(1) + Propylene(2) + Toluene(3)	1.5	80	0.0349	0.1745
CO(1) + Propylene(2) + Toluene(3)	1.5	80	0.0094	0.2816
CO(1) + Propylene(2) + Toluene(3)	1.5	80	0.0059	0.3249
CO(1) + Propylene(2) + Toluene(3)	1.5	70	0.0362	0.1446
CO(1) + Propylene(2) + Toluene(3)	1.5	70	0.0263	0.2298
CO(1) + Propylene(2) + Toluene(3)	1.5	70	0.0090	0.3118
CO(1) + Propylene(2) + Toluene(3)	1.5	70	0.0055	0.3730
Table 2.12 in Main Text				
CO(1) + propylene(2) + NX-795(3)	1.5	90	0.0921	0.1746
CO(1) + propylene(2) + NX-795(3)	1.5	90	0.0753	0.0588
CO(1) + propylene(2) + NX-795(3)	1.5	90	0.0292	0.2478
CO(1) + propylene(2) + NX-795(3)	1.5	90	0.0087	0.3593

Appendix F. Calculation of carbon and hydrogen balance deficit in Chapter 3

Since only linear and branched butyraldehydes are formed by GC analysis in most cases, the carbon and hydrogen balance deficit was estimated by calculating the moles of syngas (H_2/CO =1:1) consumed and compared the values with the moles of hydrogen and carbon added in the products. Because some syngas is also drawn into the reactor from the reservoir when some propylene is transferred from the vapor phase to the liquid phase upon reaction. The total moles of hydrogen and carbon depleted from the external reservoir is generally more than what can be accounted for by product formation.

A sample calculation of reaction in toluene (Table 3-5, Entry 1) at 343.15 K with total pressure of 1.2 MPa is shown below to consider its effect.

Initial toluene injected: 0.1882 mol

Total propylene injected: 0.0539 mol

Syngas needed to reach 1.2 MPa by simulation: 0.0058 mol

Propylene remained in reactor after 20% conversion: 0.0432 mol

Syngas needed to reach 1.2 MPa after 20% conversion by simulation: 0.0070 mol

Syngas consumption in reservoir after 20% conversion: 0.0216 mol

The discrepancy is (0.0070-0.0058)/0.0216 =5.5%

However, even at the highest conversion in this manuscript (20%), this discrepancy is no greater than 8%.

A sample calculation of propylene conversion, TOF and carbon and hydrogen balance deficit of Rh-catalyzed hydroformylation of propylene with TPP in propane-expanded toluene (PXL) at 343.15 K and 1.7 MPa (Table 3-5, Entry 4) is shown below.

Moles of syngas consumed

The moles of syngas consumed were calculated from the pressure decrease (ΔP) in the external reservoir and the reservoir temperature. The volume of the external reservoir (V_{res}) is 300 ml. The reservoir exists at room temperature (T_{res}). R is the gas constant.

$$N_{sygas\ consumed} = \frac{\Delta P * V_{res}}{R * T_{res}} = \frac{190.51\ kPa * 0.3\ L}{8.314\ (L \cdot kPa \cdot K^{-1} \cdot mol^{-1}) * 293.15K} = 23.45\ \text{mmol}$$

Moles of hydrogen and carbon added in the products

Hydroformylation reaction entails the net addition of a formyl group (CHO) and a hydrogen atom to a carbon-carbon double bond. For each mole of butyraldehyde formed consume equal amount of H_2 and CO. The moles of linear and branched butyraldehydes formed in the case study are 8.31 mmol and 2.66 mmol, respectively. The total moles of hydrogen and carbon added in the products ($N_{sygas\ added}$) are 8.31*2+2.66*2 = 21.94 mmol.

Propylene conversion

The propylene conversion is defined as moles of monoaldehyde products formed over the moles of propylene fed. The moles of propylene fed to the reactor are estimated from the volume of liquefied propylene injected by the syringe pump into the reactor. The moles of propylene feed in the case study is 63.8 mmol. The monoaldehydes products including the linear and branched butyraldehydes formed in the case study is 10.97 mmol.

Propylene conversion (%)=10.91/63.8= 17.10 %

TOF

The TOF is estimated assuming negligible propylene transfer from the vapor phase to the liquid phase at low (~5%) propylene conversion.

$$\text{TOF}\ (\text{min}^{-1}) = \frac{\text{Half of moles of syngas consumed corresponding to 5\% substrate conversion}}{(\text{moles of Rh})(\text{min})} \quad (4)$$

In the case study, half of syngas consumed corresponding to 5% substrate conversion is 3.19 mmol, the Rh is 0.0552 mmol, reaction time is

$$\text{TOF } (\text{min}^{-1}) = \frac{3.19 \text{ mmol}}{(0.0442\text{mmol})(2.27\text{min})} = \ 25.4\ min^{-1}$$

Carbon and hydrogen balance deficit

The carbon and hydrogen balance deficit ($n_{deficit}$) is estimated as follows:

$$n_{deficit} = \frac{N_{sygas\ consumed} - N_{sygas\ added}}{N_{sygas\ consumed}} = \frac{23.45 - 21.94}{23.45} = 6.44\ \%$$

The carbon and hydrogen balance deficit for all the runs in this work are summarized in Table F1.

Table F1. Carbon and hydrogen balance deficit for various reaction system

System	Aldehyde formation, mmol	Syngas depletion from reservoir, mmol	$n_{deficit}$, %
Table 3.4 in Main Text			
Entry 1	3.61	7.61	5.13
Entry 2	3.72	7.76	4.08
Entry 3	3.77	7.95	5.22
Entry 4	4.73	10.15	6.87
Entry 5	3.56	7.70	7.53
Table 3.5 in Main Text			
Entry 1	11.36	23.75	4.33
Entry 2	6.65	14.30	6.94
Entry 3	9.62	19.89	3.27
Entry 4	10.97	23.45	6.44
Entry 5	6.60	14.09	6.22
Entry 6	8.42	18.10	6.98
Table 3.6 in Main Text			
Entry 1	11.36	23.75	4.33
Entry 2	12.15	26.16	7.12
Entry 3	12.17	24.45	4.81
Entry 4	10.97	23.59	7.00
Entry 5	12.10	25.01	3.21
Entry 6	12.19	26.07	6.50
Table 3.7 in Main Text			
Entry 1	11.36	23.75	4.33
Entry 2	10.97	25.45	4.80
Entry 3	10.95	23.17	5.53
Entry 4	10.49	22.43	6.44
Entry 5	15.25	32.05	4.85
Entry 6	20.09	42.59	5.66
Entry 7	23.69	50.31	5.82
Table 3.8 in Main Text			
Entry 1	11.36	23.75	4.33
Entry 2	10.38	23.41	11.34
Entry 3	9.15	22.39	18.21
Entry 4	10.97	23.45	6.44
Entry 5	11.14	25.57	12.88
Entry 6	9.70	27.45	19.22

Appendix G. Volumetric expansion of mixtures containing various dissolved Rh catalyst complexes in Chapter 3

Volumetric expansion of mixtures containing various dissolved Rh catalyst complexes by propane that are not shown in the main text is shown in Figure S1. No catalyst precipitation was observed in the investigated P and T ranges indicating that under reaction conditions, the investigated catalyst complexes remains dissolved in these PXL phases.

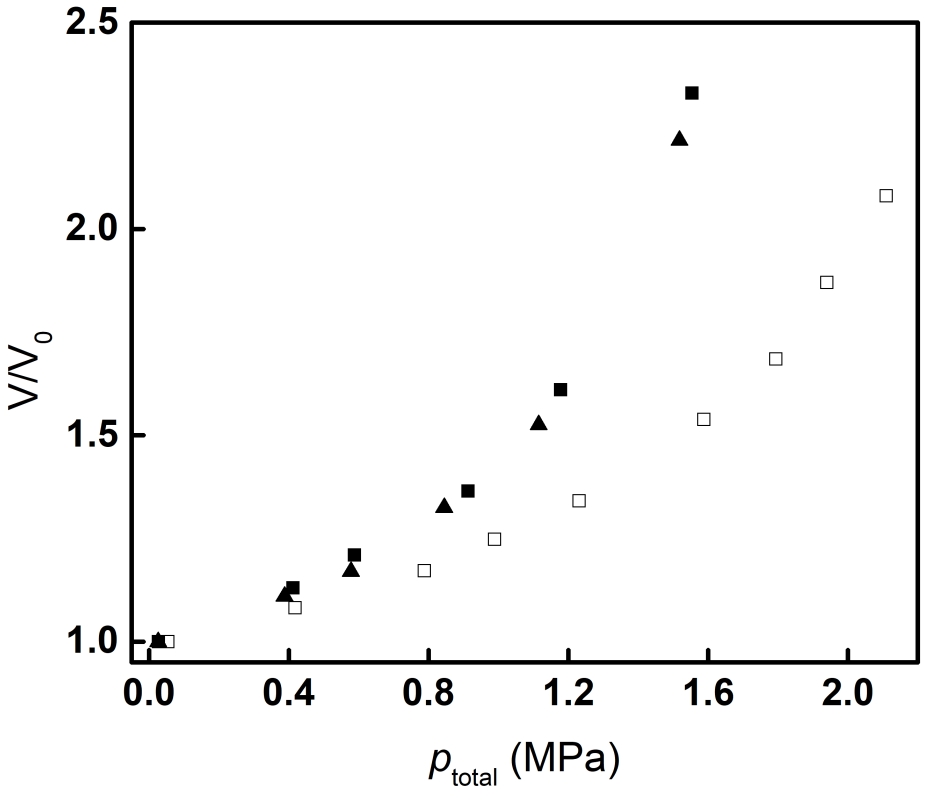

Figure G1 Volumetric expansion of mixtures containing various dissolved Rh catalyst complexes by propane (▲, [Rh] = 2.21 mmol/L, molar [CHDP/Rh] = 80. T = 343.15 K; ■, [Rh] = 2.21 mmol/L, molar [TPPA/Rh] = 80. T = 343.15 K; □, [Rh] = 2.21 mmol/L, molar [BiPhePhos/Rh] = 2. T = 363.15 K)

Appendix H. Overall compositions for the ternary and quaternary systems studied in Chapter 3

In a typical measurement, a predetermined amount of the liquid solvent (10 mL, 0.87g) is syringed into the view cell. The dense propane or propylene was gradually introduced into the cell by a syringe pump followed by the addition of syngas (H_2/CO=1:1) from a syngas reservoir to reach the final desired pressure. The amounts of propane or propylene inserted into the system were measured from the pump volume change. The syngas addition was calculated from the reservoir pressure change. The overall composition for measured ternary and quaternary systems are shown below.

Table H1 Mole fractions (x) of overall compositions in neat and propane- or propylene- expanded toluene at 70 ℃

				Propane-expanded toluene			Propylene-expanded toluene		
		Syngas Only		0.60MPa syngas + Propane			0.60 MPa syngas + Propylene		
Entry #	*P*, MPa	x, H_2	x, CO	x, H_2	x, CO	x, propane	x, H_2	x, CO	x, propylene
1	0.60	0.0117	0.0120	-	-	-		-	-
2	1.00	0.0195	0.0199	0.0101	0.0103	0.142	0.0102	0.0104	0.133
3	1.20	0.0233	0.0238	0.0093	0.0095	0.208	0.0095	0.0097	0.194
4	1.40	0.0270	0.0276	0.0086	0.0088	0.270	0.0088	0.0090	0.252
5	1.80	0.0342	0.0349	0.0073	0.0075	0.376	0.0076	0.0077	0.356
6	2.00	0.0378	0.0385	0.0068	0.0069	0.420	0.0070	0.0072	0.401

Table H2 Mole fractions (x) of overall compositions in neat and propane- or propylene-expanded NX-795 at 90 ℃

				Propane-expanded toluene			Propylene-expanded toluene		
		Syngas Only		0.60MPa syngas + Propane			0.60 MPa syngas + Propylene		
Entry #	*P*, MPa	x, H_2	x, CO	x, H_2	x, CO	x, propane	x, H_2	x, CO	x, propylene
1	0.60	0.0197	0.0201	-	-	-		-	-
2	1.00	0.0319	0.0326	0.0163	0.0167	0.173	0.0166	0.0169	0.159
3	1.20	0.0378	0.0385	0.0146	0.0149	0.248	0.0152	0.0155	0.229
4	1.40	0.0434	0.0443	0.0135	0.0138	0.317	0.0140	0.0142	0.293
5	1.80	0.0543	0.0554	0.0112	0.0114	0.435	0.0117	0.0119	0.407
6	2.00	0.0564	0.0575	0.0102	0.0104	0.483	0.0107	0.0110	0.456

Appendix I. Calculations of total capital investment in Chapter 4

Table I1. Calculations of total capital investment

Units		Percentage
Purchased cost, $ PC		
Purchased-equipment delivery	Per. of PC	0.1
Concrete foundation	Per. of PC	0.1
Piping	Per. of PC	0.6
Instrumentation	Per. of PC	0.1
Steel support	Per. of PC	0.1
Electrical	Per. of PC	0.1
Insulation	Per. of PC	0.1
Painting	Per. of PC	0.03
Equipment setting	Per. of PC	0.1
Installation equipment costs, $ IEC	**PC +above**	
Freight	per. of PC	0.03
Yard improvements	per. of PC	0.1
Environmental control	per. of PC	0.02
Buildings	per. of PC	0.4
Direct costs, $ DC	**IEC +above**	
Engineering costs	per. of DC	0.2
Construction overhead	per. of DC	0.3
Contingency	per. of DC	0.2
Contractor's fee	per. of DC	0.2
Indirect costs, $ IDC	above	0.7
Auxiliaries/Off-site, $ AO	per. of DC	0.3
Fixed Capital Investment, $ FCI	**DC + IDC +AO**	
Working Capital, $WC	per. of FCI	0.2
Total Capital Investment, $TCI	FCI + WC	

Appendix J. Raw material and utility unit price for production cost in Chapter 4

Table J1. Raw material unit prices

Chemical	Unit Price
Propane	0.61 $/kg
Syngas	0.09 $/$m^3$
Rh	74.82 $/g
Cr_2O_3	0.40 $/kg
Al_2O_3	0.30 $/kg
Solvent	1.12 $/kg

Table J2. Unit price of utilities

Chemical	Unit Price
Electricity	0.071 $/kwh
Steam	0.52 $/$m^3$
Cooling water	0.25 $/$m^3$
Refringent	8.23 $/$m^3$

Appendix K. Calculation of annual production cost in Chapter 4

Table K1. Itemized Annual Production Cost (million $) for Conventional and PXL Processes

Category	Conventional Process, million $	PXL Process, million $
Raw materials		
Propane	67.20	67.20
Syngas	12.31	12.31
HDF catalysts	0.05	0.05
HXF catalysts	4.50	4.50
Solvents	0.47	0.35
Utilities		
HP steam	3.28	1.59
Electricity	2.04	2.45
Cooling water	0.02	0.03
Refrigerant	0.17	0.20
Labor	1.11	1.11
Fixed charges	4.99	3.85
Maintenance and repairs (2% of fixed capital investment)	3.12	2.41
Operating supplies (10% of maintenance and repairs)	0.31	0.24
Patents and royalties (1% fixed capital investment)	1.56	1.20
Plant overhead cost (50% of the sum of labors and maintenance**)**	2.11	1.76
Other production costs		
Local taxes (1% of fixed capital investment)	1.56	1.20
Insurance (0.5% of fixed capital investment)	0.78	0.60
Depreciation (10% of fixed capital investment)	15.59	12.04
General Expenses		
Administrative costs (25% of overhead)	0.53	0.44
Distribution and selling expenses (10% of total expense)	15.59	12.04
Research and development (5% of total expense)	7.79	6.02
Total	140.08	127.74

Appendix L. EIO sectors used for assessing the major categories of the capital and production costs in Chapter 4

Table L1. Capital investment EIO

Input	EIO Sector	Conventional process, million $	PXL process, million $
Reactors	Metal tank, heavy gauge manufacturing	5.40	6.20
Separators and distillation columns	Metal tank, heavy gauge manufacturing	20.88	11.53
Heat exchangers	Power boiler and heat exchanger manufacturing	6.25	7.58
Pump and compressors	Pump and pumping equipment manufacturing	3.94	4.82
Equipment delivery	Truck transportation	3.60	2.80
Piping	Iron, steel pipe and tube manufacturing from purchased steel	21.61	16.72
Concrete foundations	Other concrete product manufacturing	3.60	2.80
Electrical service	Specialized design service	3.60	2.80
Building constructions	Nonresidential manufacturing structures	14.39	11.18
Painting	Paint and coating manufacturing	1.08	0.84
Engineering cost	Architectural and engineering services	6.77	5.59

The major capital investment and production costs were normalized from 2017 (used in estimating capital and operating costs) to 2002 values based on the consumer price index (CPI-U) published by the U.S. Census Bureau*

*https://www.bls.gov/regions/midwest/data/consumerpriceindexhistorical_us_table.pdf

Table L2. Major production cost EIO

Input	EIO Sector	Conventional process, million $	PXL process, million $
Propane	Industrial gas manufacturing	49.05	49.05
Syngas	Industrial gas manufacturing	8.99	8.99
Solvent	Other basic organic chemical manufacturing	0.34	0.26
Catalysts	Primary smelting and refining of nonferrous meta	3.32	3.32
Electricity	Power generation and supply	1.49	1.79
Cooling water	Water, sewage and other systems	0.01	0.02
Refrigerant	Household refrigerator and home freezer manufacturing	0.12	0.15
Direct labor	All other professional, scientific, and technical services	0.81	0.81
Maintenance	Commercial machinery repair and maintenance	2.28	1.76
Distribution and marketing	Wholesale trade	11.38	8.79
Research and development	Scientific research and development services	5.69	4.39

The major capital investment and production costs were normalized from 2017 (used in estimating capital and operating costs) to 2002 values based on the consumer price index (CPI-U) published by the U.S. Census Bureau*

*https://www.bls.gov/regions/midwest/data/consumerpriceindexhistorical_us_table.pdf

Appendix M. Calculation of carbon and hydrogen balance deficit in Chapter 5

The carbon balance deficit is estimated by calculating the moles of syngas consumed (from the observed pressure drop in the syngas reservoir) and comparing the value with the moles of hydrogen and carbon added in the products. Each mole of nonanol formed consumes 2 moles of hydrogen and 1 mole of carbon monoxide. Each mole of nonanal formed consumes 1 mole of hydrogen and 1 mole of carbon monoxide. Each mole of octane formed consumes 1 mole of hydrogen. A sample calculation for carbon and hydrogen balances at 180°C and 6.0 MPa (Table 3, Entry #6) is shown below.

The moles of syngas depletion were calculated from the pressure decrease (ΔP) in the reservoir and the reservoir temperature. The volume of the external reservoir (V_{res}) is 300 ml. The reservoir exists at room temperature (T_{res}). R is the gas constant.

$$N_{syngas} = \frac{\Delta P * V_{res}}{R * T_{res}} = \frac{1573\ kPa * 0.3\ L}{8.314\ (L \cdot kPa \cdot K^{-1} \cdot mol^{-1}) * 293.15 K} = 193.6\ mmol$$

Table M1. Sample calculation of carbon and hydrogen balance deficit

Compound		Measured value	CO	H_2
Syngas depletion from reservoir / mmol		193.6	-	-
Measured nonanal formation/ mmol		0	0	0
Measured nonanol fomation/ mmol		58.2	58.2	116.4
Measured octane formation / mmol		11.2	0	11.2
H_2 and CO addition to the product / mmol	CO		58.2	
	H_2			127.6
	H_2 + CO	185.8		
carbon and hydrogen balance deficit: $n_{deficit} = \frac{193.6 - 185.8}{193.6} * 100\% = 3.99\ \%$				

T=180°C, P = 6.0 MPa, H_2/CO = 2:1; [Co] = 1000 ppm,

The carbon and hydrogen balance deficit for all the runs are summarized in Table M2.

Table M2. Carbon and hydrogen balance deficits for various runs

System	H_2 and CO addition to the product, mmol	Syngas depletion from reservoir, mmol	$n_{deficit}$, %
Table 5-2 in Main Text			
Entry 1	184.6	189.4	2.55
Table 5-3 in Main Text			
Entry 1	73.6	75.1	1.95
Entry 2	182.7	187.8	2.76
Entry 3	184.9	191.0	3.20
Entry 4	127.3	129.0	1.38
Entry 5	165.3	167.7	1.43
Entry 6	185.9	193.6	3.99
Entry 7	118.0	122.4	3.57
Entry 8	183.8	189.8	3.19
Entry 9	147.5	153.6	3.92
Entry 10	182.8	187.7	2.62
Entry 11	190.2	194.9	2.44
Table 5-4 in Main Text			
Entry 1	186.7	192.4	2.98
Entry 2	189.5	196.1	3.35
Entry 3	191.6	195.5	1.95
Entry 4	136.7	139.9	2.28
Table 5-5 in Main Text			
Entry 1	205.0	207.2	1.08
Entry 2	206.8	211.3	2.13
Entry 3	203.3	208.1	2.30
Entry 4	202.8	209.3	3.10
Entry 5	173.1	176.2	1.75